horticulturae

MDPI

Review

A Review of the Main Process-Based Approaches for Modeling N_2O Emissions from Agricultural Soils

Mara Gabbrielli [1], Marina Allegrezza [1,*], Giorgio Ragaglini [1], Antonio Manco [2], Luca Vitale [2] and Alessia Perego [1]

[1] Department of Agricultural and Environmental Sciences, University of Milan, Via Celoria 2, 20133 Milan, Italy; mara.gabbrielli@unimi.it (M.G.); giorgio.ragaglini@unimi.it (G.R.); alessia.perego@unimi.it (A.P.)

[2] Institute for Agriculture and Forest Systems in the Mediterranean (ISAFoM), P.le Enrico Fermi 1, 80055 Portici, Italy; antonio.manco89@gmail.com (A.M.); luca.vitale@cnr.it (L.V.)

* Correspondence: marina.allegrezza@unimi.it

Abstract: Modeling approaches have emerged to address uncertainties arising from N_2O emissions variability, representing a powerful methodology to investigate the two emitting processes (i.e., nitrification and denitrification) and to represent the interconnected dynamics among soil, atmosphere, and crops. This work offers an extensive overview of the widely used models simulating N_2O under different cropping systems and management practices. We selected process-based models, prioritizing those with well-documented algorithms found in recently published scientific articles or having published source codes. We reviewed and compared the algorithms employed to simulate N_2O emissions, adopting a unified symbol system. The selected models (APSIM, ARMOSA, CERES-EGC, CROPSYST, CoupModel, DAYCENT, DNDC, DSSAT, EPIC, SPACSYS, and STICS) were categorized by the approaches used to model nitrification and denitrification processes, discriminating between implicit or explicit consideration of the microbial pool and according to the formalization of the main environmental drivers of these processes (soil nitrogen concentration, temperature, moisture, and acidity). Models' setting and performance assessments were also discussed. From the appraisal of these approaches, it emerged that soil chemical–physical properties and weather conditions are the main drivers of N cycling and the consequent gaseous emissions.

Keywords: nitrogen cycle; nitrification; denitrification; nitrous oxide emissions; greenhouse gas emissions; cropping system simulation model

Citation: Gabbrielli, M.; Allegrezza, M.; Ragaglini, G.; Manco, A.; Vitale, L.; Perego, A. A Review of the Main Process-Based Approaches for Modeling N_2O Emissions from Agricultural Soils. *Horticulturae* **2024**, *10*, 98. https://doi.org/10.3390/horticulturae10010098

Academic Editors: Moreno Toselli, Elena Baldi and Donato Cillis

Received: 21 December 2023
Revised: 15 January 2024
Accepted: 17 January 2024
Published: 19 January 2024

1. Introduction

Commonly adopted agricultural practices aimed at improving cropping systems' economic profitability have the potential to strongly influence, together with soil and environmental conditions, greenhouse gas (GHG) emissions, specifically those of carbon dioxide (CO_2) nitrous oxide (N_2O) and methane (CH_4) [1]. These GHGs have the potential to impact ozone chemistry (N_2O) and atmospheric oxidation status (CO_2) [2]. The concern about increasing N_2O emissions is related to its global warming potential, which is 265–298 times that of CO_2 for a 100-year time horizon [3]. Furthermore, N_2O is also considered the major stratospheric ozone-depleting substance. Agricultural practices, such as N amendment and fertilization, legume cropping, residue retention, and irrigation, tend to increase N_2O production and emission above background levels and contribute to indirect reactive nitrogen volatilization and nitrate leaching [4].

Soil N_2O emissions are influenced by the soil characteristics that affect primary processes that are indirectly or directly responsible for the emissions themselves: mineralization (indirectly), nitrification, and denitrification. Organic nitrogen, contained in crop residues and manure, is decomposed and mineralized by the soil microbial communities, resulting in the production of ammonium (NH_4^+) [5]. During nitrification, which is

operated by nitrifying bacteria and involves the oxidation of ammonium to nitrate (NO_3^-) by key enzymes (e.g., ammonia monooxygenase, hydroxylamine dehydrogenase, nitric oxide oxidase, nitrite oxidoreductase) [6], a small proportion of N is lost as N_2O. In contrast, denitrification, conducted by denitrifying bacteria, involves the reduction of nitrate and nitrite to gaseous N_2 and N_2O [7], respectively, by nitrate and nitrite reductases [8]. Nitrification mainly occurs in well-aerated soils with moderate water content, while denitrification takes place in anaerobic conditions, mainly found in heavy soil with scarce drainage. The contribution of each process to N_2O emissions is controlled and limited by soil biogeochemical characteristics (soil texture, pH, temperature, moisture, oxygen accessibility, and microbial activity), environmental conditions, and the type and amount of applied N fertilizer [9]. Finer-textured soils tend to release higher amounts of N_2O compared to sandy soils [10]. This phenomenon can be attributed to the presence of predominant capillary pores in finer-textured soils, which retain water more effectively and create favorable conditions for N_2O emissions from denitrification [11,12]. Soil temperature is another key element that impacts N_2O emissions. An increase in soil temperature positively affects microbial growth but also reduces oxygen concentration, leading to an increase in anaerobic conditions [13,14]. Moreover, it was found that the N_2/N_2O ratio increased exponentially with the increasing temperature [15]. Soil acidity influences the N_2/N_2O ratio, too, but its effect on the nitrification and denitrification process needs further investigation [16].

Direct applications of N synthetic fertilizers increase the available pool for N cycle transformations [17]. As previous research reported [18], the time of fertilizer application influences the efficiency of fertilizer use and crop yield. When mineral fertilizer or manure is applied at rates greater than the effective crop need, N_2O emission can increase because of the large pool of soil N that cannot be assimilated by the crop and remains available for the biological transformations involved in N_2O production. Furthermore, N_2O emissions can be enhanced due to rainfall events that increase soil moisture [19,20]. Several strategies have been developed to reduce the amount of N available for soil microorganisms, thereby decreasing nitrification and denitrification rates [21], by reducing nitrogen fertilizer inputs and applying them precisely and strategically so that nitrogen supply becomes synchronized with a specific crop demand. Also, to increase the N efficiency and delay detrimental processes, the use of urease and nitrification inhibitors is recommended [16]. This alignment minimizes the portion of N in the soil and its potential losses through volatilization of NH_3, NO_3^- leaching, and N_2O emission [22].

Quantifying N_2O emissions from agricultural soils has always been challenging due to the significant spatial and temporal variations observed in this condition during field trials [23,24]. Several replications or integrations over a larger area are generally applied to capture the spatial variability at the field level, resulting from biological, chemical, and physical conditions of the soil [25]. Temporal variability in this context is assessed through several factors including measurement frequency, emission-related events timing, and the specific time of day when measurements are conducted [26–28].

In most research studies, direct N_2O flux measurements during field trials are conducted using either manual or automated chambers in combination with a gas chromatograph or infrared analyzer [29]. These measurement techniques are conducted at relatively small spatial domains, mostly plot scales, and are suitable to capture topographic and treatment effects on N_2O emissions [30]. They are cost effective and labor intensive but might effectively address the challenge of spatial variability on reported fluxes within the studied plot [31]. Automated chambers have the advantage of allowing frequent measurements of N_2O soil flux since this methodology is less time consuming and dependent on human intervention. They require less data gap filling than manual chambers, which are very manpower demanding [27]. Continuous measurements of N_2O fluxes at fine temporal scales (ranging from minutes to hours) are possible with the use of micrometeorological techniques [32,33] that are non-intrusive and suitable to overcome the inherent spatial variability in the process of soil N_2O emission while providing reliable and accurate high-

frequency measurements of turbulent fluxes of GHGs. The most adopted approach by international ecological station networks (https://fluxnet.org/, accessed on 16 November 2023) is eddy covariance [34], a well-established method relying on fast-response sonic anemometers and spectrometers. Its use is widespread at larger spatial (between 100 m and several kilometers) and temporal scales (from hours to years) [35].

The abovementioned advancements in measurement techniques have unveiled a clear diurnal pattern in N_2O fluxes. This pattern, as observed in previous studies [36,37], implies that daily temperature variations and interactions between plants, soil microbial activities, and water content play significant roles in governing daily N_2O fluxes. Consequently, neglecting these diurnal variations could result in errors when estimating N_2O emissions. Chambers remain a valuable tool for measuring the impacts of soils, climate, and management on N_2O emissions from a range of sources. However, for pragmatic reasons, observational study periods usually cover only a few years under a narrow range of conditions and are often not continuous over that time [38]. In parallel, researchers use incubation experiments to gain a deeper understanding of nitrogen dynamics [39]. During these experiments, soil samples are analyzed under controlled conditions to assess the impact of factors such as soil moisture, texture, temperature, and various fertilization treatments on gas emissions [40]. The experiments conducted under incubation offer advantages in terms of experimental control and economic viability, but they may present some limitations, as the direct measure, in representing the real conditions of soil and agricultural environment [41]. Scale and representativeness restrictions are due to the typical small-scale trial conditions and difficulty in addressing real-world variability. Furthermore, the timeframe is commonly short and, therefore, not adequate to capture long-term trends and is not suitable for ex ante assessment [42].

To address the challenge of scaling up from an agricultural field to a regional level, improve accuracy and reproducibility, and estimate N losses associated with agricultural scenarios, various estimations' methodologies and models have been devised, spanning from straightforward regression models to fully process-based ones [43]. Commonly, the choice between one of the various estimation and modeling approaches is related to the rationale of each study and the researcher's level of familiarity with the available models, the agricultural system involved, and data requirements and availability [44]. The IPCC Guidelines for National Greenhouse Gas Inventories proposed a simplified estimation methodology that relates estimates of direct N_2O emissions from agricultural land to the quantities of nutrient N being applied [45,46]. This relation is defined by the emission factor, calculated for each type of input addition (mineral N fertilizer, organic manure, crop residue, and others) [46].

The models can either be empirical, derived from observed statistical or mathematical relationships, or process-based, developed to emulate the underlying process mechanisms [38]. Models of both types are also suitable to test hypotheses regarding biogeochemical process drivers and can be used to analyze the results of laboratory and field experiments [11]. While empirical approaches are limited to summarizing experimental data, process-based models mathematically represent one or several processes characterizing the functioning of well-delimited biological systems of fundamental or economic interest [47].

Process-based dynamic models simulate, at fine spatial and temporal scales, N_2O emissions by explicitly modeling the underlying biogeochemical processes that produce N_2O in soils and ecosystems, as influenced by pedoclimatic conditions and management practices. Data demand, which represents a common limitation [48,49], includes inputs such as soil properties, meteorological data, and cropping systems management practices, in addition to experimental observations required for model calibration and evaluation. Also, they often need site-specific information for accurate modeling [50–52]. The main advantage of using detailed input is the possibility of simulating daily soil conditions (soil temperature, soil water content, bulk density) and daily crop management (sowing and harvest, fertilization, irrigation, tillage). Indeed, process-based models' time step is

frequently 1 day, sometimes 1 h for submodels, which is appropriate to overcome the biogeochemical variation of agricultural systems that directly influence, as we reported above, the nitrification and denitrification processes. Another advantage of using detailed input data is the possibility of dividing the soil into discrete layers to describe management operations more finely (depth of soil tillage operation, fertilizer application, and crop residue burial). When differences in results arise from the application of simulation models, they can frequently be attributed to a lack of input data, to input data uncertainty, or to the inadequate resolution of biogeochemical processes. In these situations, model improvements in terms of algorithms and structure are recommended.

The aim of this work is to review and compare N_2O simulation approaches, with a major focus on dynamic process-based simulation models that provide a whole cropping system representation. A recently published and comprehensive review providing insights on the algorithms employed in the simulation of the N fluxes, particularly N_2O, is lacking. This work focuses on algorithm details reported for the selected models with a unified symbol system and is aimed at facilitating modeling approach comparisons and supporting algorithm implementation for further practical applications. In previous studies [53–55], process-based simulation approaches were successfully reviewed with, respectively, a major focus on model application scale (laboratory, field, and regional scale); model structure, strengths, and weaknesses; and emissions drivers representation (in three selected models). Comparing enforced algorithms for nitrification, denitrification, and GHG emissions provides an insightful tool for the analysis of the biogeochemical interactions concurring with N_2O emissions, thus allowing the evaluation of cropping system management practices' impacts on these processes. A comparative overview of the performances of the selected models, based on common evaluation criteria as reported by authors, is also provided.

2. Materials and Methods

2.1. Literature Search Details

The objective of the present literature search was to review the main available modeling approaches for N_2O emissions simulation. Since only process-based models offer a detailed mechanistic understanding of the underlying processes responsible for N_2O emissions, the study remained focused on this type of approach while the other modeling methodologies are summarized in the Supplementary Materials. We constrained the study to the process-based models simulating nitrous oxide emissions in a cropping system environment, where such losses are of particular concern. The analysis was restricted to process-based models for which detailed documentation of algorithms was available, preferably in recently published scientific articles or in published source codes. Models who took part in international model comparison exercises or model ensemble projects were also preferred. The selection of the models was carried out based on (i) the availability of recently published and highly cited/used materials and (ii) the inclusion of the mathematical description/algorithms/mathematical functions of the system processes considered in each model for simulating N_2O. Among the process-based models emerging from the literature analysis, we specifically looked for those explicitly considering both nitrification and denitrification as contributors to N_2O emissions.

For each model, we reported the mathematical equations used to describe the key physiological process involved in N_2O emissions simulation. Concurrently, we also reviewed published materials relative to models' application and evaluation for cropping system N_2O emissions simulation performance.

The literature search was conducted both on Scopus and Web of Science databases through the implementation of the following query:

(TITLE-ABS-KEY (model OR modeling OR simulate OR simulating OR simulation OR estimation OR estimate OR approach) AND ALL (N_2O OR nitrous AND oxide OR greenhouse AND gasses OR emission) AND TITLE-ABS-KEY (crop OR cropland AND soil OR agricultural AND environment) AND TITLE-ABS-KEY (flux OR fluxes OR emission)

As a result, we collected 439 papers on Scopus and 947 papers on the Web of Science. Another specific query has also been settled to identify scientific works where each model has been assessed considering its capability to simulate N_2O emissions in comparison to experimentally observed data. For this purpose, we added the terms (calibrate OR validation OR evaluation OR assessment) to the first query, and we obtained 134 papers in Scopus and 281 in Web of Science. From the results of both queries, redundant titles were removed, the topic was restricted to a model with a field scale approach and a daily timestep, and the abovementioned criteria were applied. Consequently, we selected 57 papers.

2.2. Overview of the Selected Models

The following process-based models (Table 1) were the result of the abovementioned selection activity. ARMOSA—Analysis of cRopping systems for Management Optimization and Sustainable Agriculture [56], APSIM—The Agricultural Production Systems sIMulator [57], CERES-EGC—Crop Environment REsource Synthesis—Environnement et Grandes Cultures [58], CROPSYST—Cropping Systems simulation model [59], and STICS—Simulateur mulTIdisciplinaire pour les Cultures Standard [60] are five dynamic models whose primary purpose is to operate as analytical tools aimed at the impact evaluation of cropping system management on both crop production and environment. They are able to simulate a range of critical processes such as crop growth, soil C and N dynamics, and soil and water management, including nitrogen transformation like net mineralization, nitrification, and denitrification processes.

DSSAT—Decision Support System For Agrotechnology Transfer [61] has been designed to address several application contexts such as genetic modeling, on-farm and precision management, and regional environmental assessments; thus, it supports a range of utilities comprising weather, soil, and genetics tools.

EPIC—Environmental Policy Integrated Climate model [62] is an agricultural dynamic model primarily developed to address the effect of soil erosion on crop productivity.

DNDC—DeNitrification-DeComposition [52,63] and DAYCENT—DAYly CENTury [64] are specially designed to simulate nitrogen and carbon fluxes, considering soil, crop, and water dynamics. CoupModel—Coupled heat and mass transfer model for soil–plant–atmosphere systems [65] was also designed to simulate water and heat fluxes; it has later adopted high-level submodules of nitrification, denitrification, and gas transport from DNDC [52]. Both feature a detailed microbial approach to trace gas emissions forms (e.g., N_2O, NO, N_2, NH_3, CH_4, and CO_2).

SPACSYS [66] is a process-based model simulating water, C, and N cycling between plants, soils, and microbes. It has been widely used to assess the impact of climate change tillage, fertilizer application, and different cultivars on agricultural systems in terms of crop yields, C and N budgets, soil physical properties, and soil water redistribution.

2.3. Statistical Indices for Model Evaluation

When reporting the application areas of the selected models, the evaluation criteria used by the authors and published in the articles were also included in this review. These evaluation indices were derived from experiments conducted for model validation and/or calibration. Typical statistical indices (Appendix A.1, Appendix A) for performance evaluations in modeling applications include Pearson's correlation coefficient (r), coefficient of determination (R^2), root mean squared error ($RMSE$), relative root mean squared error ($RRMSE$), and modeling efficiency (EF). These metrics describe the error associated with model estimates ($RMSE$), the total variation in observations captured by simulated data (R^2), and whether the model outperforms a mean observation in the prediction of observed data (EF). When present, the other indexes have also been organized and reported in Appendix A (Appendix A.3, Table A9).

Table 1. Reviewed model overview. Nitrification simulation (Nit), denitrification simulation (Denit), microbial biomass explicit simulation, environmental factors considered: soil temperature ($f(T)$), soil moisture ($f(W)$), soil acidity ($f(pH)$), and substrate (other than ammonium and nitrate) concentration effect ($f(substrate)$).

Reference	Author	Year	Model	Nit	Denit	Microbial Biomass	$f(T)$	$f(W)$	$f(pH)$	$f(substrate)$
[67]	Thorburn et al.	2010	APSIM	yes	yes	no	yes	yes	only for Nit	active carbon only for Denit
[56]	Perego et al.	2013	ARMOSA	yes	yes	no	yes	yes	only for Nit	-
[58]	Gabrielle et al.	2005	CERES-EGC	yes	yes	no	yes	yes	no	-
[68]	Jansson and Karlberg	2010	CoupModel	yes	yes	optional for both Nit and Denit	yes	yes	yes	DOC for Nit in the microbial explicit approach
[69]	Stockle et al.	2012	CROPSYST	yes	yes	only for SOC mineralization	only for Nit	yes	only for Nit	CO_2 for Denit
[11]	Parton et al.	2001	DAYCENT	yes	yes	no	only for Nit	yes	only for Nit	CO_2 for Denit
[52]	Li	2000	DNDC	yes	yes	yes	yes	only for Nit	yes (indirectly for Nit)	indirectly DOC for both
[70]	Hoogenboom et al.	2019	DSSAT	yes	yes	no	only for CERES-Denit and Nit	yes	only for Nit	CO_2 for DAYCENT-Denit, water-extractable C for CERES-Denit
[62]	Sharpley and Williams	1990	EPIC	yes	yes	no	yes	yes	only for Nit	CO_2 for Denit (Kemanian option)
[71]	Wu et al.	2015	SPACSYS	yes	yes	optional for both Nit and Denit	yes	only for Nit	yes	DOC for Nit and Denit
[60]	Brisson et al.	2008	STICS	yes	yes	no	yes	yes	only for Nit	-

3. Results

These sections report the main approaches for nitrous oxide simulation, with a major focus on process-based models. The other concurrent alternative approaches for the prediction and estimate of soil N_2O releases—such as IPCC approaches, statistical models, meta-models, and whole farm models—are reported in the Supplementary Material.

3.1. Process-Based Models

All the processes described are simulated for selected discrete soil layers at each time step unless otherwise specified. All the state and auxiliary variable values employed in the formulas correspond to the current time step value unless otherwise specified. In the following paragraphs, parameters are presented with their definition, symbol, unit of measure, and default value (when available). In this review, all variables and parameters are associated with a common symbol for all the models. The model-specific original symbols of variables (Appendix A.3, Tables A1, A3, A5 and A7) and parameters (Appendix A.3, Tables A2, A4, A6 and A8) are reported in Appendix A.

3.1.1. Nitrification

Approaches Based on Implicit Microbial Pools

In **APSIM** [67], the potential nitrification rate (R_{nit}, mg N g^{-1} soil d^{-1}, Equation (1)) follows a Michaelis–Menten kinetics [72] and employs two parameters: the maximum reaction velocity (V_{max}, mg N g^{-1} soil d^{-1}, 40), and the ammonium concentration ([NH_4]) to obtain half of V_{max} (K_m, mg N g^{-1} soil, 90). The nitrification rate is obtained by limiting the potential rate with the response function to soil acidity, soil moisture, and temperature.

$$R_{nit} = \frac{V_{max} \cdot [NH_4]}{K_m + [NH_4]} \cdot min[f(T),\ f(W),\ f(pH)] \quad (1)$$

In the **ARMOSA** [56] and **CROPSYST** [69,73] models, the nitrification rate (R_{nit}, kg N ha^{-1} d^{-1}, Equation (2)) is simulated using the SOILN approach [74,75]. A daily nitrification coefficient (k_{nit}, d^{-1}, 0.2) is employed, together with the nitrate–ammonium ratio for nitrification ($r_{NO3/NH4}$, unitless, 8, from 1 to 15 in agricultural soils). **ARMOSA** also employs a multiplicative aerobic factor ($f_n(OX)$, unitless) that simulates the effect of tillage operations within 45 days of the first application. After this period, or if meanwhile 100 mm of rain has fallen, the factor is no longer considered in the rate estimate.

$$R_{nit} = k_{nit} \cdot \left(\frac{N_{NH4} - N_{NO3}}{r_{NO3/NH4}} \right) \cdot f_n(T) \cdot f_n(W) \cdot f_n(pH) \quad (2)$$

In **CERES-EGC** [76], the nitrification rate (R_{nit}, kg N ha^{-1} d^{-1}, Equation (3)) is obtained by limiting the maximum nitrification rate (k_{nit}, kg N ha^{-1} d^{-1}), representing the site-specific nitrification rate at 20 °C, with three unitless response functions to soil ammonium concentration, water-filled pore space, and temperature.

$$R_{nit} = k_{nit} \cdot f_n(T) \cdot f_n(W) \cdot f_n(NH_4) \quad (3)$$

In **CoupModel** [68], the nitrification rate (R_{nit}, g N m^{-2} d^{-1}, Equation (4)) can be estimated with a simplified approach or with an explicit microbial biomass approach (Equation (10)). In the simplified approach, the nitrification rate (R_{nit}, g N m^{-2} d^{-1}) depends on a soil acidity coefficient (k_{pH}, unitless, 1), which is limited by the response functions to soil temperature, water-filled pore space, ammonium, and nitrate concentrations.

$$R_{nit} = f(T) \cdot f_n(W) \cdot f_n(NH_4, NO_3) \cdot k_{pH} \quad (4)$$

In **DAYCENT** [11] version 4.7, the nitrification rate (R_{nit}, g N m^{-2} d^{-1}, Equation (5)) consists of a fraction of the daily net mineralization from the SOM submodel (Net_{mm},

g N m^{-2}), which is assumed to be nitrified each day (K_{nit2}, d^{-1}, 0.2), and in a maximum nitrified fraction (K_{nit}, d^{-1}, 0.1) of the soil ammonium concentration (NH_4, g N m^{-2}).

$$R_{nit} = Net_{mm} \cdot k_{nit2} + k_{nit} \cdot NH_4 \cdot f_n(T) \cdot f_n(W) \cdot f_n(pH) \quad (5)$$

In **DSSAT** [70] V4.8.2.0 [77], the nitrification rate (R_{nit}, kg N ha^{-1} d^{-1}, Equation (6)) is limited through response functions to soil temperature, moisture, and acidity, which range between 0 and 1, and it is further reduced in the presence of a nitrification inhibitor compound.

$$R_{nit} = NH_4 \cdot [f_{n1}(T) \cdot f_n(W) + f_n(pH) + f_{n2}(T)] \quad (6)$$

In **EPIC** [62] version 1102 [78], the nitrification rate (R_{nit}, kg N ha^{-1} d^{-1}, Equation (7)) is simulated as depending on the ammonium availability, net of nitrogen volatilization (R_{vol}, kg N ha^{-1} d^{-1}). The response function of nitrification to soil moisture is based on soil water content ($f_1(W)$), and it is also employed in the denitrification estimate. The auxiliary variable ($AKAV$, unitless) estimate depends on the considered layer: for the first layer, it depends on soil temperature and wind speed; for the deeper layers, it depends on temperature and a cationic exchange capacity factor. The parameter employed (k_{nit3}, unitless, between 0 and 1) represents the upper limit of nitrification—volatilization as a fraction of the present ammonium.

$$R_{nit} = min\left\{k_{nit3},\ 1 - e^{-[AKAV + (f_n(T) \cdot f_1(W) \cdot f_n(pH))]}\right\} \cdot NH_4 - R_{vol} \quad (7)$$

In **the SPACSYS** model [66], the nitrification rate (R_{nit}, g N m^{-2} d^{-1}, Equation (8)) in the implicit microbial biomass approach depends on the maximum rate of nitrification (k_{nit}, d^{-1}) parameters, which is limited by the response functions to soil temperature, water-filled pore space, and ammonium and nitrate concentration.

$$R_{nit} = k_{nit} \cdot f(T) \cdot f_n(W) \cdot f_n(NH_4, NO_3) \quad (8)$$

In **STICS** [60], nitrification occurs only in the biologically active soil layer, which is constrained by a maximum depth parameter (z_{nit}, cm, 30). The nitrification rate in each layer (R_{nit}, kg N ha^{-1} cm^{-1}, Equation (9)) depends on the daily maximum fraction of ammonium converted in nitrate (k_{nit}, d^{-1}) and on the ratio between N_2O emissions and total nitrification ($r_{N2O/nit}$, unitless). The total nitrification is obtained as the sum of each layer's nitrification rate above the maximum depth.

$$R_{nit} = (1 - r_{N2O/nit}) \cdot k_{nit} \cdot NH_4 \cdot f_n(T) \cdot f_n(W) \cdot f_n(pH) \quad (9)$$

Approaches Based on Explicit Microbial Pools

In **CoupModel** [68], when nitrifying microbials are explicitly taken into account, the nitrification rate (R_{nit}, g N m^{-2} d^{-1}, Equation (10)) is directly proportional to a rate coefficient (k_{nit}, mg ha d^{-1} kg^{-1}, 0.25) and to the nitrifiers microbial biomass (B_{nit}, g m^{-2}), limited by the response functions to environmental factors and to ammonium solute concentration.

$$R_{nit} = k_{nit} \cdot f(T) \cdot f_n(W) \cdot f_n(NH_4) \cdot k_{pH} \cdot B_{nit} \quad (10)$$

In **DNDC** model version 9.5 [79], the nitrification rate (R_{nit}, kg N ha^{-1} d^{-1}, Equation (11)) is calculated on the base of a nitrification coefficient (k_{nit}, d^{-1}, 0.005), the ammonium amount (kg N ha^{-1}), the soil acidity (pH, unitless), and the nitrifiers biomass (B_{nit}, kg C ha^{-1}).

$$R_{nit} = k_{nit} \cdot NH_4 \cdot B_{nit} \cdot pH \quad (11)$$

For the explicit microbial pools approach of the **SPACSYS** model [71], the nitrification rate (R_{nit}, g N m^{-2} d^{-1}, Equation (12)) depends on the nitrifier biomass (B_{nit}, g C m^{-2}) and on the maximum rate of nitrification (k_{nit}, d^{-1}, 0.004) parameters, which is limited

by the response functions to soil temperature, water-filled pore space, soil acidity, and ammonium concentration.

$$R_{nit} = k_{nit} \cdot f(T) \cdot f(W) \cdot f_n(pH) \cdot f_n(NH_4) \cdot B_{nit} \quad (12)$$

3.1.2. Denitrification

Approaches Based on Implicit Microbial Pools

In the **APSIM** model [67], the denitrification rate (R_{denit}, kg N ha^{-1} d^{-1}, Equation (13)) is simulated as a fraction (k_{denit}, unitless, 0.0006) of the nitrate (kg N ha^{-1}) amount, limited by active carbon concentration ([C_A], ppm, Appendix A.2, Appendix A) and soil temperature moisture response functions.

$$R_{denit} = k_{denit} \cdot NO_3 \cdot [C_A] \cdot f_d(T) \cdot f_d(W) \quad (13)$$

In **ARMOSA** [56], the denitrification rate (R_{denit}, kg N ha^{-1} d^{-1}, Equation (14)) is simulated using SOILN approach [75]: a daily denitrification rate (k_{denit}, kg N ha^{-1} d^{-1}, 0.04, between 0.04 and 0.2) is employed, together with a denitrification half-saturation constant (K_m, mg N L^{-1}, 10, between 5 and 15) defining the nitrate concentration ([NO_3], kg N L^{-1}) at which denitrification activity is half of the activity at optimum nitrate concentration.

$$R_{denit} = k_{denit} \cdot \frac{[NO_3]}{[NO_3] + \frac{K_m}{10^6}} \cdot f(T) \cdot f_d(W) \quad (14)$$

In **CERES-EGC** [76], the denitrification rate (R_{denit}, kg N ha^{-1} d^{-1}, Equation (15)) is obtained by limiting the potential rate (k_{denit}, kg N ha^{-1} d^{-1}), representing the site-specific denitrification rate at 20 °C, with three unitless response functions to soil nitrate concentration, water-filled pore space, and temperature.

$$R_{denit} = k_{denit} \cdot f_d(T) \cdot f_d(W) \cdot f_d(NO_3) \quad (15)$$

In **CoupModel** [68], the denitrification rate (R_{denit}, g N m^{-2} d^{-1}) is either not accounted for (denitrification not simulated), or it can be calculated with a simplified approach (where the rate depends on response functions for soil temperature, soil moisture, and nitrate concentration in the soil with denitrifying microorganisms not explicitly simulated, Equation (16)) or with an explicit denitrifying microorganisms biomass approach (Equation (25)). The denitrification rate, when simulated, can be differentiated through the soil profile: it can be evenly distributed (constant), or it can decrease linearly or exponentially with the depth of the soil layer (Δz). A factor (z_{adj}, unitless) adjusts the potential denitrification rate parameter (k_{denit}, g N m^{-2} d^{-1}, 0.04) for each soil layer.

$$R_{denit} = k_{denit} \cdot f(T) \cdot f_d(W) \cdot f_d(NO_3) \cdot z_{adj}(\Delta z) \quad (16)$$

In the **CROPSYST** model [59,69,73], the actual denitrification rate (R_{denit}, kg N ha^{-1} d^{-1}, Equation (17)) is obtained by limiting a potential denitrification rate (k_{denit}, kg N ha^{-1} d^{-1}) with environmental factors response functions [80] to soil nitrate, soil heterotrophic respiration, and water content.

$$R_{denit} = k_{denit} \cdot min[f_d(NO_3), f_d(CO_2)] \cdot f_d(W) \quad (17)$$

In **DAYCENT** model 4.7 [11], the total N flux (R_{denit}, µg N g soil^{-1} d^{-1}, Equation (18)) from denitrification [81] is obtained using a response function to nitrate level ($f_d(NO_3)$, µg N g soil^{-1} d^{-1}) and a response function to heterotrophic respiration ($f_d(CO_2)$, µg N g soil^{-1} d^{-1}), which surrogates labile C availability, together with a response function to *WFPS* ($f_d(W)$, unitless), which surrogates O_2 soil status.

$$R_{denit} = min[f_d(NO_3), f_d(CO_2)] \cdot f_d(W) \quad (18)$$

In **DSSAT** model [70] V4.8.2.0 [77], the denitrification of NO_3 to N_2O and N_2 gases can be simulated using the DAYCENT or CERES denitrification subroutine. In the DAYCENT subroutine, the NO_3 denitrification rate (R_{denit}, kg N ha^{-1} d^{-1}, Equation (19)) is derived from the DAYCENT model [81]. The denitrification rate is calculated for each soil layer and is accelerated for the soil layer whose depth (z, m) comprises 0 and the parameter z_{denit} (m, 0.3 default).

$$R_{denit} = \begin{cases} f_d(W) \cdot min[f_d(NO_3), f_d(CO_2)] & if\ z > z_{denit} \\ f_d(W) \cdot max\{min[f_d(NO_3), f_d(CO_2)],\ 0.066\} & if\ z < z_{denit} \end{cases} \quad (19)$$

In the CERES denitrification subroutine, denitrification only occurs when nitrate is present (NO_3 > 0.01 kg N ha^{-1}), the soil water content (SWC, m^3 m^{-3}) is higher than the drained upper limit (DUL, m^3 m^{-3}), and the soil temperature (T, K) is higher than 5. The denitrification rate (R_{denit}, kg N ha^{-1} d^{-1}, Equation (20)) depends on a denitrification coefficient (k_{denit}, d^{-1}, 0.0006), water-extractable soil carbon (C_W), nitrate content, and water and temperature response functions.

$$R_{denit} = k_{denit} \cdot NO3 \cdot C_W \cdot f_d(W) \cdot f_d(T) \quad (20)$$

In **EPIC** model v. 1102 [62], three methods for the denitrification routine can be selected from the control file: IMWJ [82], Armen Kemanian denitrification method, and the original EPIC denitrification method [78]. The IMWJ (Izaurralde, McGill, Williams, and Jones) denitrification option (not reported) calculates the total number of electrons released by C oxidation and accepted by O_2 and oxides of N (NO_3^-, NO_2^- and N_2O) during an hour for a given layer. The movement of N_2O through the soil profile and of N_2O and N_2 through the liquid phase are also simulated. In the Armen Kemanian denitrification method, the denitrification rate (R_{denit}, kg N ha^{-1} d^{-1}, Equation (21)) is estimated by considering a parameter (k_{denit}, unitless, 32), the soil layer weight (WT), and the response functions to nitrate content, soil moisture, and respiration level.

$$R_{denit} = f_d(NO_3) \cdot f_d(W) \cdot f_d(CO_2) \cdot k_{denit} \cdot WT \cdot 10^{-3} \quad (21)$$

In the original EPIC denitrification method, the denitrification rate (R_{denit}, kg N ha^{-1} d^{-1}, Equation (22)) employs a soil temperature factor, and two soil moisture factors ($f_1(W)$, also employed in the nitrification subroutine, and $f_d(W)$ also employed in Equation (21)).

$$R_{denit} = NO_3 \cdot \sqrt{f_d(T) \cdot f_1(W)} \cdot f_d(W) \quad (22)$$

In the implicit microbial biomass approach of the **SPACSYS** model [66], the denitrification rate (R_{denit}, g N m^{-2} d^{-1}, Equation (23)) depends on the maximum rate of denitrification (k_{denit}, g N m^{-2} d^{-1}) parameter, which is limited by the response functions to soil temperature, water-filled pore space, and nitrate concentration.

$$R_{denit} = k_{denit} \cdot f(T) \cdot f_d(W) \cdot f_d(NO_3) \quad (23)$$

In the **STICS** model [60], the daily denitrification rate (R_{denit}, kg N ha^{-1} d^{-1}, Equation (24)) is simulated with the approach of [83] only for a denitrifying soil layer (z_{denit}, cm, 20). A potential denitrification rate (k_{denit}, kg N ha^{-1} d^{-1}, 16) is limited by the nitrate content, soil temperature, and moisture response functions.

$$R_{denit} = \frac{k_{denit}}{z_{denit}} \cdot f_d(T) \cdot f_d(NO_3) \cdot f_d(W) \quad (24)$$

Approaches Based on Explicit Microbial Pools

In **CoupModel** [68], when denitrifying microbes are explicitly considered, the denitrification rate is a function of their biomass (B_{denit}, g C m^{-2}) and of their activity ($M_{activity}$,

g C m^{-2}). In this approach, NO_3 concentration is obtained by dividing the nitrate amount of the z_{th} layer for the soil water content of the layer, while NO_2, NO, and N_2O concentrations ($N_{AnNxOyConc}$, Appendix A) are estimated by also considering the volumetric anaerobic fraction of the layer (f_{Anvol}, auxiliary variable). These concentrations and the corresponding amount (N_{AnNxOy}) in the considered soil layers are employed to define the total denitrification rate (R_{denit}, g N m^{-2} d^{-1}, Equation (25)), as the sum of the nitrogen fluxes ($N_{AnNO2\rightarrow AnNO}$, $N_{AnNO\rightarrow AnN2O}$ and $N_{AnN2O\rightarrow AnN2}$, i.e., out fluxes from anaerobic N pools due to microbial growth and respiration, that consumes all N from all the nitrogen anaerobic pools except for N_2) of the denitrification processes steps. The nitrogen content in the anaerobic NO_3 pool, i.e., soil nitrate ($AnNO_3$, g N m^{-2}), is employed. The equation structure describing the flux between N_{NO3} and $AnNO_2$ is also used for estimating the fluxes between $AnNO_2$ and $AnNO$ and between $AnNO$ and AnN_2O. The equation for growth respiration (N_{rg}) and maintenance respiration (N_{rm}) are reported in Appendix A (Appendix A.2).

$$\begin{aligned} R_{denit} &= N_{AnNO2\rightarrow AnNO} + N_{AnNO\rightarrow AnN2O} + N_{AnN2O\rightarrow AnN2} \\ N_{NO_3\rightarrow AnNO2} &= min\left[AnNO_3,\ \left(N_{rgNO3} + N_{rmNO3}\right)\cdot M_{activity}\cdot B_{denit}\right] \\ N_{AnNO_2\rightarrow AnNO} &= min\left[AnNO_2,\ \left(N_{rgNO2} + N_{rmNO2}\right)\cdot M_{activity}\cdot B_{denit}\right] \\ N_{AnNO\rightarrow AN2O} &= min\left[AnNO,\ \left(N_{rgNO} + N_{rmNO}\right)\cdot M_{activity}\cdot B_{denit}\right] \\ N_{AnN_2O\rightarrow AnN_2} &= min\left[AnN_2O,\ \left(N_{rgN2O} + N_{rmN2O}\right)\cdot f_d(NO_3)\cdot M_{activity}\cdot B_{denit}\right] \end{aligned} \quad (25)$$

In **DNDC** model version 9.5 [79], the consumption rate of N_xO_y through denitrification ($R_{c,NxOy}$, kg N ha^{-1} d^{-1}, Equation (26)) depends on the growth rate of each denitrifier group (u_{NxOy}), the denitrifiers maximum growth yield on the corresponding substrate (Y_{NxOy}, kg C kg N^{-1}), the maintenance coefficient on the corresponding substrate (M_{NxOy}, kg N kg^{-1} h^{-1}), the denitrifier biomass (B_{denit}, kg N ha^{-1}), the total N oxides amount (sum of NO_3^-, NO_2^-, NO, and N_2O; $\sum N_xO_y$, kg N ha^{-1}). Furthermore, in the DNDC model, the soil aeration status intended as a redox potential (oxygen or other oxidants content in the soil profile) is simulated. Then, the soil in each layer is divided into aerobic and anaerobic parts where nitrification and denitrification occur, respectively. When the anaerobic parts increase, more substrates (DOC, ammonium, and N oxides) are allocated to the anaerobic microsites to intensify denitrification. When the anaerobic parts decrease, nitrification will be increased due to the reallocation of the substrates into the aerobic microsites.

$$R_{c,NxOy} = \left(\frac{u_{NxOy}}{Y_{NxOy}} + \frac{M_{NxOy}\cdot N_xO_y}{\sum N_xO_y}\right)\cdot B_{denit}\cdot f_{d,NxOy}(pH)\cdot f_d(T) \quad (26)$$

In the explicit microbial biomass approach of the **SPACSYS** model [71], the consumption rate ($R_{c,NxOy}$, kg N m^{-3} d^{-1}, Equation (26)) of each N oxide (NO_3^-, NO_2^-, NO, N_2O) depends on two parameters: the maintenance coefficient on each N oxides (M_{NxOy}; g C g^{-1} N d^{-1}, Table A8), and the maximum growth yield on each N oxides (Y_{NxOy}, g C g^{-1} N, Table A8). The concentration of each N oxides ($[N_xO_y]$, kg N m^{-3}) and of all N oxides ($\sum[N_xO_y]$, kg N m^{-3}), together with the growth rate of the N_xO_y denitrifiers ($R_{g,NxOy}$, kg C m^{-3} d^{-1}) and their total biomass (B_{denit}, g C m^{-2}) are used. The difference from the DNDC model consists in the use of the same soil temperature response function structures for both nitrification and denitrification.

3.1.3. Emissions

In **APSIM** [67], ARMOSA [56], **DAYCENT** [11] version 4.7, **DNDC** version 9.5 [79], and **DSSAT** model [70] V4.8.2.0 [77], the N_2O emissions rate during nitrification (N_2O_{nit}, kg N ha^{-1} d^{-1}, Equation (27)) is estimated as a fraction ($r_{N2O/nit}$, unitless, Table A6) of the nitrified N (R_{nit}, kg N ha^{-1} d^{-1}).

$$N_2O_{nit} = r_{N2O/nit}\cdot R_{nit} \quad (27)$$

In the **APSIM** model, N_2O emissions during denitrification (N_2O_{denit}, kg N ha^{-1} d^{-1}, Equation (28)) are obtained using the N_2/N_2O ratio reported by [81], the heterotrophic CO_2 respiration rate ($CO_{2,resp}$, µg C g soil^{-1} d^{-1}), the *WFPS* and a parameter related to gas diffusivity in the soil at field capacity (g_{diff}, unitless, 25.1). The soil nitrate concentration considered is the one on a dry weight basis ([NO_3], µg N g^{-1}). In the **ARMOSA** model, N_2O emissions due to denitrification (N_2O_{denit}, kg N ha^{-1} d^{-1}) are also simulated with a modified APSIM approach by applying the N_2/N_2O ratio to the denitrification rate. In Equation (28), the ratio between soil water content (*SWC*, m^3 m^{-3}) and saturation soil water content (SWC_{sat}, m^3 m^{-3}) substitutes the *WFPS*.

$$\frac{N_2}{N_2O_{denit}} = max\left[0.16 \cdot g_{diff},\quad k_1 \cdot e^{\left(\frac{-0.8 \cdot [NO_3]}{CO_{2,resp}}\right)}\right] \cdot max[0.1,\ ((1.5 \cdot WFPS) - 0.32)] \tag{28}$$

In **CERES-EGC** [76], N_2O emissions (kg N ha^{-1} d^{-1}, Equation (29)) from both nitrification and denitrification are simulated by employing site-specific parameters representing the fraction of denitrified N ($r_{N2O/denit}$, unitless) and of nitrified N ($r_{N2O/nit}$, unitless) emitted as nitrous dioxide.

$$N_2O = r_{N2O/nit} \cdot R_{nit} + r_{N2O/denit} \cdot R_{denit} \tag{29}$$

In **CoupModel** [68], N_2O and NO emissions (N_2O_{nit} and NO_{nit}, Equation (30)) from nitrification can be simulated using the simplified approach or the microbial biomass explicit one for nitrification rate simulation, while the emissions deriving from denitrification require the explicit simulation of the denitrifiers microbial biomass. NO and N_2O emissions from denitrification depend on the nitrification rate (R_{nit}), the maximum *NO* ($r_{NO/nit}$, unitless, 0.004) or N_2O ($r_{N2O/nit}$, unitless, 0.0006) fraction parameters, and on the value of the response function for soil moisture, temperature, and acidity (Equations (45), (74), and (77)). The gaseous N forms can be emitted directly into the atmosphere from the layer in which they were formed, or the transportation of the gases through the soil profile can be simulated explicitly. Emissions from denitrification, when transportation of the gases through the soil profile is not considered, correspond to the nitrogen fluxes ($N_{NO2 \rightarrow AnNO}$, $N_{AnNO \rightarrow AnN2O}$, $N_{AnN2O \rightarrow AnN2}$, Equation (25)) estimated for each pool.

$$\begin{aligned} N_2O_{nit} &= r_{N2O/nit} \cdot f_e(W) \cdot f_e(T) \cdot R_{nit} \\ NO_{nit} &= r_{NO/nit} \cdot f_e(W) \cdot f_e(T) \cdot f_e(pH) \cdot R_{nit} \end{aligned} \tag{30}$$

In the **CROPSYST** model [59,69,73], N_2O emissions (µg N kg^{-1} d^{-1}) deriving from nitrification are modeled as a fraction of the nitrification rate (µg N kg^{-1} d^{-1}), obtained through a function of soil moisture and temperature [15].

N_2O emissions from denitrification (N_2O_{denit}, µg N kg^{-1} d^{-1}, Equation (31)) are modeled based on concepts and data from [81] through the application of a N_2/N_2O ratio ($R_{N2/N2O}$, unitless, Equation (31)), which is dependent on soil nitrate ($f_e(NO_3)$, unitless, Equation (99)), heterotrophic respiration ($f_e(CO_2)$, unitless, Equation (100)), and water content ($f_e(W)$, unitless, Equation (72)) response functions, derived from [80].

N_2 emissions from denitrification are obtained by dividing the denitrification rate by the inverse of the N_2/N_2O ratio plus one.

$$\begin{aligned} N_2O_{denit} &= \frac{R_{denit}}{(1+R_{N2/N2O})} \\ R_{N2/N2O} &= min[f_e(NO_3), f_e(CO_2)\ ] \cdot f_e(W) \end{aligned} \tag{31}$$

In **DAYCENT** model [11] version 4.7, N_2O emissions from denitrification are simulated with the approach of [81]. In Equation (32), $f_e(NO_3/CO_2)$ is a unitless function, constrained between 0 and 1, of soil gas diffusivity at field capacity (g_{diff}, unitless), and $f_e(W)$ is a disturbance-specific multiplier (unitless, not limited to 1, Equation (73)) that considers

the effect of soil moisture (*WFPS*, unitless) on N_2/N_2O ratio (the ratio is obtained by multiplying the two functions).

$$N_2O_{denit} = \frac{R_{denit}}{\left\{1 + \left[f_e\left(\frac{NO_3}{CO_2}\right) \cdot f_e(W)\right]\right\}} \quad (32)$$

The $NO_{x,nit+denit}$ (g N ha^{-1} d^{-1}, Equation (33)) emissions from soils are estimated on the base of the simulated N_2O emission flux (N_2O_{denit} and N_2O_{nit}) by means of a NO_x/N_2O ratio ($R_{NOx/N2O}$, unitless, Equation (33)) and of a pulse multiplier (P, unitless) that is employed to take into account pulses in NO_x emissions due to precipitation events.

$$\begin{aligned} NO_{x,\ nit+denit} &= R_{NOx/N2O} \cdot N_2O_{denit} + R_{NOx/N2O} \cdot N_2O_{nit} \cdot P \\ R_{NOx/N2O} &= 15.2 + \frac{\left\{35.5 \cdot atan\left[0.68 \cdot \pi \cdot \left(10 \cdot g_{diff} - 1.86\right)\right]\right\}}{\pi} \end{aligned} \quad (33)$$

In **DNDC** model version 9.5 [79], NO and N_2O produced in either nitrification or denitrification are subject to further transformation during their diffusion through the soil matrix. The emitted fractions of the total N_2O and of the total N_2 evolved in a day from denitrification ($P(N_2O)$ and $P(N_2)$, unitless, Equation (34)), depending on the air-filled fraction of the total porosity (1-*WFPS*, unitless) and on an adsorption factor depending on clay content in the soil ($f_e(AD)$, unitless, [0–2]). In the **SPACSYS** model [71], the emissions rates are derived from the DNDC approach [63].

$$\begin{aligned} P(N_2O) &= [0.0006 + 0.0013 \cdot f_e(AD)] + [0.013 - 0.005 \cdot f_e(AD)] \cdot (1 - WFPS) \\ P(N_2) &= 0.017 + [0.025 - 0.0013 \cdot f_e(AD)] \cdot (1 - WFPS) \end{aligned} \quad (34)$$

In the GHG module of **DSSAT** [70] V4.8.2.0 [77], the N_2O amount produced in any layer and diffused upward is directly proportional to $(1 - WFPS)$, while the N_2O not diffused from the layer ($WFPS$) is added to the next day's total N_2O. NO emissions are estimated through a NO_x/N_2O ratio ($R_{NOx/N2O}$, unitless, Equation (35)) and a NO_x pulse multiplier derived from DAYCENT (P, unitless, calculated on the base of rain and snow). The NO_x/N_2O ratio employs the soil gas diffusivity at field capacity (g_{diff}, unitless, from [81]).

$$NO_{nit} = \left\{8 + \left[\frac{18 \cdot atan\left(0.75 \cdot \pi \cdot \left(10 \cdot g_{diff} - 1.86\right)\right)}{\pi}\right]\right\} \cdot 0.5 \cdot P \cdot N_2O_{nit} \quad (35)$$

N_2O fluxes (N_2O_{denit}, kg N ha^{-1} d^{-1}, Equation (36)) from denitrification are calculated using the same approach [81] both in the DAYCENT denitrification subroutine and in the CERES-EGC denitrification subroutine; the only difference is the equation of an auxiliary variable ($ratio_1$, unitless, Appendix A.2, Appendix A) employed in the estimate of the N_2/N_2O ratio ($R_{N2/N2O}$, unitless). The ratio is modified by considering the number of consecutive days (n_{day}, its maximum used value is 7) during which $WFPS > 0.8$ using an additional auxiliary variable ($ratio_2$, unitless, Appendix A.2, Appendix A). N_2 fluxes ($N_{2,denit}$, kg N ha^{-1} d^{-1}) are obtained by removing N_2O emission from the denitrification rate.

$$\begin{aligned} N_2O_{denit} &= \frac{R_{denit}}{R_{N2/N2O}} \\ R_{N2/N2O} &= max(ratio_1,\ ratio_2) \end{aligned} \quad (36)$$

In **EPIC** model [62] v. 1102 [78], the Armen Kemanian denitrification method simulates N_2O emissions due to denitrification (N_2O_{denit}, kg N ha^{-1} d^{-1}, Equation (37)) as depending on the estimated denitrification rate, the nitrate factor, the water factor, and the respiration factor.

$$N_2O_{denit} = R_{denit} \cdot f_d(NO_3) \cdot \left[1 - \sqrt{f_d(W)}\right] \cdot \left[1 - f_d(CO_2)^{0.25}\right] \quad (37)$$

In the original EPIC denitrification method, N_2 emission due to denitrification (kg N ha^{-1} d^{-1}, Equation (38)) is estimated as a fraction of denitrification using a parameter describing the N_2 fraction partitioning ($r_{N2/denit}$, unitless, between 0.1 and 0.9) while N_2O emissions are complimentary estimated ($N_2O_{,denit}$, kg N ha^{-1} d^{-1}, Equation (38)).

$$N_2O_{denit} = R_{denit} - (r_{N2/denit} \cdot R_{denit}) \quad (38)$$

In the **STICS** model [60], N_2O emissions during nitrification (N_2O_{nit}, kg N ha^{-1} d^{-1}, Equation (39)) are obtained through the ratio between N_2O and the total nitrification ($r_{N2O/nit}$, unitless). N_2O emissions during denitrification (N_2O_{denit}, kg N ha^{-1} d^{-1}, Equation (39)) are obtained by assuming a constant ratio ($r_{N2O/denit}$, unitless) between N_2O emissions and total denitrification.

$$\begin{aligned} N_2O_{nit} &= r_{N2O/nit} \cdot R_{nit} \cdot NH_4 \\ N_2O_{denit} &= r_{N2O/denit} \cdot R_{denit} \end{aligned} \quad (39)$$

3.1.4. Environmental Factors

Soil Temperature Factor

In the **APSIM** model [67], the temperature factor limiting nitrification is the same as that used for the mineralization estimate [72]. It consists of an exponential function, whose minimum value (0) is obtained for a 0 °C soil temperature and whose maximum value (1) is obtained for a 30 °C soil temperature [84]. The temperature factor (Figure 1, Equation (40)) limiting denitrification is an exponential function of the soil temperature (T, °C) [67].

$$f_d(T) = 0.1 \cdot e^{(0.46 \cdot T)} \quad (40)$$

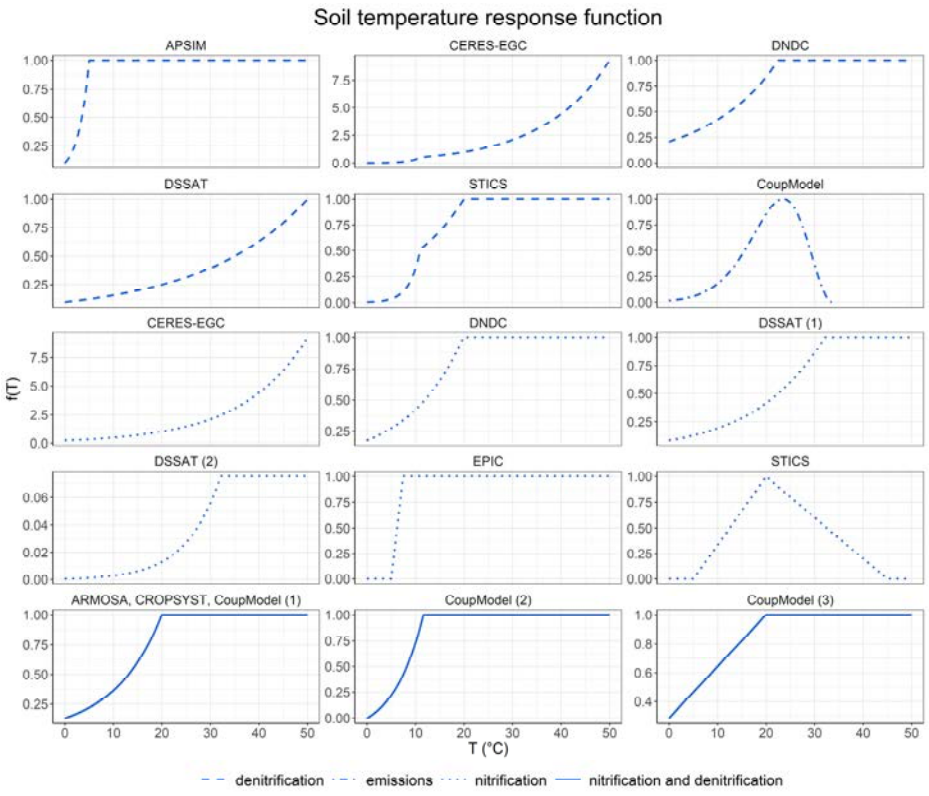

Figure 1. Soil temperature response functions employed for denitrification (dashed lines), nitrification (dotted lines), both processes (solid lines), and emissions (dot-dashed lines) simulation with parameter default values. For the DSSAT model are reported both $f_{n1}(T)$, DSSAT (1), and $f_{n2}(T)$, DSSAT (2), from Equation (48), while for CoupModel are reported all the three alternative functions from Equation (44): $f(T)_1$, CoupModel (1), $f(T)_2$, CoupModel (2), $f(T)_3$, CoupModel (3).

In the **ARMOSA** model, the same soil temperature factor ($f(T)$, unitless, Equation (41)) is employed both for nitrification and denitrification, and it is derived from the SOILN approach [75]. It consists of an exponential function, constrained between 0 and 1, having a Q_{10}-value as a base (t_{Q10}, unitless, between 1.5 and 4) that describes the response to a 10 °C soil temperature change. A base temperature (T_{opt}, °C, 20) at which the temperature effect is equal to 1 is also employed. **CROPSYST** model [59,69,73] employs the same response function (Equation (41)) to limit only the nitrification rate.

$$f(T) = t_{Q10}^{\left(\frac{T-T_{opt}}{10}\right)} \tag{41}$$

In the **SPACSYS** model [71], a Q_{10} equation having different Q_{10} for the various processes is employed, while in **DAYCENT** model 4.7 [11], the response function of nitrification to soil temperature, $f_n(T)$, is represented by a generalized Poisson density function.

In **CERES-EGC** [76], the response function of nitrification to soil temperature (T, °C) is an exponential function (Equation (42)) that is not limited to 1 and employs a Q_{10} factor parameter (t_{Q10}, unitless, 2.1) describing the relative increase in the process activity for a 10 °C increase in soil temperature.

$$f_n(T) = e^{\left[\frac{(T-20)\cdot ln(t_{Q10})}{10}\right]} \tag{42}$$

The exponential response function of denitrification to soil temperature (Equation (43)) is not limited to 1 and employs a threshold temperature parameter (T_{denit}, °C, 11) and two Q_{10} factors: one for low temperature ($t_{Q10,1}$, unitless, 89.0) and one for high temperature ($t_{Q10,2}$, unitless, 2.1).

$$f_d(T) = \begin{cases} e^{\left[\frac{(T-T_{denit})\cdot ln(t_{Q10,1}) - 9ln(t_{Q10,2})}{10}\right]} & if\ T < T_{denit} \\ e^{\left[\frac{(T-20)\cdot ln(t_{Q10,2})}{10}\right]} & if\ T \geq T_{denit} \end{cases} \tag{43}$$

In **CoupModel** [68], the response function of denitrification and of nitrification to soil temperature (T, °C, for the topsoil layer, it is equal to the air temperature) in a considered layer can be selected among three different options (Figure 1, Equation (44)). A function that becomes a Q_{10}-type function above a certain temperature threshold ($f(T)_1$), a Q_{10}-type function for the whole range of temperatures ($f(T)_2$), and a Ratkowsky function consisting in a quadratic function ($f(T)_3$). The employed parameters are the following: response to a 10 °C soil temperature change on the microbial activity, nitrification and denitrification (t_{Q10}, unitless, 2), base temperature for the microbial activity, nitrification and denitrification at which the response is 1 (T_{opt}, °C, 20), threshold temperature for the microbial activity, nitrification and denitrification below which the response is stronger than above and ceases at 0 °C ($T_{Q10thres}$, °C, 5), minimum temperature for nitrification and denitrification (T_{min}, °C, −8), and temperature at which the response of nitrification and denitrification is equal to 1 (T_{max}, °C, 20).

$$\begin{aligned} f(T)_1 &= t_{Q10}^{\left(\frac{T-T_{opt}}{10}\right)} \\ f(T)_2 &= \frac{T}{T_{Q10thres}} \cdot f_d(T)_1 \\ f(T)_3 &= \begin{cases} 1 & if\ T > T_{max} \\ \left(\frac{T-T_{min}}{T_{max}-T_{min}}\right)^2 & if\ T_{min} < T < T_{max} \\ 0 & if\ T < T_{min} \end{cases} \end{aligned} \tag{44}$$

The response function ($f_e(T)$, unitless, Equation (45)) to soil temperature for N_2O and NO emissions during nitrification employs three parameters: the maximum ($g_{TmaxNxO}$, °C, 33.5) and optimum ($g_{ToptNxO}$, °C, 23.5) soil temperature for the formation of nitrous trace

gases during nitrification, and the parameter determining the response function shape ($g_{TshapeNxO}$, unitless, 1.5).

$$\begin{aligned} f_e(T) &= \left(\frac{g_{TmaxNxO} - T}{g_{TmaxNxO} - g_{ToptNxO}}\right)^{f(T_{exp})} \\ f(T_{exp}) &= g_{TshapeNxO} \cdot \frac{T - g_{ToptNxO}}{g_{TmaxNxO} - g_{ToptNxO}} \end{aligned} \quad (45)$$

In **DNDC** model version 9.5 [79], the soil temperature (T, °C) factor employed in the nitrification is an exponential function of soil temperature (Figure 1, Equation (46)).

$$f_n(T) = 3.503^{\left[\frac{(60-T)}{25.78}\right]} \cdot e^{\left[\frac{3.503 \cdot (T-34.22)}{25.78}\right]} \quad (46)$$

The soil temperature factor employed in the denitrification estimate (Figure 1, Equation (47)) is a Q_{10}-type function with a base equal to 2 and an optimum temperature of 22.5 °C, with a soil temperature threshold parameter ($T_{max,denit}$, °C, 60). The function is equal to zero when the soil temperature is higher than the threshold value.

$$f_d(T) = 2^{\frac{T-22.5}{10}} \quad if\ T \le T_{max,denit} \quad (47)$$

In **DSSAT** model [70] V4.8.2.0 [77], two functions are used for the response of nitrification to soil temperature: the first one is constrained between 0 and 1 and describes soil temperature (T, K) effect on nitrification ($f_{n1}(T)$, unitless, Figure 1, Equation (48)), while the second one is a function ($f_{n2}(T)$, unitless, Figure 1, Equation (48)) of the temperature response function of the previous time step ($f_{n1}(T)_{t-1}$, unitless).

$$\begin{aligned} f_{n1}(T) &= e^{\left(\frac{-6572}{T} + 21.4\right)} \\ f_{n2}(T) &= min\left[0.075 \cdot f_{n1}(T)_{t-1}{}^2, 1\right] \end{aligned} \quad (48)$$

The response function of denitrification to soil temperature (T, K) is only present in the CERES denitrification subroutine, and it is limited between 0 and 1 ($f_d(T)$, unitless, Figure 1, Equation (49)).

$$f_d(T) = 0.1 \cdot e^{0.046 \cdot T} \quad (49)$$

In **EPIC** model [62] v. 1102 [78], the response function of nitrification to soil temperature (T, °C) is a linear function (Equation (50)).

$$f_n(T) = 0.41 \cdot (T - 5) \quad (50)$$

In the **STICS** model [60], the response function of nitrification to soil temperature (T, °C) is limited between 0 and 1 (Figure 1, Equation (51)), and it is defined by the following parameters: minimum cardinal temperature for nitrification ($T_{min,nit}$, °C), optimum cardinal temperature for nitrification ($T_{opt,nit}$, °C), and maximum cardinal temperature for nitrification ($T_{max,nit}$, °C).

$$f_n(T) = \begin{cases} \frac{T - T_{min,nit}}{T_{opt,nit} - T_{min,nit}} & if\ T \le T_{opt,nit} \\ \frac{T - T_{max,nit}}{T_{opt,nit} - T_{max,nit}} & if\ T \ge T_{opt,nit} \end{cases} \quad (51)$$

The response function of denitrification to soil temperature (T, °C) is limited between 0 and 1 (Figure 1, Equation (52)), and it is defined by two cardinal temperatures for denitrification ($T_{1,denit}$, °C, 11; $T_{2,denit}$, °C, 20).

$$f_d(T) = \begin{cases} e^{[(T - T_{1,denit}) \cdot 0.449 - 0.668]} & if\ \ T \le T_{1,denit} \\ e^{[(T - T_{2,denit}) \cdot 0.0742]} & if\ \ T > T_{1,denit} \end{cases} \quad (52)$$

Soil Moisture Factor

In the **APSIM** model [67], the soil moisture factor limiting nitrification is a trapezoidal function whose value is 0 at the lower limit soil water content and at the saturation soil water content (SWC_{sat}), and it is equal to 1 at the drained upper limit. All the considered soil water contents are volumetric ones [84]. The soil moisture factor limiting denitrification (Figure 2, Equation (53)) is defined by the following parameters: water content at which denitrification ceases (SWC_{lim}, in the default configuration, is equal to the value of *WFPS* at *DUL*) and empirical coefficient (x, in the default configuration equal to 1) [67].

$$f_d(W) = \left(\frac{SWC - SWC_{lim}}{SWC_{sat} - SWC_{lim}} \right)^x \quad (53)$$

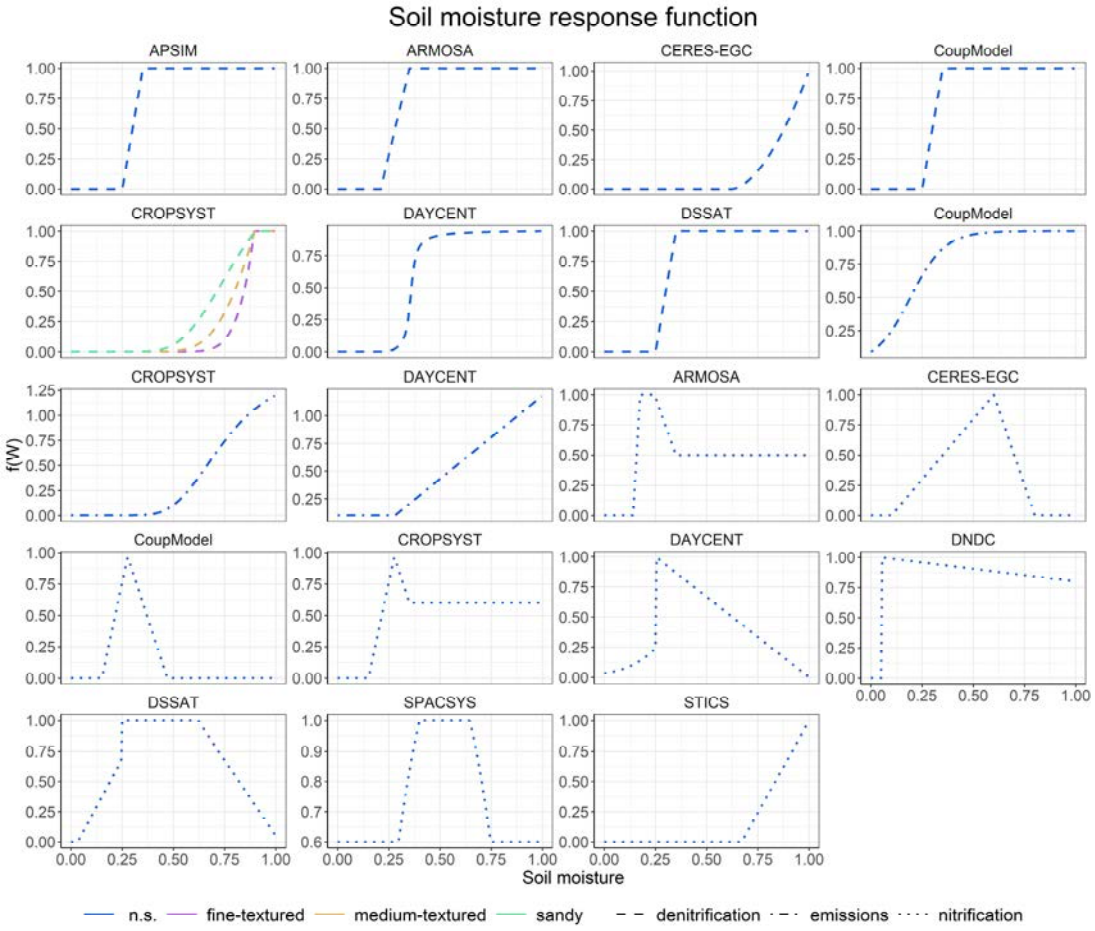

Figure 2. Soil moisture (expressed as *SWC* or *WFPS* depending on the considered model) response functions employed for nitrification (dotted lines), denitrification (dashed lines) and emissions (dot-dashed lines) simulation, with parameter default values. When the model considers diversified response functions for different soil texture classes, they are reported in the same panel with different colors; otherwise, the soil texture class is not specified (n.s.).

In **ARMOSA**, the soil moisture effect on nitrification is described through a response function ($f_n(W)$, unitless, Figure 2, Equation (54)) limited between 0 and 1, which employs four soil water content thresholds (SWC_{min}, SWC_{optmin}, SWC_{optmax}, and SWC_{max}, $m^3\ m^{-3}$, Appendix A.2, Appendix A) that are estimated as fractions of the saturation water content (SWC_{sat}, $m^3\ m^{-3}$). The function is defined by the following parameters: microbial activity below SWC_{min} (f_{min}, unitless, 0), microbial activity above SWC_{max} (f_{max}, unitless, 0.5), microbial activity curvature coefficients (a and b, unitless, 1). When $SWC \leq SWC_{min}$, the response function is equal to f_{min}; when $SWC > SWC_{max}$, the response function is equal

to f_{max}, while the function is equal to 1 when SWC is comprised between SWC_{optmin} and SWC_{optmax}.

$$f_n(W) = \begin{cases} f_{min} + (1 - f_{min}) \cdot \left(\frac{SWC - SWC_{min}}{SWC_{optmin} - SWC_{min}} \right)^a & \langle 1 \rangle \\ f_{max} + (1 - f_{max}) \cdot \left(\frac{SWC_{max} - SWC}{SWC_{max} - SWC_{optmax}} \right)^b & \langle 2 \rangle \end{cases} \quad (54)$$
$$\langle 1 \rangle \; SWC_{min} < SWC \leq SWC_{optmin}$$
$$\langle 2 \rangle \; SWC_{optmax} < SWC \leq SWC_{max}$$

The soil moisture effect on denitrification is described through a response function, constrained between 0 and 1 ($f_d(W)$, unitless, Figure 2, Equation (55)), that is derived from the APSIM approach (Equation (53)). This response function uses three parameters: the saturation threshold (thr_{sat}, unitless, 0.6), an empirical coefficient (x, unitless, 1, between 0.9 and 5), and a lower threshold for soil water content (thr_{denit}, unitless, 0.05) under which no denitrification occurs (response function equal to 0).

$$f_d(W) = \left(\frac{SWC - thr_{sat} \cdot SWC_{sat}}{SWC_{sat} - thr_{sat} \cdot SWC_{sat}} \right)^x \quad (55)$$

In **CERES-EGC** [76], the nitrification response function to soil water content (Equation (56)) increases linearly from a minimum $WFPS$ value ($WFPS_{min,nit}$, %, 0.1) to an optimum value ($WFPS_{opt,nit}$, %, 0.6). The function then decreases linearly to a maximum value ($WFPS_{max,nit}$, %, 0.8). It is equal to zero otherwise.

$$f_n(W) = \begin{cases} \frac{WFPS - WFPS_{min,nit}}{WFPS_{opt,nit} - WFPS_{min,nit}} \; if \; WFPS_{min,nit} < WFPS \leq WFPS_{opt,nit} \\ \frac{WFPS_{max,nit} - WFPS}{WFPS_{max,nit} - WFPS_{opt,nit}} \; if \; WFPS_{opt,nit} \leq WFPS < WFPS_{max,nit} \end{cases} \quad (56)$$

The denitrification response function to soil water content (Equation (57)) is equal to zero when the soil $WFPS$ is lower than a threshold value ($WFPS_{denit}$, %, 0.62); otherwise, it consists of a function having a parameter as exponent (x, unitless, 1.74).

$$f_d(W) = \left(\frac{WFPS - WFPS_{denit}}{1 - WFPS_{denit}} \right)^x if \; WFPS \geq WFPS_{denit} \quad (57)$$

In **CoupModel** [68], the soil moisture response function for denitrification (Figure 2, Equation (58)) is estimated differently on the base of the simulated soil water content (SWC, $m^3\ m^{-3}$) and of the soil water content at saturation (SWC_{sat}, $m^3\ m^{-3}$). The response function is defined by the following parameters: a coefficient in the function for soil moisture effect on denitrification ($p_{\theta Dp}$, unitless, 10) and a water content range from saturation in the function for soil moisture on denitrification ($p_{\theta DRange}$, %, 10). The function is equal to 1 when SWC is equal to SWC_{sat}, while it is equal to zero when $SWC - SWC_{sat} > p_{\theta Dp}$.

$$f_d(W) = \left(\frac{SWC - SWC_{sat} - p_{\theta DRange}}{p_{\theta DRange}} \right)^{p_{\theta Dp}} \quad if \; SWC - SWC_{sat} < p_{\theta Dp} \quad (58)$$

The soil moisture response function for nitrification (Figure 2, Equation (59)) is estimated differently on the base of the simulated soil water content at saturation and at wilting point (SWC_{wilt}, $m^3\ m^{-3}$) and is defined by the following parameters: saturation activity in soil moisture response function ($p_{\theta satact}$, unitless, 0.6, 0 is equal to no activity, 1 is equal to optimum activity at saturation), water content interval lower limit in the soil moisture response for nitrification and denitrification ($p_{\theta Low}$, %, 13, range 8–15), the coefficient for the soil moisture function ($p_{\theta p}$, unitless, 1 corresponds to a linear response, 0–1 corresponds to a convex response, >1 corresponds to a concave response), water content interval upper limit in the soil moisture response function for nitrification and denitrification ($p_{\theta Upp}$, %, 8,

range 1–10). The function is equal to $p_{\theta satact}$ when SWC is equal to SWC_{sat}, while it is equal to zero when $SWC < SWC_{wilt}$.

$$f_n(W) = min\left[\left(\frac{SWC_{sat} - SWC}{p_{\theta Upp}}\right)^{p_{\theta p}} \cdot (1 - p_{\theta satact}) + p_{\theta satact'}\left(\frac{SWC - SWC_{wilt}}{p_{\theta Low}}\right)^{p_{\theta p}}\right] \quad (59)$$

In the **CROPSYST** model [59,69,73], the response function of nitrification (Figure 2, Equation (60)) to the volumetric soil water content (SWC, $m^3\ m^{-3}$) is modeled with the SOILN approach [74,75]. The response function is equal to zero below the wilting point (SWC_{wilt}, %); it increases to one in the interval delimited by a parameter ($p_{\theta Low}$, %, 13), and near the saturation water content (SWC_{sat}, %), it decreases to a saturation activity ($p_{\theta satact}$, unitless, 0.6, range 0–1) in an interval confined by a parameter ($p_{\theta Upp}$, %, 8). The shape of the response curve between $p_{\theta Low}$ and $p_{\theta Upp}$ is given by a parameter ($p_{\theta p}$, unitless), the linear response is obtained with a value of 1; between 0 and 1, the response function is convex, and for values higher than 1, the response is concave. $p_{\theta Low}$ is the water content interval defining increasing activity from 0 (no activity) at SWC_{wilt} to 1 (optimum activity) at $p_{\theta Low}$ + SWC_{wilt}; its normal range is 8–15, depending on soil type. $p_{\theta Upp}$ is the water content interval defining decreasing activity from 1 (optimum activity) at $SWC_{sat} - p_{\theta Upp}$ to the activity given by parameter $p_{\theta satact}$ at SWC_{sat}; its normal range is 1–10, depending on soil type.

$$\begin{array}{l} f_n(W) = \begin{cases} p_{\theta satact} + (1 - p_{\theta satact}) \cdot \left(\frac{SWC_{sat} - SWC}{p_{\theta Upp}}\right)^{p_{\theta p}} & \langle 1 \rangle \\ \left(\frac{SWC - SWC_{wilt}}{p_{\theta Low}}\right)^{p_{\theta p}} & \langle 2 \rangle \end{cases} \\ \langle 1 \rangle\ if SWC_{sat} - p_{\theta Upp} < SWC < SWC_{sat} \\ \langle 2 \rangle\ if\ SWC_{wilt} < SWC < SWC_{wilt} + p_{\theta Upp} \end{array} \quad (60)$$

The response function ($f_d(W)$, unitless, Equation (61)) describing $WFPS$ (unitless) effect on denitrification is limited, between 0 and 1 [80], its parameters values vary with soil texture (sandy, medium and fine): a (1.56, 4.82, and 60.0), b (12.0, 14.0, and 18.0), c (16.0, 16.0, and 22.0), and d (2.01, 1.39, and 1.06).

$$f_d(W) = \frac{a}{b^{\left[\frac{c}{b^{(d \cdot WFPS)}}\right]}} \quad (61)$$

In **DAYCENT** model 4.7 [11], the response function of nitrification and denitrification, $f_n(W)$ and $f_d(W)$, consider the second and the third soil layer moisture status only (Figure 2). The response function for nitrification (Equation (62)) employs available soil water content (SWC_{avail}, $m^3\ m^{-3}$) and the weighted average of the $WFPS$ of the considered layers, respectively, for soils drier or wetter than field capacity (SWC_{fc}, $m^3\ m^{-3}$).

$$f_n(W) = \begin{cases} \frac{1}{1 + 30 \cdot e^{-9 \cdot SWC_{avail}}} & if\ SWC \le SWC_{fc} \\ \frac{-1}{1 - SWC_{fc}} \cdot (WFPS_{avg} - 1) & else \end{cases} \quad (62)$$

The $WFPS$ curve (Equation (63)) of the denitrification submodel [81] was modified [11] to stop the denitrification process for $WFPS$ < 55%, and it is defined by a parameter corresponding to the $WFPS$ level at which the denitrification reaches half of its maximum velocity (a, unitless). The $WFPS$ [11,85] for the two response functions is calculated as a function of gravimetric soil water content (θ_g, g water g $soil^{-1}$) and bulk density (BD, g cm^{-3}).

$$\begin{array}{l} f_d(W) = 0.45 + \frac{atan[0.6 \cdot \pi \cdot (0.1 \cdot WFPS - a)]}{\pi} \\ WFPS = \theta_g \cdot \frac{BD}{\left(1 - \frac{BD}{2.65}\right)} \end{array} \quad (63)$$

In **DNDC** model version 9.5 [79], a soil moisture factor (Figure 2, Equation (64)) is employed in the nitrification estimate, for which the soil water content is expressed as water-filled porosity (*WFPS*).

$$f_n(W) = \begin{cases} 0.8 + 0.21 \cdot (1 - WFPS) & if\ WFPS > 0.05 \\ 0 & if\ WFPS \leq 0.05 \end{cases} \quad (64)$$

In **DSSAT** model [70] V4.8.2.0 [77], the response function ($f_n(W)$, unitless, Figure 2, Equation (65)) of nitrification to soil water content (SWC, $m^3\ m^{-3}$) is based on water-filled porosity ($WFPS$, unitless), and it is limited between 0 and 1. The function uses as soil water content thresholds the drained upper limit (DUL, $m^3\ m^{-3}$) and the saturation water content (SWC_{sat}, $m^3\ m^{-3}$). The $WFPS$ is obtained as the ratio between SWC and SWC_{sat}.

$$f_n(W) = \begin{cases} -2.5 \cdot WFPS + 2.55 & if\ SWC > DUL \\ 1 & if\ SWC < DUL\ and\ WFPS > 0.4 \\ 3.15 \cdot WFPS - 0.1 & else \end{cases} \quad (65)$$

In the DAYCENT denitrification subroutine, the response function of denitrification ($f_d(W)$, unitless, Equation (66)) to soil moisture is constrained between 0 and 1 and considers the soil gas diffusivity at field capacity (g_{diff}, unitless), the $WFPS$ and an auxiliary variable ($CO_{2correct}$, Equation (91)).

$$\begin{aligned} f_d(W) &= 0.45 + \frac{atan\{0.6 \cdot \pi \cdot [10 \cdot WFPS - (9.0 - M \cdot CO_{2correct})]\}}{\pi} \\ M &= \left\{ min\left[0.113,\ g_{diff} \cdot (-1.25)\right] \right\} + 0.145 \end{aligned} \quad (66)$$

In the CERES denitrification subroutine, the response function of denitrification ($f_d(W)$, unitless, Equation (67)) to soil moisture is constrained between 0 and 1 and is calculated when soil moisture (SWC, $m^3\ m^{-3}$) is higher than the drained upper limit (DUL, $m^3\ m^{-3}$).

$$f_d(W) = 1 - \left(\frac{SWC_{sat} - SWC}{SWC_{sat} - DUL} \right) \quad (67)$$

In **EPIC** model [62] v. 1102 [78], the Armen Kemanian denitrification method employs a water factor ($f_d(W)$, Equation (68)) that considers the soil layer porosity (PO, $m^3\ m^{-3}$), its soil water storage (SWT, $m^3\ m^{-3}$, fraction of field capacity), its thickness (z_{layer}, m), and its clay amount ($CLAY$, %).

$$\begin{aligned} f_d(W) &= \begin{cases} \frac{1}{1 + \left(\frac{1 - AIRV}{0.9 + 0.01 \cdot CLAY} \right)^{-60}} & if\ \left(\frac{1 - AIRV}{0.9 + 0.01 \cdot CLAY} \right) > 0.8 \\ 0 & else \end{cases} \\ AIRV &= \frac{PO - SWT}{z_{layer}} \end{aligned} \quad (68)$$

In the **SPACSYS** model [71], the water-filled pore space ($WFPS$) response function is applied only to nitrification (Figure 2, Equation (69)), and it is expressed with a quadratic function, with the $WFPS$ estimate approach derived from [86,87]. Its value depends on volumetric soil water content (SWC, $m^3\ m^{-3}$), soil bulk density (BD, $g\ cm^{-3}$), and soil particle density (PD, $g\ cm^{-3}$) parameters.

$$\begin{aligned} f_n(W) &= \begin{cases} min\left[1; \left(-11.25 \cdot WFPS^2 + 11.75 \cdot WFPS - 1.9\right)\right] & if\ 0.3 \leq\ WFPS \leq 0.75 \\ 0.6\ if\ 0.3 < WFPS\ or\ WFPS > 0.75 \end{cases} \\ WFPS &= \frac{SWC}{1 - \frac{BD}{PD}} \end{aligned} \quad (69)$$

In the **STICS** model [60], the response function (Equation (70)) of nitrification to soil water content (SWC, mm water cm^{-1} soil) is limited between 1 and 0, and it employs an optimal water content parameters ($SWC_{opt,nit}$, unitless, 1) that is different from the one used

for mineralization, and a minimal soil water content for nitrification process ($SWC_{min,nit}$, unitless, 0.67). All the soil water content parameters are expressed as a proportion of field capacity water content (SWC_{fc}, mm water cm^{-1} soil).

$$f_n(W) = \frac{SWC - SWC_{min,nit} \cdot SWC_{fc}}{(SWC_{opt,nit} - SWC_{min,nit}) \cdot SWC_{fc}} \quad (70)$$

The response function of denitrification to soil moisture is defined using the auxiliary variable saturation soil status ($WFPS$, unitless), and it is related to the mineralization process through the reference temperature for soil mineralization parameter (T_{miner}, °C, 15). The function (Figure 2, Equation (71)) is limited between 0 and 1. It considers the amount of water remaining in the soil macroporosity (SWC_{sat}, mm) and the bulk density (g cm^{-3}).

$$f_d(W) = \left[\frac{WFPS - \left(0.62 - \frac{T - T_{miner}}{100}\right)}{1 - \left(0.62 - \frac{T - T_{miner}}{100}\right)} \right]^{1.74}$$
$$WFPS = \frac{SWC + SWC_{sat}}{10 \cdot \left(1 - \frac{BD}{2.66}\right)} \quad (71)$$

In the **CROPSYST** model [59,69,73], the response function ($f_e(W)$, unitless, Equation (72)) describing the $WFPS$ (unitless) effect on N_2/N_2O ratio for denitrification gas fluxes is not constrained between 0 and 1, and it is derived from [80].

$$f_e(W) = \frac{1.4}{13^{\left[\frac{17}{13^{(2.2 \cdot WFPS)}}\right]}} \quad (72)$$

In **DAYCENT** model 4.7 [11], a $WFPS$ effect on the N_2/N_2O ratio ($f_e(W)$, Equation (73)) is also applied.

$$f_e(W) = max(0.1,\ 0.015 \cdot WFPS \cdot 100 - 0.32) \quad (73)$$

In **CoupModel** [68], the soil moisture response function limiting the production of NO and N_2O during nitrification ($f_e(W)$, unitless, Equation (74)) is defined by two parameters: the relative saturation level in the response function for soil moisture when NO or N_2O is formed during nitrification ($g_{\theta satcrit}$, unitless, Table A8, Appendix A.3, Appendix A) and the parameter describing the shape of the moisture response function for NO or N_2O emissions ($g_{\theta satform}$, unitless, Table A8, Appendix A.3, Appendix A).

$$f_e(W) = 1 - \frac{1}{1 + e^{\left(\frac{SWC/SWC_{sat} - g_{\theta satcrit}}{g_{\theta satform}}\right)}} \quad (74)$$

Soil Acidity Factor

In the **APSIM** model [67], the soil acidity factor limiting nitrification is a trapezoidal function [84] whose value is equal to 0 when $pH < pH_{min}$ (unitless, 4.5) or $pH > pH_{max}$ (9, unitless) and whose value is equal to 1 for $pH_{optmin} \leq pH \leq pH_{optmax}$ (unitless, 6 and 8, respectively). The response function of nitrification to soil acidity in **ARMOSA**, **CROPSYST** [59,69,73], and **STICS** [60] models employs the SOILN approach [74,75]: it is a linear function (Figure 3, Equation (75)) defined by two parameters. The function is equal to 0 for $pH < pH_{min}$ (unitless, 3), while it is equal to 1 for $pH > pH_{max}$ (unitless, 5.5).

$$f_n(pH) = \frac{pH - pH_{min}}{pH_{max} - pH_{min}} \quad (75)$$

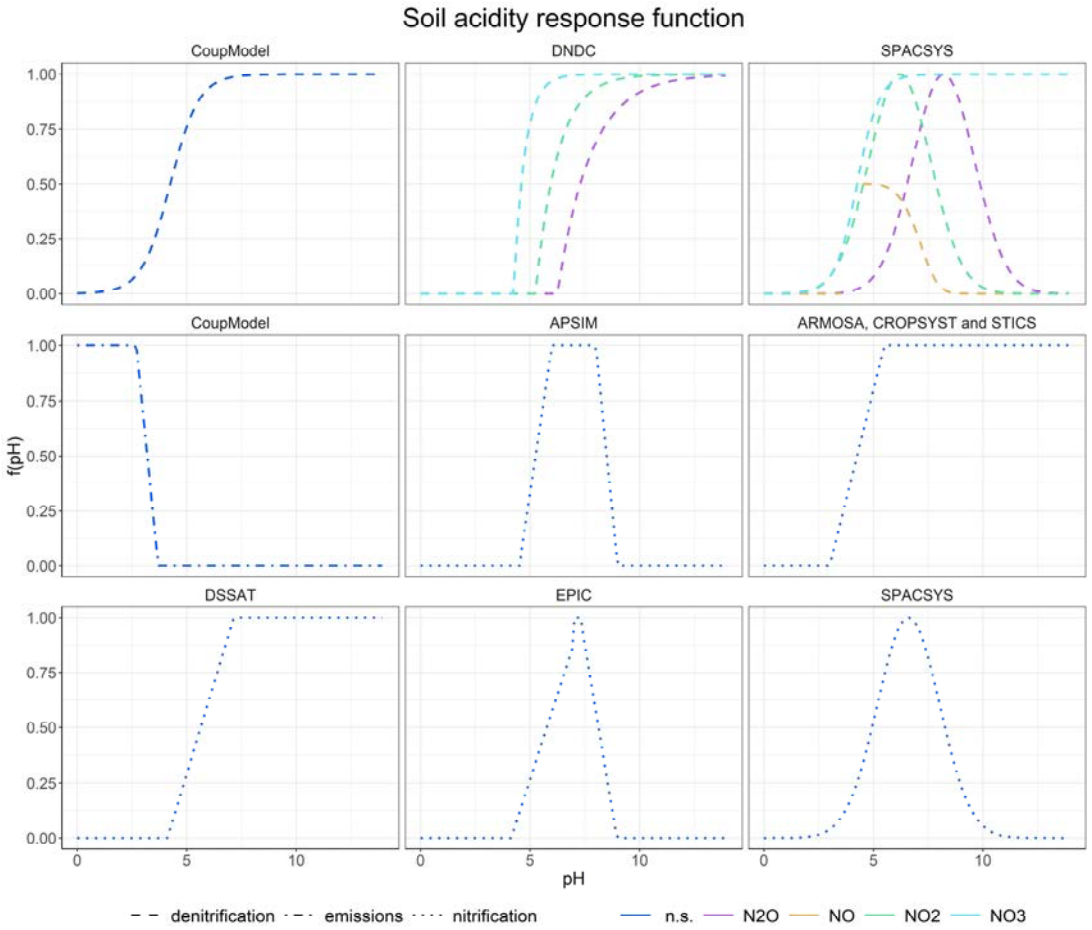

Figure 3. Soil acidity response functions employed for nitrification (dotted lines), denitrification (dashed lines) and emissions (dot-dashed lines) simulation, with parameter default values. When the model considers diversified response functions for each N_xO_y oxide, they are reported in the same panel with different colors; otherwise, the N_xO_y oxide is not specified (n.s.).

In **CoupModel** [68], the response function of denitrification (Figure 3, Equation (76)) to soil acidity is defined by two parameters: the pH half rate (d_{pHrate}, unitless, 4.25) and a shape coefficient ($d_{pHshape}$, unitless, 0.5).

$$f_d(pH) = 1 - \frac{1}{1 + e^{\left(\frac{pH - d_{pHrate}}{d_{pHshape}}\right)}} \tag{76}$$

In **CoupModel** [68], the response function of NO and N_2O production during nitrification to soil acidity (Equation (77)) employs a parameter (pH_{min}, unitless, 4.7) describing the pH value below, in which the function is equal to 1.

$$f_e(pH) = pH_{min} - pH \tag{77}$$

In **DAYCENT** model 4.7 [11,85], the response function of nitrification to soil acidity (Equation (78)) is calculated as an inverse function of the tangent function (atan is a standard C arctangent function from the library math.h).

$$f_n(pH) = atan(pH,\ a) \tag{78}$$

In **DNDC** model version 9.5 [79], a pH factor for denitrification is employed ($f_d(pH)_{NxOy}$, Figure 3, Equation (79)).

$$f_d(pH)_{NxOy} = \begin{cases} 1 - \frac{1}{e^{(pH-4.25)/0.5}} \; if \; N_xO_y = NO_3 \\ 1 - \frac{1}{e^{(pH-5.25)/1}} \; if \; N_xO_y = NO_2 \; or \; NO \\ 1 - \frac{1}{e^{(pH-6.25)/1.5}} \; if \; N_xO_y = N_2O \end{cases} \quad (79)$$

In **DSSAT** model [70] V4.8.2.0 [77], the response function of nitrification to soil acidity ($f_n(pH)$, unitless) is limited between 0 and 1. It is equal to 0 and 1 when $pH < pH_{min}$ and when $pH > pH_{opt,}$ respectively, and linear in between (Figure 3, Equation (80)).

$$f_n(pH) = min(1,\ 0.33 \cdot pH - 1.36) \quad (80)$$

In **EPIC** model [62] v. 1102 [78], a trapezoidal response function (Figure 3, Equation (81)) of nitrification to soil acidity (pH, unitless) is employed: it is constrained between 0 and 1 and defined by two parameters: pH optimum minimum threshold (pH_{optmin}, unitless, 7) and pH optimum maximum threshold (pH_{optmax}, unitless, 7.4).

$$f_n(pH) = \begin{cases} (0.307 \cdot pH) - 1.269 & if \; pH < pH_{optmin} \\ 1 & if \; pH_{optmin} \le pH \le pH_{optmax} \\ 5.367 - 0.599 \cdot pH & if \; pH > pH_{optmax} \end{cases} \quad (81)$$

In the **SPACSYS** model [71], the response functions of nitrification and denitrification to soil acidity are unitless and limited between 0 and 1 (each step of the denitrification process presents its own function, Figure 3, Equation (82)).

$$\begin{aligned} f_n(pH) &= e^{-\left(\frac{pH-6.6}{2}\right)^2} \\ f_{d,NO_3}(pH) &= 1 - \frac{1}{1+e^{\left(\frac{pH-4.25}{0.5}\right)}} \\ f_{d,NO}(pH) &= \frac{1}{1+e^{\left(\frac{pH-4.5}{2.5}\right)^{5.5}}} \\ f_{d,NO_2}(pH) &= e^{-\left(\frac{pH-6.2}{2}\right)^2} \\ f_{d,N_2O}(pH) &= e^{-\left(\frac{pH-8.2}{2}\right)^2} \end{aligned} \quad (82)$$

Substrate Concentration Effect

In **CERES-EGC** [76], the response function of nitrification (Equation (83)) to soil ammonium content (mg N kg soil^{-1}) employs a half-saturation constant parameter ($K_{m,nit}$, mg N kg soil^{-1}, 10) that is modified on the base of the soil water content value.

$$f_n(NH_4) = \frac{NH_4}{K_{m,nit} \cdot SWC + NH_4} \quad (83)$$

In the response function of denitrification (Equation (84)) to soil nitrate content (mg N kg soil^{-1}), using a dedicated half-saturation constant ($K_{m,denit}$, mg N kg soil^{-1}, 22), the soil water content is not considered.

$$f_d(NO_3) = \frac{NO_3}{K_{m,denit} + NO_3} \quad (84)$$

In **CoupModel** [68], the response function of denitrification (Equation (85)) to nitrate concentration ([NO_3], mg N L^{-1}) employs a parameter describing the half-saturation

constant (K_m, mg N L^{-1}, 10, range 5–15), i.e., the nitrate concentration at which the activity is half of the activity at optimum nitrate concentration.

$$f_d(NO_3) = \frac{\frac{[NO_3]}{SWC \cdot z_{layer}}}{\left(\frac{[NO_3]}{SWC \cdot z_{layer}}\right) + K_m} \tag{85}$$

The response function of nitrification rate (Equation (86)) to nitrate and ammonium ($[NH_4]$, mg N L^{-1}) concentrations in the simplified approach, i.e., when microbes are not considered, employs two parameters: the nitrate–ammonium ratio ($r_{NO3/NH4}$, unitless, 8, range 1–15) and the specific nitrification rate (k_{nit}, d^{-1}, 0.2).

$$f_n(NH_4, NO_3) = max\left(0, \frac{[NH_4] - [NO_3]}{r_{NO3/NH4}}\right) \cdot k_{nit} \tag{86}$$

The response function of nitrification rate (Equation (87)) to ammonium concentration in the microbial biomass explicit approach employs the nitrification half rate parameters (K_m, mg N L^{-1}, 6.18).

$$f_n(NH_4) = \frac{\frac{[NH_4]}{SWC \cdot z_{layer}}}{\frac{[NH_4]}{SWC \cdot z_{layer}} + K_m} \tag{87}$$

In **CROPSYST** [59,69,73], the response function ($f_d(NO_3)$, g N ha^{-1} d^{-1}, Equation (88)) describing the maximum denitrification for a certain NO_3 (µg N g^{-1}) soil level is derived from [80].

$$f_d(NO_3) = 11.00 + \frac{40.00 \cdot atan[\pi \cdot 0.002 \cdot (NO_3 - 180)]}{\pi} \tag{88}$$

The response function ($f_d(CO_2)$, g N ha^{-1} d^{-1}, Equation (89)) describing the maximum denitrification for a certain soil respiration ($CO_{2,resp}$, kg C N ha^{-1} d^{-1}) level is derived from [80].

$$f_d(CO_2) = \frac{24}{\left(1 + \frac{200}{e^{0.35 \cdot CO_{2,resp}}}\right)} - 100 \tag{89}$$

In **DAYCENT** model 4.7 [11], the two substrate concentration effect functions ($f_d(NO_3)$, $f_d(CO_2)$, µg N g $soil^{-1}$ d^{-1}, Equation (90)) are not limited between 0 and 1 (they cannot be negative), but they correspond to the potential total N flux not limited by CO_2 and H_2O for $f_d(NO_3)$ by NO_3 and H_2O for $f_d(CO_2)$ [81].

$$\begin{aligned} f_d(NO_3) &= atan(NO_3, a) \\ f_d(CO_2) &= 0.1 \cdot (CO_2)^{1.3} - 0.1 \end{aligned} \tag{90}$$

In **DSSAT** model [70] V4.8.2.0 [77], the DAYCENT denitrification subroutine employs a denitrification response function to NO_3^- ($f_d(NO_3)$, kg N ha^{-1} d^{-1}, Equation (91)) that has a lower bound equal to zero.

$$f_d(NO_3) = 1.556 + \left(\frac{76.91}{\pi}\right) \cdot atan[\pi \cdot 0.00222 \cdot (NO_3 - 9.23)] \tag{91}$$

In the DAYCENT denitrification subroutine, the denitrification response function to CO_2 ($f_d(CO_2)$, unitless, Equation (92)) is derived from [81] and has a lower bound equal to zero. It considers a minimum amount of nitrate ($NO_{3,min}$, kg N ha^{-1} d^{-1}, 0.1) and an auxiliary variable ($CO_{2correct}$, Equation (91)), derived from the CO_2 produced daily ($CO_{2,resp}$)

in the first two soil layers (first soil layer, $L = 0$, and second soil layer, $L = 1$, the first soil layer also includes the mulch layer).

$$\begin{aligned} f_d(CO_2) &= \left[0.1 \cdot \ CO_{2correct}{}^{1.3}\right] - NO_{3,min} \\ CO_{2correct} &= \begin{cases} [CO_2] & if\ WFPS \le thr_{WFPS} \\ [CO_2]\cdot(1 + a\cdot(WFPS - thr_{WFPS})) & else \end{cases} \\ [CO_2]\ (L) &= \begin{cases} CO_{2,\ resp}(0) + CO_{2,\ resp}(1) & if\ L = 1 \\ CO_{2,\ resp}(L) & else \end{cases} \\ thr_{WFPS} &= \begin{cases} 0.8\ if\ g_{diff} \ge 0.15 \\ \frac{g_{diff}\cdot 250 + 43}{100}\ else \end{cases} \\ a &= \begin{cases} 0.004 & if\ g_{diff} \ge 0.15 \\ -0.1\cdot g_{diff} + 0.019 & else \end{cases} \end{aligned} \quad (92)$$

In the CERES denitrification subroutine, the water-extractable soil carbon amount (C_W, Equation (93)) depends on the availability of C from the humic fraction (C_{SSOM}) and of the fresh C from the carbohydrate pool (C_{LIT}).

$$C_W = 24.5 + 0.0031\cdot(C_{SSOM} + 0.2\cdot C_{LIT}) \quad (93)$$

In **EPIC** model [62] v. 1102 [78], the Armen Kemanian denitrification method uses a nitrate factor ($f_d(NO_3)$, Equation (94)).

$$f_d(NO_3) = \frac{max\left(1e^{-5}, \frac{1000\cdot NO_3}{WT}\right)}{max\left(1e^{-5}, \frac{1000\cdot NO_3}{WT}\right) + 60} \quad (94)$$

In the Armen Kemanian denitrification method, the respiration factor ($f_d(CO_2)$, Equation (95)) considers the CO_2 respiration ($CO_{2,resp}$, kg C N ha^{-1} d^{-1}) of the layer and the soil weight (WT).

$$f_d(CO_2) = min\left(1, \frac{\frac{1000\cdot CO_{2,resp}}{WT}}{50}\right) \quad (95)$$

In the **SPACSYS** model [71], the substrate concentration effects, $f_d(DOC)$, $f_d(NO_3)$, and $f_n(NH_4)$ are described by a Michaelis–Menten-like equation (Equation (96)), and they depend on substrate concentration ([S], g C m^{-3} or g N m^{-3}) and on the Michaelis constant for the substrate (K_m, g C m^{-3} or g N m^{-3}). The constant default values are 9.45, 16.65, and 18.53, respectively, for DOC, $NO_3{}^-$, and $NH_4{}^+$.

$$f([S]) = \frac{[S]}{[S] + K_m} \quad (96)$$

In the **STICS** model [60], nitrate (NO_3, kg N ha^{-1} cm^{-1}) concentration effect on denitrification (Equation (97)) also depends on soil bulk density (BD, g cm^{-3}).

$$f_d(NO_3) = \frac{NO_3}{NO_3 + 2.2\cdot BD} \quad (97)$$

In the DAYCENT denitrification subroutine **DSSAT** model [70] V4.8.2.0 [77], a nitrate effect on the N_2/N_2O ratio ($f_e(NO_3)$, Equation (98)) is also applied.

$$\begin{aligned} f_e(NO_3) &= \begin{cases} max\left(0.16\cdot K_1, K_1\cdot e^{\frac{-0.8\cdot NO_3}{CO_{2correct}}}\right) & if [CO_2] > 0.001 \\ 0.16\cdot K_1 & else \end{cases} \\ K_1 &= max\left(1.5,\ 38.4 - 350\cdot g_{diff}\right) \end{aligned} \quad (98)$$

In the **CROPSYST** model [59,69,73], the response function ($f_e(NO_3)$, Equation (99), unitless, not constrained between 0 and 1) describing NO_3 (μg N g^{-1}) effect on N_2/N_2O ratio for denitrification gas fluxes is derived from [80].

$$f_e(NO_3) = 1 - \left\{0.5 + \frac{1 \cdot atan[\pi \cdot 0.01 \cdot (NO_3 - 190)]}{\pi}\right\} \cdot 25 \quad (99)$$

The response function (f_e (CO_2), Equation (100), unitless, not constrained between 0 and 1) describing soil respiration ($CO_{2,resp}$, kg C N ha^{-1} d^{-1}) effect on N_2/N_2O ratio for denitrification gas fluxes is derived from [80].

$$f_e(CO_2) = 13 + \frac{30.78 \cdot atan\left[\pi \cdot 0.07 \cdot \left(CO_{2,resp} - 13\right)\right]}{\pi} \quad (100)$$

3.1.5. Model Evaluation

This section evaluates 8 (i.e., APSIM, CERES-EGC, CoupModel, DAYCENT, DNDC, EPIC, SPACSYS, and STICS) of the reviewed models, for which the model assessment of N_2O simulation performance was available in published articles. Due to limited data availability of the following models' application and evaluation, CROPSYST, DSSAT, and ARMOSA, were not included in this section. In total, we analyzed 16 papers (Table 2) related to the application of these models, with 10 aimed at validation, 3 at calibration, and 3 reporting the results of both evaluation processes. The 83% of these papers were published between 2015 and 2023. In these studies, measured N_2O emissions were derived both from field and laboratory experiments conducted by the authors of the articles and from experiments carried out by other researchers. The experiment sites were categorized according to the Köppen climate classification, considering their geographical positions, to obtain an overview of the climatic conditions in which the experiments and the simulations were carried out. The most common climatic group that emerged was Cfb, corresponding to a temperature of the warmest month greater than or equal to 10 °C, and temperature of the coldest month less than 18 °C but greater than 3 °C, and precipitation evenly distributed throughout the year [88].

In more than half of the studies, measurements of N_2O emissions in the field were conducted intermittently (i.e., not-continuous measurements). Most of the studies that employed intermittent measurement approaches dealt with a large number of experimental treatments. In contrast, in studies where measurements were taken continuously, the maximum number of tested treatments was limited to 4. Simulated and measured N_2O emissions were reported by the individual studies both as cumulative and daily values. More in detail, 7 of the reviewed model evaluations used cumulated N_2O emissions, 9 used both cumulated and daily N_2O emissions, and 4 employed only daily N_2O emissions.

A comprehensive overview of the statistical indices extracted from the studies is reported in Table A9 (Appendix A.3, Appendix A), and it is organized according to the treatment(s) for which they were calculated. The most frequently reported index in the reviewed studies, determination coefficient (R^2), allowed us to compare model performances concerning both cumulated and daily emissions. Other performance indices (*r*, *RMSE*, *RRMSE*, *EF*) were seldom used. Furthermore, the different time periods employed to obtain cumulated N_2O emissions values and the associated *RMSE* values prevented the possibility of this accuracy index comparisons, while relative errors (*RRMSE*) were rarely reported.

Table 2. Overview of the selected model evaluation studies analyzed in this review. The type of model evaluation is reported: calibration (CAL.) and validation (VAL.), as well as the type of environment (Env.), soil texture (Soil), Köppen climate group (Climate), and the number of treatments (n°).

Model	Ref.	Type	Country	Env.	Soil	Climate	Measure Type	n°	Measure Methodology	Simulated Emissions
APSIM	[16]	VAL.	China	Arable	Silty–loam	Cfb	Continuous fluxes field measures	3	Manual static chambers	Cumulated/daily
	[16]	CAL.	China	Arable	Silty–loam	Cfb	Continuous fluxes field measures	1	Gas chromatography	Cumulated/daily
CERES-EGC	[89]	VAL.	Sweden	Arable	Sandy–loam	Cfb	Not-continuous fluxes field measures	1	Manual static chambers	Daily
	[90]	VAL.	Italy	Arable	Clay–loam	Cfa	Continuous fluxes field measures	1	Automatic chambers	Daily
CoupModel	[7]	CAL.	Sweden	Lab. experiment	Silty–loam	Cfb	Not-continuos fluxes measures	16	Manual static chambers	Cumulated
	[91]	VAL.	Germany	Arable	Silty–loam	Cfb	Not-continuous fluxes field measures	3	Manual static chambers	Daily
DAYCENT	[92]	VAL.	Switzerland	Arable	Silty soil	Cfb	Not-continuous fluxes field measures	5	Manual static chambers	Cumulated
	[11]	VAL.	Colorado	Grassland	Sandy–loam, sandy–clay, clay–loam	Bsk	Not-continuous fluxes field measures	5	Automatic chambers	Cumulated/daily
	[93]	VAL.	Colorado	Arable	Sandy–loam, clay–loam	Bsk	Not-continuous fluxes field measures	2	Automatic chambers	Cumulated
DNDC	[94]	CAL.	China	Rice/arable	Clay–loam	Cfa	Not-continuous fluxes field measures	6	Manual static chambers	Cumulated/daily
	[95]	VAL.	China	Rice/arable	Silty–clay–loam	Bsk	Continuous fluxes field measures	3	Manual static chambers	Cumulated/daily
EPIC	[96]	CAL.	USA	Arable	Silty–loam	Dfa	Not-continuous fluxes field measures	7	Manual static chambers	Cumulated/daily
	[96]	VAL.	USA	Arable	Silty–loam	Dfa	Not-continuous fluxes field measures	7	Manual static chambers	Cumulated/daily
	[82]	CAL.	USA	Arable	Sandy–loam	Dfa	Not-continuous fluxes field measures	6	Manual static chambers	Cumulated/daily
SPACSYS	[71]	VAL.	Scotland	Grassland	Clay–loam	Cfb	Not-continuous fluxes field measures	3	Manual static chambers	Cumulated
	[97]	VAL.	England	Grassland	Clayey	Cfb	Not-continuous fluxes field measures	1	Manual static chambers	Cumulated
	[98]	VAL.	England	Grassland	Various	Cfb	Continuous fluxes field measures	1	Automatic chambers	Cumulated
	[97]	CAL.	England	Grassland	Clayey	Cfb	Not-continuous fluxes field measures	1	Manual static chambers	Daily
STICS	[99]	VAL.	Spain Spain–Catalogna France	Arable	Silty–clay–loam (SP), clay–loam (SP-C, FR)	Cfa (SP), Csa (SP-C), Cfb (FR)	Continuous fluxes field measures	3	Automatic chambers	Cumulated

In general, the reported determination coefficient values are higher when estimated with cumulated N_2O emissions values than the ones obtained from daily values (Figure 4). When considering the combination of measure methodology (continuous and not-continuous measures) and model output (daily and cumulated emissions), differences in models' performance are more relevant for validation studies than for calibration ones (Table A9). In the reviewed studies, the average R^2 obtained after calibration with continuous measures corresponds to 0.48 (with R^2 values reported for daily emissions ranging from 0.31 to 0.56 and from 0.30 to 0.67 for cumulated emissions), while it is equal to 0.65 for calibration studies that employed not-continuous measures (0.1–0.92 and 0.41–0.96, respectively, for daily and cumulated emissions). The average R^2 value, deriving from the published validation coefficient of determinations, were equal to 0.55 and 0.29, respectively, for continuous (0.05–0.74 and 0.4–0.95, respectively, for daily and cumulated emissions) and not continuous (0.02–0.5 and 0.02–0.89, respectively, for daily and cumulated emissions) measures. Frequently, models that were calibrated with continuous measures obtained higher R^2 when subjected to validation using the same type of measured data (particularly when the fitting index is calculated on cumulated emissions). The choice between using cumulated or daily values appears to be primarily linked to measured data frequency, which is associated with the specific research objectives and resource availability. It should be noted that the use of cumulated emissions values for model evaluation tends to reduce the disagreement between measured and simulated data, which can represent both an advantage and a disadvantage. Indeed, the use of cumulated values allows for obtaining higher determination coefficients in the calibration phase, but it does not always ensure the same results at validation (particularly when carried on independent datasets). Conversely, daily emissions values provide a more detailed view but may reveal greater discrepancies between observations and simulations (Table A9).

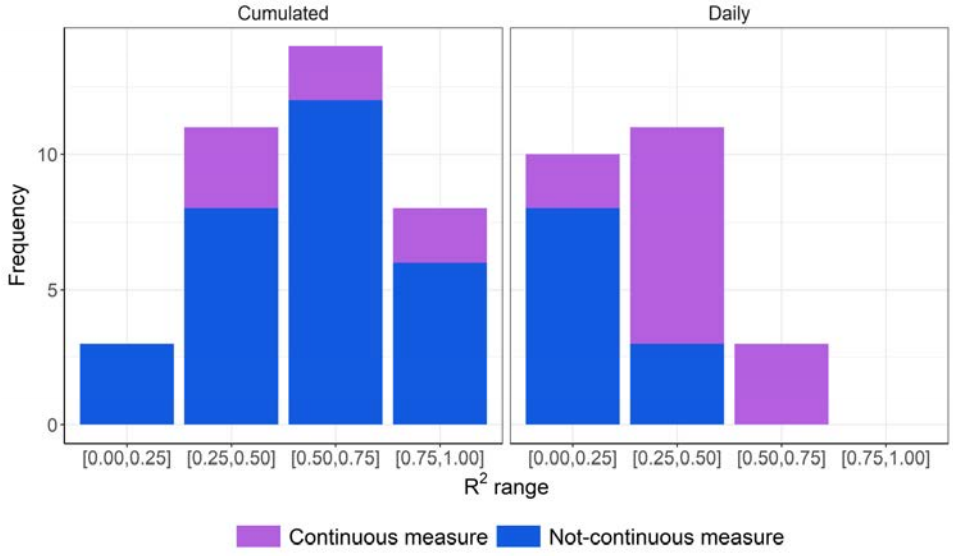

Figure 4. Coefficient of determination (R^2) classes and frequencies in the reviewed evaluation studies, divided for the combination of the type of values considered in the model evaluation process (Cumulated and Daily N_2O emissions) and the type of N_2O emissions measure methodology (Continuous and Not-continuous measure).

When considering only mineral N fertilization treatments, as expected, R^2 values reported in calibration studies that employed not-continuous measures (average R^2 0.66) are higher than the ones obtained after calibration with continuous measures (average R^2 0.48). In validation studies simulating these treatments, average R^2 values were, however, higher in studies that employed continuous measures (0.46) than in the ones that used not-continuous measures (0.27). Probably, this difference is due to the fact that studies that employed continuous emissions measures for validation purposes also employed model

parameter sets calibrated on continuous emissions. Determination coefficients deriving from the reviewed zero N control treatments were generally low (average R^2 equal to 0.065 and 0.31, respectively, for continuous and not-continuous measures) since they were estimated for validation datasets of daily emissions.

4. Discussion

From the appraisal of the main approaches for N_2O emissions modeling, and in agreement with [54], it emerged that soil and weather conditions variability representation is the main driver employed for describing the interactions network that connects soil chemical–physical properties and weather conditions to soil N cycling and the consequent gaseous emissions. In the reviewed process-based models, the level of detail of weather variability representation is obtained by the adoption of a daily time step and of specific parameter values for each simulated process, thus differentiating these approaches from the statistical ones (e.g., IPPC guidelines and statistical models). Soil physical properties are adequately described by the employment of soil hydrological parameters, which allows the simulation of soil water content and temperature variations as influenced by weather trends, soil cover type (bare soil, vegetal soil cover derived from crop growth and development modules) and soil tillage operations. Differences in WFPS simulation or in soil hydrological parameters calculation arise from each model's specific characteristics. The reviewed algorithms generally estimate nitrification and denitrification rates as potential rates limited by soil temperature and moisture response functions, both for the implicit and explicit microbial pool approaches. The main differences that lead to simulated output behaviors, specifically after calibration, are given by the formalization of response functions. Nitrification, in the majority of the approaches, is also limited by soil acidity, while denitrification in the implicit microbial pools approaches is influenced by soil respiration. Indeed, soil organic carbon pool simulation contributes to improving the quality of N_2O emissions representation in process-based models since it allows a more detailed description of the soil mineral nitrogen fluxes. When microbial biomass is explicitly simulated, nitrification and denitrification rates are directly proportional to the microbial biomass itself.

With respect to other types of modeling approaches, process-based models also allow daily representations of management operations (tillage, organic and mineral fertilization, irrigation, residue retention, or removal) and their influence on soil C and N cycles in a specific soil layer. The majority of the reviewed approaches employ dynamic assessment of the fraction of nitrified or denitrified N that is lost as N_2O, and in some cases, further emissions response functions to soil conditions are considered. The major limitation of the IPCC methodology, also shared by statistical models, is not being representative of the reality of crop and soil dynamics since environmental factors influence, and their spatial–temporal heterogeneity is not taken into account. Emission factors, produced by the application of IPCC guidelines, rely on simpler relations that assume a linear proportionality between the N mineral pool and nitrous oxide emission. While this approach is straightforward and of universal applicability, it might lead to sensible underestimation or overestimation of the total emission in case of deficiency or abundance in the N mineral pool, respectively.

Process-based approaches' effectiveness largely depends on the quality and precision of the input data used for calibration and validation. As mentioned before [24–28], quantifying N_2O emissions represents a challenge, primarily due to the spatio-temporal variability of fluxes. Therefore, the chosen methodology for measuring gas fluxes plays a crucial role. Measured data uncertainty, arising, for example, from linear interpolation of manual measurements, considerably impacts the model's performance. On the other hand, the use of automated chambers in manipulative experiments demands intensive labor, advanced sensor technology, and proficient users, while long-term unattended observations of emission fluxes and environmental driver variables by networks of permanent micrometeorological observation sites are an easy way of disposing of datasets collected in contrasting environments for calibration, validation, and comparison.

To address this uncertainty, it is necessary to increase the quantity and accuracy of measurements, even though this requires significant efforts in data collection and processing [13,50,51] and in terms of resource availability.

However, as mentioned earlier, the use of automatic systems for measures acquisition requires complex technology adoption by expert users, often presenting challenges in terms of availability and resources. When such data are available, the models can effectively represent the phenomenon accurately [43]. The current availability of long-term continuous time series of semi-hourly GHG flux data—such as ICOS Carbon Portal (https://www.icos-cp.eu/, accessed on 16 November 2023) or FLUXNET2015 dataset (https://fluxnet.org/data/fluxnet2015-dataset/, accessed on 16 November 2023)—coupled with high-quality biophysical variables as well as ancillary data and metadata represents a useful tool for carrying on multiple model comparison exercises [100]. In this regard, subsets of data might be assembled from selected permanent ecological sites of worldwide networks and be the object of relative simulation confrontation of an ensemble of models. Another consideration arises from the variable diffusivity of N_2O within the soil at different depths, making it challenging to select the appropriate simulation setup and, as a consequence, to calibrate according to measured values that are taken in the soil–atmosphere interface (usually a few centimeters depth from topsoil). This is a critical issue as the majority of selected papers do not provide information about the thickness of the topsoil layer to which the simulated emissions are referred.

One of the most used indicators of the agreement between simulated and observed data is the coefficient of determination, R^2. However, it is important to note that an optimal R^2 value (close to 1) does not necessarily guarantee the model's ability to reproduce the processes accurately and efficiently. In the reviewed model evaluations, high R^2 was frequently associated with discrete *RMSE* values, even if the latter are reported in a few studies. In general, it is good practice to use a combination of different criteria to address model performance evaluation, adopting a broader set of indices that evaluate several aspects of model performance [101]. To truly appreciate the efforts put into measuring and modeling N_2O emissions, a set of model performance indices should be estimated for emissions and other N pools to allow a comprehensive evaluation of the modeling approaches.

5. Conclusions

In the present paper, we have undertaken a comprehensive examination of the main approaches for modeling N_2O. The modeling approaches review was based on their operational principles, although consideration was also given to the model evaluation as presented in published articles. One of the main limitations of the N_2O process-based modeling, underlined by this review, is connected to the inherent difficulties in the direct measure of emissions, which increases model evaluation process uncertainty. In particular, long-period field trials concerning representative cropping systems are required to support models' calibration and improvement. Methodological limitations are also linked to the dynamic simulations of the other cropping system components (crop N uptake, soil organic matter pool evolution, and mineralization in particular) and their accuracy, efficiency, and robustness. This review schematically reports approaches and equations with the aim of easing the comparison of the mechanisms underlying the N_2O emissions simulation. Given the increasing interest in N_2O emissions and their environmental drivers in the agroecosystems, the application of process-based modeling to evaluate cropping system management practices constitutes a powerful tool, even with the abovementioned methodological limitations. Furthermore, process-based models allow the estimate of conditions-specific emission factors for given climate, soil, and cropping system (including annual or perennial crops) combinations that stakeholders (researchers, administrations, and farmers) can evaluate complementarily to IPCC emissions factors, thus deepening N_2O emissions dynamics assessment. Given the uncertainty associated with N_2O simulated emissions, an advisable approach is represented by multi-model ensemble applications to assess possible emissions ranges.

Supplementary Materials: The following supporting information can be downloaded at: https://www.mdpi.com/article/10.3390/horticulturae10010098/s1. Supplementary Materials: overview of the other N_2O modeling approaches. Refs. [41,45,102–117] are cited in Supplementary Material.

Author Contributions: Conceptualization, M.G., M.A., G.R. and A.P.; methodology, M.G., M.A., G.R. and A.P.; investigation, M.G. and M.A.; writing—original draft preparation, M.G. and M.A.; writing—review and editing, G.R., A.M., L.V. and A.P.; supervision, G.R. and A.P. All authors have read and agreed to the published version of the manuscript.

Funding: This study was carried out within the Agritech National Research Center and received funding from the European Union Next-Generation EUGeneration EU (PIANO NAZIONALE DI RIPRESA E RESILIENZA (PNRR)—MISSIONE 4 COMPONENTE 2, INVESTIMENTO 1.4—D.D. 1032 17 June 2022, CN00000022). This manuscript reflects only the authors' views and opinions, and neither the European Union nor the European Commission can be considered responsible for them.

Data Availability Statement: No new data were created or analyzed in this study. Data sharing is not applicable to this article.

Acknowledgments: We gratefully thank Acutis M. and Magliulo V. for their constructive comments, which helped to improve the manuscript.

Conflicts of Interest: The authors declare no conflict of interest. The funders had no role in the design of the study; in the collection, analyses, or interpretation of data; in the writing of the manuscript; or in the decision to publish the results.

Appendix A

Appendix A.1 Model Evaluation Indices

The root mean squared error (*RMSE*) [118] is a difference-based measure of model performance expressed in a quadratic form. It corresponds to the squared root of the mean differences between simulated (S_i) and measured values (O_i).

$$RMSE = \sqrt{\frac{\sum_{i=1}^{n}(S_i - O_i)^2}{n}}$$

The relative root mean squared error (*RRMSE*) [118] represents *RMSE* on a 0–100% scale, and it is obtained by dividing *RMSE* by the mean of the observed values ($\bar{O}$). It has a minimum and optimum value corresponding to zero.

$$RRMSE = \sqrt{\frac{\sum_{i=1}^{n}(S_i - O_i)^2}{n}} \cdot \frac{100}{\overline{O}}$$

The modeling efficiency (*EF*) [119] has an optimum and maximum value equal to one. Its negative values derive from a worse fit than the mean of the observed values.

$$EF = \frac{\sum_{i=1}^{n}\left(O_i - \overline{O}\right)^2 - \sum_{i=1}^{n}(O_i - S_i)^2}{\sum_{i=1}^{n}\left(O_i - \overline{O}\right)^2}$$

Pearson's correlation coefficient (*r*) [120] has an optimum value equal to one. It measures the correlation between simulated and observed values, which does not necessarily involve their coincidence.

$$r = \frac{\sum_{i=1}^{n}\left(O_i - \overline{O}\right)\cdot\left(S_i - \overline{S}\right)}{\sqrt{\sum_{i=1}^{n}\left(O_i - \overline{O}\right)^2 \cdot \sum_{i=1}^{n}\left(S_i - \overline{S}\right)^2}}$$

The coefficient of determination (R^2) ranges between 0 and 1 (its maximum and optimum value).

$$R^2 = \frac{\sum_{i=1}^{n}(S_i - \overline{O})}{\sum_{i=1}^{n}(O_i - \overline{O})}$$

Appendix A.2 Process-Based Models Auxiliary Variables

In the **APSIM** model [67], the auxiliary variable active carbon ([C_A], ppm) concentration in the *i*th soil layer is defined as a fraction of soil organic carbon ([*SOC*], ppm). *SOC* is estimated as the sum of the carbon concentration of the *HUM* ([C_{SSOM}], ppm) and *FOM* ([C_{FOM}], ppm) soil pool. *FOM* corresponds to the fresh organic matter pool; from its mineralization, two pools are derived: *BIOM*, more labile soil microbial biomass and microbial products, and *HUM*, the rest of the soil organic matter [121].

$$[C_A] = 0.0031 \cdot [SOC] + 24.5$$

$$[SOC] = [C_{SSOM}] + [C_{FOM}]$$

In the **ARMOSA** model, the soil content thresholds employed in the soil moisture response function are estimated as fractions of the saturation water content (*SWCsat*, $m^3\ m^{-3}$). The following parameters are employed: microbial activity minimum water threshold coefficient (thr_{min}, unitless, 0.4), microbial activity minimum optimal water threshold coefficient (thr_{optmin}, unitless, 0.5), microbial activity maximum optimal water threshold coefficient (thr_{optmax}, unitless, 0.7), and microbial activity maximum water threshold coefficient (thr_{max}, unitless, 1).

$$SWC_{min} = thr_{min} \cdot SWC_{sat}$$

$$SWC_{optmin} = thr_{optmin} \cdot SWC_{sat}$$

$$SWC_{optmax} = thr_{optmax} \cdot SWC_{sat}$$

$$SWC_{max} = thr_{max} \cdot SWC_{sat}$$

In **CoupModel** [68], the nitrifiers microbial biomass (B_{nit}, $g\ m^{-2}$) is estimated as a function of their growth ($R_{g,nit}$, $g\ m^{-2}\ d^{-1}$), death ($R_{d,nit}$, $g\ m^{-2}\ d^{-1}$), and respiration ($R_{resp,nit}$, $g\ m^{-2}\ d^{-1}$) rates. The growth rate is influenced by response functions to soil temperature, moisture, and solute concentrations (dissolved organic carbon and nitrate) and by a growth coefficient parameter (γ_n, d^{-1}, 2). The nitrate response function is the same employed in the simplified approach for denitrification, and the same equation structure is maintained for the DOC response function (the nitrate half rate parameter is substituted with a *DOC* half rate parameter). The death rate depends on a death rate parameter (d_n, d^{-1}, 1) and on the squared nitrifier biomass, while the respiration rate considers the CN ratio of the decomposing microbial biomass (cn_b, unitless, 10).

$$B_{nit} = B_{nit,\ i-1} + R_{g,nit} - R_{d,nit} - R_{resp,nit}$$

$$R_{g,nit} = \gamma_n \cdot f(T) \cdot f(W) \cdot f(DOC) \cdot f_d(NO_3) \cdot n_{pH} \cdot B_{nit}$$

$$R_{d,nit} = d_n \cdot f(T) \cdot f(W) \cdot f(DOC) \cdot k_{pH} \cdot {B_{nit}}^2$$

$$r_r = d_n \cdot f(T) \cdot f(W) \cdot k_{pH} \cdot \left(\frac{1}{cn_b} - 1\right) \cdot B_{nit}$$

For denitrification simulation (in the microbial biomass explicit approach), NO_2, NO, and N_2O concentrations ($N_{AnNxOyConc}$, Supplementary Material) are estimated by also considering the volumetric anaerobic fraction of the layer (f_{Anvol}, auxiliary variable).

$$N_{AnNxOxConc} = \frac{N_{AnNxOy}}{SWC \cdot f_{Anvol}}$$

The total denitrifiers biomass (B_{denit}, g m^{-2}) depends on its growth ($\sum R_{g,NxOy}$, g m^{-2} d^{-1}) and death ($R_{d,denit}$, g m^{-2} d^{-1}) rate. The growth rate corresponds to the sum of the N fluxes from each N pool to the microbial biomass one, depending on which growth parameter ($\gamma_{d,NxOy}$, d^{-1}) is used: $R_{g,1}$ corresponds to $N_{NO3 \to microDN}$ (when using the parameter $\gamma_{d,NO3}$), $R_{g,2}$ corresponds to $N_{NO2 \to microDN}$ (when using the parameter $\gamma_{d,NO2}$), $R_{g,3}$ corresponds to $N_{NO \to microDN}$ (when using the parameter $\gamma_{d,NO}$), and $R_{g,4}$ corresponds to $N_{N2O \to microDN}$ (when using the parameter $\gamma_{d,N2O}$, in this case, a response function taking into account the nitrate inhibition effect is used). The death rate calculation employs a death rate coefficient (d_d, d^{-1}, 0.09), while the microbial activity ($M_{activity}$, g m^{-2}) depends on a pH response function (different than the one used for the nitrification rate) on a soil temperature function and on a response function to the total amount of N in the anaerobic pools ($f(N_{AnTot})$). The equation for growth respiration (N_{rg}) employs an efficiency parameter ($d_{effNxOy}$, unitless) and is applied to each N pool (N_xO_y equal to NO_3, NO_2, NO, and N_2O). Similarly, the equation for maintenance respiration (N_{rm}) employs a respiration coefficient (d_{rcNxOy}, d^{-1}), and it is applied to each N pool (N_{NxOy}, the amount of N in a certain pool is represented by N_{NxOy}, while the total amount of the anaerobic N pool is represented by N_{AnTot})

$$B_{denit,i} = B_{denit,\, i-1} + \sum R_{g,NxOy} - R_{d,denit}$$

$$R_{g,NxOy} = \gamma_{d,NxOy} \cdot f(DOC) \cdot f(N_xO_y) \cdot M_{activity} \cdot B_{denit}$$

$$R_{d,denit} = d_d \cdot M_{activity} \cdot B_{denit}$$

$$M_{activity} = f(T) \cdot f_{micr}(pH) \cdot f(N_{AnTot}) \cdot f_{Anvol}(z) \cdot d_{actratecoef}$$

$$N_{rgNxOy} = \frac{R_{g,NxOy}}{d_{effNxOy} - R_{g,NxOy}}$$

$$N_{rmNxOy} = \frac{d_{rcNxOy} \cdot N_{NxOy}}{N_{AnTot}}$$

In **DNDC** model version 9.5 [79], the relative growth ($R_{g,nit}$, kg C ha^{-1} d^{-1}) and death ($R_{d,nit}$, kg C ha^{-1} d^{-1}) rates of nitrifiers microbes employ the dissolved organic carbon content (DOC, kg C ha^{-1}) of the soil layer and the same soil moisture factor ($f_n(W)$) employed for nitrification rate calculation.

$$R_{g,nit} = 0.0166 \cdot \left[\frac{DOC}{1 + DOC} + \frac{f_n(W)}{1 + f_n(W)} \right]$$

$$R_{d,nit} = 0.008 \cdot B_{nit} \cdot \frac{1}{(1 + [DOC]) \cdot (1 + f_n(W))}$$

The nitrifier biomass (B_{nit}, kg C ha^{-1}) is estimated considering their relative growth and death rates, a soil temperature factor ($f_n(T)$), and a soil moisture factor ($f_n(W)$).

$$B_{nit,i} = B_{nit,i-1} + \left[\left(R_{g,nit} - R_{d,nit} \right) \cdot B_{nit,i-1} \cdot f_n(T) \cdot f_n(W) \right]$$

The relative growth rate of denitrifiers ($\sum R_{g,NxOy}$, kg C ha^{-1} d^{-1}) is simulated on the base of the maximum growth rates of NO_3^-, NO_2^-, NO, or N_2O denitrifiers ($\gamma_{d,NxOy}$, d^{-1}). N_xO_y represents the concentration of NO_3^-, NO_2^-, NO, or N_2O in soil water (kg N ha^{-1}),

K_C is the half-saturation constant of soluble C in the Monod model (kg C m soil water^{-3}), K_N is the half-saturation constant of NO_3^-, NO_2^-, NO, or N_2O in the Monod model (kg N m soil water^{-3}), $f_d(T)$ is a temperature factor, and $f_d(pH)_{NO3}$, $f_d(pH)_{NO2}$, $f_d(pH)_{NO}$, and $f_d(pH)_{N2O}$ are soil pH factors.

$$\sum R_{g,NxOy} = \left\{ f_d(T) \cdot \left[R_{g,NO3} \cdot f_d(pH)_{NO3} + R_{g,NO2} \cdot f_d(pH)_{NO2} + R_{g,NO} \cdot f_d(pH)_{NO} + R_{g,N2O} \cdot f_d(pH)_{N2O} \right] \right\} \cdot B_{denit}$$

$$R_{g,NxOy} = \gamma_{d,NxOy} \cdot \left(\frac{[DOC]}{K_c + [DOC]} \right) \cdot \left(\frac{[N_xO_y]}{K_N + [N_xO_y]} \right)$$

The relative death rate of denitrifiers ($R_{d,denit}$, kg C ha^{-1} d^{-1}) depends on denitrifier biomass, maintenance respiration coefficient (M_C, kg C kg C^{-1} h^{-1}), and maximum growth yield on soluble carbon (Y_C, kg C kg C^{-1}). Furthermore, denitrifiers DOC consumption, N assimilation, and CO_2 production through denitrification are also simulated.

$$R_{d,denit} = M_C \cdot Y_C \cdot B_{denit}$$

In the GHG module of **DSSAT** model [70] V4.8.2.0 [77], both in the DAYCENT denitrification subroutine and in the CERES denitrification subroutine, the only difference is the equation of an auxiliary variable ($ratio_1$, unitless) employed in the estimate of the N_2/N_2O ratio ($R_{N2/N2O}$, unitless). The ratio is modified by considering the number of consecutive days (n_{day}, its maximum used value is 7) during which $WFPS > 0.8$ using an additional auxiliary variable ($ratio_2$, unitless).

$$ratio_{1,\ DAYCENT} = max[0.1,\ f_e(NO_3) \cdot f_e(W)]$$

$$ratio_{1,CERES} = \frac{1}{\left(\frac{NO_3}{NO_3 + 30} - 1 \right)}$$

$$ratio_2 = max\left[0, -330 + (334 \cdot WFPS) + \left(18.4 \cdot n_{day} \right) \right]$$

The SPACSYS model [71] derives its approach to microbial evolution for nitrification from [122]. The nitrifier biomass at the current time step (B_{nit}, g C m^{-2}) depends on the gross microbial growth rate ($R_{g,nit}$, kg C m^{-3} d^{-1}), microbial death rate ($R_{d,nit}$, kg C m^{-3} d^{-1}), and microbial maintenance respiration rate ($R_{resp,nit}$, kg C m^{-3} d^{-1}). The employed parameters are the maximum nitrifier gross growth (γ_n, d^{-1}), the maximum nitrifier death rate (d_n, d^{-1}), and an assimilation factor (ε_n, unitless).

$$B_{nit,i} = B_{nit,i-1} + R_{g,nit} - R_{d,nit} - R_{resp,nit} \quad (i = time\ step)$$

$$n_g = \gamma_n \cdot f(T) \cdot f_n(W) \cdot f_n(pH) \cdot f_n(DOC) \cdot f(NO_3) \cdot B_{nit,i-1}$$

$$n_d = d_n \cdot f(T) \cdot f_n(W) \cdot f_n(pH) \cdot f_n(DOC) \cdot B_{nit,i-1}$$

$$r_r = \left(\frac{1}{\varepsilon_n} - 1 \right) \cdot B_{nit,i-1}$$

The growth rate of N_xO_y denitrifiers ($R_{g,NxOy}$, kg C m^{-3} d^{-1}) depends on parameters quantifying the maximum growth rate of the N_xO_y denitrifiers ($\gamma_{d,NxOy}$, d^{-1}, 4 different values), on the denitrifier biomass (B_{denit}, g C m^{-2}), and on the response function ($f_d(N_xO_y)$) to the concentration of each N_xO_y (NO_3^-, NO_2^-, NO, and N_2O).

$$R_{g,\ NxOy} = \gamma_{d,NxOy} \cdot f_d(DOC) \cdot f_d\left(N_xO_y\right) \cdot f_{d,NxOy}(pH) \cdot f(T) \cdot B_{denit} \qquad (i = 1,\ 2,\ 3)$$

The growth rate of total denitrifiers ($\sum R_{g,NxOy}$, kg C m^{-3} d^{-1}) is obtained as the sum of all the N_xO_y denitrifier growth rates, while the death rate of total denitrifiers ($R_{d,denit}$, kg C m^{-3} d^{-1}) depends on their biomass, on the C maintenance respiration rate of total denitrifiers ($R_{resp,denit}$, kg C m^{-3} d^{-1}). Two parameters are used: a maintenance coefficient on C (M_c, d^{-1}, 0.0031) and a maximum growth yield on DOC (Y_c, g C g^{-1} N, 0.503).

$$R_{d,denit} = M_c \cdot Y_c \cdot B_{denit}$$

$$R_{resp,denit} = \frac{\sum R_{g,\ NxOy}}{Y_c} + M_c \cdot B_{denit}$$

$$B_{denit,i} = B_{denit,i-1} + \sum R_{g,\ NxOy} - R_{d,denit} - R_{resp,denit} \qquad (i = time\ step)$$

Appendix A.3 Tables

Table A1. Nitrification module variables, unit of measures, original model symbols (original symbol), and symbols used in the present review (review symbol).

Model	Variable	Unit	Original Symbol	Review Symbol
APSIM	nitrification rate	mg N g^{-1} d^{-1}	R_{nit}	R_{nit}
ARMOSA	nitrification rate	kg N ha^{-1} d^{-1}	Nit_NH_4	R_{nit}
ARMOSA	nitrate amount	kg N ha^{-1}	NO_3	NO_3
ARMOSA	ammonium amount	kg N ha^{-1}	NH_4	NH_4
CERES-EGC	nitrification rate	kg N ha^{-1} d^{-1}	N_i	R_{nit}
CoupModel	nitrification rate	g N m^{-2} d^{-1}	$N_{NH4\rightarrow NO3}$	R_{nit}
CoupModel	nitrifier biomass	g m^{-2}	N_{micrN}	B_{nit}
CROPSYST	nitrification rate	kg N ha^{-1} d^{-1}	$N_{NH4\rightarrow NO3}$	R_{nit}
CROPSYST	ammonium amount	kg N ha^{-1}	N_{NH4}	NH_4
CROPSYST	nitrate amount	kg N ha^{-1}	N_{NO3}	NO_3
DAYCENT	nitrification rate	g N m^{-2} d^{-1}	FNO_3	R_{nit}
DAYCENT	mineralization rate	g N m^{-2}	Net_{mm}	Net_{mm}
DAYCENT	ammonium amount	g N m^{-2}	NH_4	NH_4
DNDC	nitrification rate	kg N ha^{-1} d^{-1}	RN	R_{nit}
DNDC	ammonium amount	kg N ha^{-1}	[NH_4^+]	NH_4
DNDC	nitrifier biomass	kg C ha^{-1}	Nitrifier	B_{nit}
DSSAT	nitrification rate	kg N ha^{-1} d^{-1}	NITRIF	R_{nit}
DSSAT	ammonium amount	kg N ha^{-1}	NH_4	NH_4
EPIC	nitrification rate	kg N ha^{-1} d^{-1}	RNIT	R_{nit}
EPIC	volatilization rate	kg N ha^{-1} d^{-1}	AVOL	R_{vol}
EPIC	ammonium amount	kg N ha^{-1}	NH_3	NH_4
EPIC	auxiliary variable	unitless	AKAV	AKAV
EPIC	soil temperature	°C	STMP	T
SPACSYS	nitrification rate (microbial explicit)	g N m^{-2} d^{-1}	n_n	R_{nit}
SPACSYS	water-filled pore space	unitless	WFPS	WFPS
SPACSYS	nitrifier biomass	g C m^{-2}	M_b	B_{nit}
SPACSYS	nitrification rate	g N m^{-2} d^{-1}	N_{nitri}	R_{nit}
STICS	nitrification rate (layer)	kg N ha^{-1} cm^{-1} d^{-1}	TNITRIF	R_{nit}
STICS	nitrification rate (total)	kg N ha^{-1} d^{-1}	NITRIF	$R_{nit(total)}$
STICS	ammonium amount	kg N ha^{-1}	AMM	NH_4
all model	nitrification response function to soil temperature	unitless	various	$f_n(T)$
all model	nitrification response function to soil moisture	unitless	various	$f_n(W)$
all model	nitrification response function to soil acidity	unitless	various	$f_n(pH)$
all model	nitrification response function to ammonium level	unitless	various	$f_n(NH_4)$

Table A2. Nitrification module parameters, unit of measure, original model symbol, and symbol used in the present review, default values [range].

Model	Parameter	Unit	Original Symbol	Review Symbol	Default
APSIM	nitrification coefficient	mg N g^{-1} d^{-1}	V_{max}	V_{max}	40
APSIM	nitrification half-saturation constant	mg N g^{-1}	K_m	K_m	90
ARMOSA	nitrification coefficient	d^{-1}	k_n	k_{nit}	0.2
ARMOSA	NO_3:NH_4 ratio	unitless	N_{ratio}	$r_{NO3/NH4}$	8 [1–15]
CERES-EGC	nitrification coefficient	kg N ha^{-1} d^{-1}	MNR	k_{nit}	-
CoupModel	pH response function coefficient	unitless	n_{pH}	k_{pH}	1
CoupModel	nitrification coefficient	mg ha d^{-1} kg^{-1}	$n_{micrate}$	k_{nit}	0.25
CROPSYST	nitrification coefficient	d^{-1}	NITK	k_{nit}	0.2
CROPSYST	NO_3:NH_4 ratio	unitless	NITR	$r_{NO3/NH4}$	8 [1–15]
DAYCENT	nitrified fraction of Net_{mm}	d^{-1}	K_1	k_{nit2}	0.2
DAYCENT	nitrified fraction of NH_{4+}	d^{-1}	K_{max}	k_{nit}	0.1
DNDC	nitrification coefficient	d^{-1}	0.005	k_{nit}	0.005
EPIC	nitrified/volatilized fraction of NH3	unitless	PARAM(64)	k_{nit3}	[0–1]
SPACSYS	nitrification coefficient (microbial explicit)	d^{-1}	n_{nmax}	k_{nit}	0.004
SPACSYS	nitrification coefficient	d^{-1}	k_{nitri}	k_{nit}	-
STICS	max depth for nitrification	cm	$PROFHUM_S$	z_{nit}	30
STICS	nitrification coefficient	d^{-1}	FNX_G	k_{nit}	0.5
STICS	N_2O:total nitrification ratio	unitless	$RATIONIT_S$	$r_{N2O/nit}$	-

Table A3. Denitrification module variables, unit of measures, original model symbols (original symbol), and symbols used in the present review (review symbol).

Model	Variable	Unit	Original Symbol	Review Symbol
APSIM	denitrification rate	kg N ha^{-1} d^{-1}	R_{denit}	R_{denit}
APSIM	nitrate amount	kg N ha^{-1}	NO_3	NO_3
APSIM	active C concentration	ppm	C_A	$[C_A]$
ARMOSA	denitrification rate	kg N ha^{-1} d^{-1}	Denit_NO_3	R_{denit}
ARMOSA	nitrate concentration	kg N L^{-1}	Conc_NO_3	$[NO_3]$
CERES-EGC	denitrification rate	kg N ha^{-1} d^{-1}	PDR	R_{denit}
CoupModel	denitrification rate	g N m^{-2} d^{-1}	$N_{NO3\rightarrow Denit}$	R_{denit}
CoupModel	N_xO_y consumption rate	g N m^{-2} d^{-1}	$N_{NxOy\rightarrow AnNxOy}$	$N_{NxOy\rightarrow AnNxOy}$
CoupModel	N_xO_y content in the anaerobic pool	g N m^{-2} d^{-1}	AnNxOy	AnNxOy
CoupModel	d_{pot} depth-adjustment coefficient	unitless	d_{dist}	z_{adj}
CROPSYST	denitrification rate	kg N ha^{-1} d^{-1}	D_a	R_{denit}
DAYCENT	denitrification rate	µg N g $soil^{-1}$ d^{-1}	D_t	R_{denit}
DNDC	N_xO_y consumption rate	kg N ha^{-1} d^{-1}	dNOx/dt	$R_{c,NxOy}$
DNDC	denitrifier biomass	kg N ha^{-1}	Denitrifier	B_{denit}
DSSAT	denitrification rate	kg N ha^{-1} d^{-1}	DENITRIF	R_{denit}
DSSAT	volumetric soil water content	m^3 m^{-3}	SW	SWC
DSSAT	drained upper limit	m^3 m^{-3}	DUL	DUL
DSSAT	soil temperature	K	ST	T
DSSAT	water-extractable soil C	kg C ha^{-1}	CW	C_W
DSSAT	nitrate amount	kg N ha^{-1}	NO_3	NO_3
EPIC	denitrification rate	kg N ha^{-1} d^{-1}	DN	R_{denit}
EPIC	soil weight	kg	WT	WT
EPIC	nitrate amount	kg N ha^{-1}	NO_3	NO_3
SPACSYS	N_xO_y consumption rate	kg N m^{-3} d^{-1}	$d_{c,i}$	$R_{c,NxOy}$

Table A3. *Cont.*

Model	Variable	Unit	Original Symbol	Review Symbol
SPACSYS	N_xO_y concentration	kg N m^{-3}	N_i	$[N_xO_y]$
SPACSYS	total N_xO_y concentration	kg N m^{-3}	N_{total}	$\sum[N_xO_y]$
SPACSYS	denitrification rate	g N m^{-2} d^{-1}	N_{deni}	R_{denit}
STICS	denitrification rate (total)	kg N ha^{-1} d^{-1}	NDENENG	R_{denit}
all model	denitrification response function to soil temperature	unitless	various	$f_d(T)$
all model	denitrification response function to soil moisture	unitless	various	$f_d(W)$
all model	denitrification response function to soil acidity	unitless	various	$f_d(pH)$
all model	denitrification response function to N_xO_y level	unitless/μg N g $soil^{-1}$ d^{-1}	various	$f_d(N_xO_y)$
all model	denitrification response function to DOC level	unitless	various	$f_d(DOC)$
all model	denitrification response function to heterotrophic respiration	unitless/μg N g $soil^{-1}$ d^{-1}	various	$f_d(CO_2)$

Table A4. Denitrification module parameters, unit of measure, original model symbol, and symbol used in the present review, default values [range].

Model	Parameter	Unit	Original Symbol	Review Symbol	Default
APSIM	denitrification coefficient	Unitless	k_{denit}	k_{denit}	0.0006
ARMOSA	denitrification coefficient	kg N ha^{-1} d^{-1}	k_d	k_{denit}	[0.04–0.2]
ARMOSA	denitrification half-saturation constant	mg N L^{-1}	Hsconst	K_m	[5–15]
CERES-EGC	denitrification coefficient	kg N ha^{-1} d^{-1}	PDR	k_{denit}	-
CoupModel	denitrification coefficient	g N m^{-2} d^{-1}	d_{pot}	k_{denit}	0.04
CROPSYST	denitrification coefficient	kg N ha^{-1} d^{-1}	D_p	k_{denit}	-
DNDC	growth yield on N_xO_y	kg C kg N^{-1}	Y_{NOx}	Y_{NxOy}	-
DNDC	maintenance coefficient on N_xO_y	kg N kg^{-1} h^{-1}	M_{NOx}	M_{NxOy}	-
DSSAT	max depth for denitrification	m	Denit_depth	z_{denit}	0.3
DSSAT	denitrification coefficient	d^{-1}	0.0006	k_{denit}	0.0006
EPIC	denitrification coefficient	Unitless	DNITMX	k_{denit}	32
SPACSYS	denitrification coefficient	g N m^{-2} d^{-1}	k_{deni}	k_{denit}	-
SPACSYS	maintenance coefficient on N_xO_y	g C g N^{-1} d^{-1}	M_{Ni}	M_{NxOy}	Table A8
SPACSYS	growth yield on N_xO_y	g C g N^{-1}	Y_{Ni}	Y_{NxOy}	Table A8
SPACSYS	growth rate on N_xO_y	d^{-1}	γ_{gd}	γ_{gd}	Table A8
STICS	denitrification coefficient	kg N ha^{-1} d^{-1}	$VPOTDENIT_S$	k_{denit}	16
STICS	max depth for denitrification	cm	$PROFDENIT_S$	z_{denit}	20

Table A5. Emissions module variables, unit of measures, original model symbols (original symbol), and symbols used in the present review (review symbol).

Model	Variable	Unit	Original Symbol	Review Symbol
APSIM	nitrification N_2O emission rate	kg N ha^{-1} d^{-1}	N_2O_{nit}	N_2O_{nit}
APSIM	denitrification N_2O emission rate	kg N ha^{-1} d^{-1}	N_2O_{denit}	N_2O_{denit}
APSIM	nitrate concentration	μg N g^{-1}	NO_{3ppm}	$[NO_3]$
APSIM	heterotrophic respiration rate	μg C g $soil^{-1}$ d^{-1}	CO_2	$CO_{2,resp}$
ARMOSA	nitrification N_2O emission rate	kg N ha^{-1} d^{-1}	Nit_N_2O	N_2O_{nit}
ARMOSA	denitrification N_2O emission rate	kg N ha^{-1} d^{-1}	Denit_N_2O	N_2O_{denit}
ARMOSA	nitrate amount	kg N ha^{-1}	NO_3	NO_3
ARMOSA	heterotrophic respiration rate	kg C ha^{-1} d^{-1}	CO_2	$CO_{2,resp}$
ARMOSA	soil water content at saturation	m^3 m^{-3}	SWC_{sat}	SWC_{sat}

Table A5. *Cont.*

Model	Variable	Unit	Original Symbol	Review Symbol
CoupModel	nitrification NO emission rate	g N m^{-2} d^{-1}	NO_{nit}	NO_{nit}
CoupModel	emissions response function to soil temperature	unitless	$f_e(T)$	$f_e(T)$
CoupModel	emissions response function to soil moisture	unitless	$f_e(W)$	$f_e(W)$
CoupModel	emissions response function to soil acidity	unitless	$f_e(pH)$	$f_e(pH)$
CoupModel	nitrification N_2O emission rate	g N m^{-2} d^{-1}	N_2O_{nit}	N_2O_{nit}
CROPSYST	denitrification N_2O emission rate	μg N kg^{-1} d^{-1}	D_{N2O}	N_2O_{denit}
CROPSYST	N_2/N_2O ratio	unitless	$R_{N2/N2O}$	$R_{N2/N2O}$
CROPSYST	denitrification N_2 emission rate	μg N kg^{-1} d^{-1}	D_{N2}	$N_{2,denit}$
CROPSYST	emissions response function to nitrate level	unitless	$f_r(NO_3)$	$f_e(NO_3)$
CROPSYST	emissions response function to heterotrophic respiration	unitless	$f_r(CO_2)$	$f_e(CO_2)$
CROPSYST	emissions response function to soil moisture	unitless	$f_r(W)$	$f_e(W)$
DAYCENT	denitrification N_2O emission rate	g N m^{-2} d^{-1}	N_2O_{denit}	N_2O_{denit}
DAYCENT	N_2/N_2O ratio	unitless	$R_{N2/N2O}$	$R_{N2/N2O}$
DAYCENT	D_{FC} function	unitless	$F_r(NO_3/CO_2)$	$f_e(NO_3/CO_2)$
DAYCENT	N_2/N_2O ratio response function to soil moisture	unitless	F_r(WFPS)	$f_e(W)$
DAYCENT	nitrification N_2O emission rate	g N m^{-2} d^{-1}	N_2O_{nit}	N_2O_{nit}
DAYCENT	NO_x emission rate	g N m^{-2} d^{-1}	NO_x	$NO_{x,nit+denit}$
DAYCENT	NO_x/N_2O ratio	unitless	RNO_x	$R_{NOx/N2O}$
DAYCENT	pulse multiplier	unitless	P	P
DNDC	nitrification N_2O emission rate	kg N ha^{-1} d^{-1}	N_2O_N	N_2O_{nit}
DNDC	denitrification N_2O emitted fraction	unitless	$P(N_2O)$	$P(N_2O)$
DNDC	denitrification N_2 emitted fraction	unitless	$P(N_2)$	$P(N_2)$
DSSAT	nitrification N_2O emission rate	kg N ha^{-1} d^{-1}	N_2O_{nit}	N_2O_{nit}
DSSAT	nitrification NO emission rate	kg N ha^{-1} d^{-1}	NO_{nit}	NO_{nit}
DSSAT	NO/N_2O ratio	unitless	NO_N2O_ratio	$R_{NOx/N2O}$
DSSAT	pulse multiplier	unitless	P	P
DSSAT	denitrification N_2O emission rate	kg N ha^{-1} d^{-1}	N_2O_{denit}	N_2O_{denit}
DSSAT	denitrification N_2 emission rate	kg N ha^{-1} d^{-1}	N_2	$N_{2,denit}$
DSSAT	N_2/N_2O ratio	unitless	Rn2n2o	$R_{N2/N2O}$
DSSAT	auxiliary variable	unitless	ratio1	$ratio_1$
DSSAT	auxiliary variable	unitless	ratio2	$ratio_2$
DSSAT	emissions response function to nitrate level	unitless	$f_e(NO_3)$	$f_e(NO_3)$
DSSAT	emissions response function to soil moisture	unitless	$f_e(W)$	$f_e(W)$
DSSAT	water-filled pore space	unitless	WFPS	WFPS
EPIC	denitrification N_2O emission rate	kg N ha^{-1} d^{-1}	DN2O	N_2O_{denit}
EPIC	denitrification N_2 emission rate	kg N ha^{-1} d^{-1}	DN2	$N_{2,denit}$
SPACSYS	denitrification N_2O emitted fraction	unitless	$P(N_2O)$	$P(N_2O)$
SPACSYS	denitrification N_2 emitted fraction	unitless	$P(N_2)$	$P(N_2)$
SPACSYS	adsorption factor	unitless	AD	f_e(AD)
SPACSYS	total porosity air-filled fraction	unitless	AP	1-WFPS
SPACSYS	nitrification N_2O emission rate	ng N g $soil^{-1}$ d^{-1}	N_2O	N_2O_{nit}
SPACSYS	soil temperature	°C	T	T
STICS	nitrification N_2O emission rate	kg N ha^{-1} d^{-1}	N_2O_{nit}	N_2O_{nit}
STICS	denitrification N_2O emission rate	kg N ha^{-1} d^{-1}	N_2O_{denit}	N_2O_{denit}

Table A6. Emissions module parameters, unit of measure, original model symbols (original symbol), and symbols used in the present review (review symbol), default values [range].

Model	Parameter	Unit	Original Symbol	Review Symbol	Default
APSIM	N_2O emission: total nitrification ratio	unitless	k_2	$r_{N2O/nit}$	0.002
APSIM	gas diffusivity	unitless	k_1	g_{diff}	25.1
ARMOSA	N_2O emission: total nitrification ratio	unitless	f_{N2O}	$r_{N2O/nit}$	0.002

Table A6. *Cont.*

Model	Parameter	Unit	Original Symbol	Review Symbol	Default
ARMOSA	gas diffusivity	unitless	$diff_d$	g_{diff}	25.1
CERES-EGC	N_2O emission: total nitrification ratio	unitless	C	$r_{N2O/nit}$	-
CERES-EGC	N_2O emission: total denitrification ratio	unitless	R	$r_{N2O/denit}$	-
CoupModel	NO emission: total nitrification ratio	unitless	$g_{mfracNO}$	$r_{NO/nit}$	0.004
CoupModel	N_2O emission: total nitrification ratio	unitless	$g_{mfracN2O}$	$r_{N2O/nit}$	0.0006
DAYCENT	gas diffusivity	unitless	D_{FC} or D/D_0	g_{diff}	-
DAYCENT	N_2O emission: total nitrification ratio	unitless	K_2	$r_{N2O/nit}$	0.02
DNDC	N_2O emission: total nitrification ratio	unitless	0.0024	$r_{N2O/nit}$	0.0024
DSSAT	N_2O emission: total nitrification ratio	unitless	0.001	$r_{N2O/nit}$	0.001
DSSAT	gas diffusivity	unitless	D_{FC}	g_{diff}	-
DSSAT	gas diffusivity	unitless	dD0	g_{diff}	-
EPIC	N_2 emission: total denitrification	unitless	PARM(80)	$r_{N2/denit}$	[0.1–0.9]
STICS	N_2O emission: total nitrification ratio	unitless	$RATIONIT_S$	$r_{N2O/nit}$	-
STICS	N_2O emission: total denitrification ratio	unitless	$RATIODENIT_S$	$r_{N2O/denit}$	-

Table A7. Parameters of the environmental response functions of nitrification (nit.), denitrification (denit.), and emissions (emiss.): unit of measures, original model symbols (original symbol), and symbols used in the present review (review symbol), default values [range].

Function	Model	Parameter	Unit	Original Symbol	Review Symbol	Default
f(T)	ARMOSA	response to a 10 °C T change	unitless	Q_{10}	t_{Q10}	2 [1.5–4.0]
f(T)	ARMOSA	base T for the microbial activity	°C	T_{base}	T_{opt}	20
f(T)	CERES-EGC	nit. response to a 10 °C T change	unitless	$Q10_{nit}$	t_{Q10}	2.1
f(T)	CERES-EGC	denit. threshold T	°C	TTr_{denit}	T_{denit}	11
f(T)	CERES-EGC	denit. response to a 10 °C T change	unitless	$Q10_{denit,1}$	$t_{Q10,1}$	89
f(T)	CERES-EGC	denit. response to a 10 °C T change	unitless	$Q10_{denit,2}$	$t_{Q10,2}$	2.1
f(T)	CoupModel	nit./denit. cardinal T_{min}	°C	t_{min}	T_{min}	−8
f(T)	CoupModel	nit./denit. cardinal T_{max}	°C	t_{max}	T_{max}	20
f(T)	CoupModel	base T for microbial activity	°C	$t_{Q10base}$	T_{opt}	20
f(T)	CoupModel	Q10 threshold	°C	$t_{Q10thres}$	$T_{Q10thres}$	5
f(T)	CoupModel	response to a 10 °C T change	unitless	t_{Q10}	t_{Q10}	2
f(T)	CoupModel	emissions T_{max}	°C	$g_{TmaxNxO}$	$g_{TmaxNxO}$	33.5
f(T)	CoupModel	emissions T_{opt}	°C	$g_{ToptNxO}$	$g_{ToptNxO}$	23.5
f(T)	CoupModel	response function shape coefficient	unitless	$g_{TshapeNxO}$	$g_{TshapeNxO}$	1.5
f(T)	CROPSYST	nitrification cardinal T_{opt}	°C	TEMBAS	$T_{opt,nit}$	20
f(T)	CROPSYST	response to a 10 °C T change	unitless	TEMQ10	t_{Q10}	3 [1.5–4.0]
f(T)	DNDC	denitrification cardinal T_{max}	°C	60	$T_{max,denit}$	60
f(T)	STICS	nitrification cardinal T_{min}	°C	$TNITMIN_G$	$T_{min,nit}$	5
f(T)	STICS	nitrification cardinal T_{opt}	°C	$TNITOPT_G$	$T_{opt,nit}$	20
f(T)	STICS	nitrification cardinal T_{max}	°C	$TNITMAX_G$	$T_{max,nit}$	45
f(T)	STICS	denitrification cardinal T_1	°C	$TDENREF1_G$	$T_{1,denit}$	11
f(T)	STICS	denitrification cardinal T_2	°C	$TDENREF2_G$	$T_{2,denit}$	20
f(W)	APSIM	SWC at which denitrification ceases	$m^3\ m^{-3}$	SWC_{lim}	SWC_{lim}	-
f(W)	APSIM	empirical coefficient	unitless	X	x	1 [0.9–5.0]
f(W)	ARMOSA	empirical coefficient	unitless	$denit_{WC}$	x	1 [0.9–5.0]
f(W)	ARMOSA	microbial activity below SWC_{min}	unitless	f_{min}	f_{min}	0
f(W)	ARMOSA	microbial activity above SWC_{max}	unitless	f_{max}	f_{max}	0.5
f(W)	ARMOSA	response function shape coefficient	unitless	A	a	1
f(W)	ARMOSA	response function shape coefficient	unitless	B	b	1
f(W)	ARMOSA	saturation threshold	unitless	thr_{sat}	thr_{sat}	0.6
f(W)	ARMOSA	lower threshold	unitless	thr_{denit}	thr_{denit}	0.05
f(W)	CERES-EGC	minimum WFPS for nitrification	%	MIN_{WFPS}	$WFPS_{min,nit}$	0.1
f(W)	CERES-EGC	optimum WFPS for nitrification	%	OPT_{WFPS}	$WFPS_{opt,nit}$	0.6
f(W)	CERES-EGC	maximum WFPS for nitrification	%	MAX_{WFPS}	$WFPS_{max,nit}$	0.8
f(W)	CERES-EGC	threshold WFPS for denitrification	%	Tr_{WFPS}	$WFPS_{denit}$	0.62

Table A7. *Cont.*

Function	Model	Parameter	Unit	Original Symbol	Review Symbol	Default
f(W)	CERES-EGC	denit. response function exponent	unitless	POW_{denit}	x	1.74
f(W)	CoupModel	SWC effect on denit. coefficient	unitless	$p_{\theta Dp}$	$p_{\theta Dp}$	10
f(W)	CoupModel	SWC range from saturation	%	$p_{\theta DRange}$	$p_{\theta DRange}$	10
f(W)	CoupModel	saturation activity	unitless	$p_{\theta satact}$	$p_{\theta satact}$	0.6 [0–1]
f(W)	CoupModel	water content interval lower limit	%	$p_{\theta Low}$	$p_{\theta Low}$	13 [8–15]
f(W)	CoupModel	function shape coefficient	unitless	$p_{\theta p}$	$p_{\theta p}$	1
f(W)	CoupModel	water content interval upper limit	%	$p_{\theta Upp}$	$p_{\theta Upp}$	8 [1–10]
f(W)	CoupModel	relative saturation level	unitless	$g_{\theta satcrit}$	$g_{\theta satcrit}$	Table A8
f(W)	CoupModel	function shape coefficient	unitless	$g_{\theta satform}$	$g_{\theta satform}$	Table A8
f(W)	CROPSYST	saturation activity	unitless	MOSSA	$p_{\theta satact}$	0.6 [0–1]
f(W)	CROPSYST	function shape coefficient	unitless	MOSM	$p_{\theta p}$	1
f(W)	CROPSYST	water content interval lower limit	%	MOS(1)	$p_{\theta Low}$	13 [8–15]
f(W)	CROPSYST	water content interval upper limit	%	MOS(2)	$p_{\theta Upp}$	8 [1–10]
f(W)	SPACSYS	soil bulk density	g cm^{-3}	ρ_d	BD	-
f(W)	SPACSYS	soil particle density	g cm^{-3}	ρ_s	PD	-
f(W)	STICS	optimal SWC for nitrification	unitless	$HOPTN_G$	$SWC_{opt,nit}$	1.0
f(W)	STICS	minimum SWC for nitrification	unitless	$HIMINN_G$	$SWC_{min,nit}$	0.67
f(W)	STICS	reference T for mineralization	°C	$TREF_G$	T_{miner}	15
f(W)	STICS	soil bulk density	g cm^{-3}	DA	BD	-
f(pH)	APSIM	nitrification pH minimum threshold	unitless	-	pH_{min}	4.5
f(pH)	APSIM	nit. pH optimum minimum value	unitless	-	pH_{optmin}	6
f(pH)	APSIM	nit. pH optimum maximum value	unitless	-	pH_{optmax}	8
f(pH)	APSIM	nitrification pH maximum threshold	unitless	-	pH_{max}	9
f(pH)	ARMOSA	nitrification pH minimum threshold	unitless	PHMIN	pH_{min}	3
f(pH)	ARMOSA	nitrification pH maximum threshold	unitless	PHMAX	pH_{max}	5.5
f(pH)	CoupModel	pH half rate	unitless	d_{pHrate}	d_{pHrate}	4.25
f(pH)	CoupModel	shape coefficient	unitless	$d_{pHshape}$	$d_{pHshape}$	0.5
f(pH)	CoupModel	nitrification pH minimum threshold	unitless	$g_{pHcoeff}$	pH_{min}	4.7
f(pH)	CROPSYST	nitrification pH minimum threshold	unitless	PHMIN	pH_{min}	-
f(pH)	CROPSYST	nitrification pH maximum threshold	unitless	PHMAX	pH_{max}	-
f(pH)	DAYCENT	parameter of arctan function	unitless	A	a	-
f(pH)	DSSAT	nitrification pH minimum threshold	unitless	-	pH_{min}	-
f(pH)	DSSAT	nitrification pH optimum threshold	unitless	-	pH_{opt}	-
f(pH)	EPIC	nit. pH optimum minimum value	unitless	-	pH_{optmin}	7
f(pH)	EPIC	nit. pH optimum maximum value	unitless	-	pH_{optmax}	7.4
f(pH)	STICS	nitrification pH minimum threshold	unitless	$PHMINNIT_G$	pH_{min}	3
f(pH)	STICS	nitrification pH maximum threshold	unitless	$PHMAXNIT_G$	pH_{max}	5.5
f(S)	CERES-EGC	nit. half-saturation constant	mg N kg^{-1}	Km_{nit}	$K_{m,nit}$	10
f(S)	CERES-EGC	denit. half-saturation constant	mg N kg^{-1}	Km_{denit}	$K_{m,denit}$	22
f(S)	CoupModel	half-saturation constant	mg N L^{-1}	$d_{Nhalfsat}$	K_m	10 [5–15]
f(S)	CoupModel	layer thickness	m	Δz	z_{layer}	-
f(S)	CoupModel	NO_3:NH_4 ratio	unitless	$r_{nitr,amm}$	$r_{NO3/NH4}$	8 [1–15]
f(S)	CoupModel	nit. coefficient	d^{-1}	n_{rate}	k_{nit}	0.2
f(S)	CoupModel	nit. half-saturation constant	mg N L^{-1}	$n_{hrateNH}$	K_m	6.18
f(S)	DSSAT	minimum nitrate amount	kg N ha^{-1} d^{-1}	min_nitrate	$NO_{3,min}$	0.1
f(S)	SPACSYS	half-saturation constant	g C m^{-3} or g N m^{-3}	k_m	K_m	[9.45–18.53]

Table A8. N_xO_y oxide-specific parameters default values.

Model	Module	Parameter	NO_3^- Value	NO_2^- Value	NO Value	N_2O Value
CoupModel	emissions	$g_{\theta satcrit}$	-	-	0.45	0.55
CoupModel	emissions	$g_{\theta satform}$	-	-	0.024	0.24
CoupModel	microbial biomass	$\gamma_{d,NxOy}$	16	16	8.2	8.2
CoupModel	microbial biomass	$d_{effNxOy}$	0.401	0.428	0.428	0.151
CoupModel	microbial biomass	d_{rcNxOy}	2.2	0.84	0.84	1.9
SPACSYS	microbial biomass	γ_{gd}	13.65	7.83	8.28	8.81
SPACSYS	denitrification	Y_{NxOy}	0.65	0.17	0.75	0.24
SPACSYS	denitrification	M_{NxOy}	2.16	8.38	1.90	1.90

Table A9. Overview of the selected model evaluation studies analyzed in this review. The type of evaluation (Ev.) is classified into calibration (CAL.) and validation (VAL.). The country code (Coun.) is reported together with the Köppen climate classification (K. C.) of the field trial site. The crop or the crop rotation (Crop) for which each treatment was tested are reported: potatoes, winter wheat, white cabbage, winter barley, grass-clover ley (rotation 1); rice, pepper, Chinese cabbage, white radish, cowpea (rotation 2); tomato, lettuce, cabbage, packchoi (rotation 3); corn, soybean, winter wheat (rotation 4); corn, soybean, and alfalfa (rotation 5). The tested treatment (Tr.) reviewed are the following: zero N control (N_0), mineral N fertilization (N_{min}), organic N fertilization (N_{org}), sandy–loam soil (SL), sandy–clay–loam soil (SCL), clay–loam soil (CL), crop management ($Crop_{mng}$), and soil moisture conditions (SWC). Averaged values of the fitting indices, referring to several tested treatments, are also reported (Overall) if published in the original evaluation study. The progressive number within each reference (Ref.) and type of evaluation combination of the tested treatments (n°) are also reported. The type of measure (Meas.) is classified into continuous measure (C) and not-continuous measure (N), while the value employed for N_2O emissions fitting (Fit.) is classified as daily value (d) and as cumulated value (c). The following evaluation metrics are reported: Pearson's correlation coefficient (*r*), coefficient of determination (R^2), root mean squared error (*RMSE*, kg N-N_2O ha^{-1}), *RMSE* at the 95% confidence level ($RMSE_{95}$, kg N-N_2O ha^{-1}), modeling efficiency (*EF*), relative root mean squared error (*RRMSE*, %), R^2 significance level (*p*-value).

Model	Ref.	Ev.	Coun.	K. C.	Crop	Meas.	Fit.	n°	Tr.	*r*	R^2	*RMSE*	$RMSE_{95}$	*EF*	*RRMSE*	*p*-Value
APSIM	[16]	CAL.	CHN	Cfb	corn	C	d	2	N_{min}	-	0.31	-	-	-	-	-
	[16]	CAL.	CHN	Cfb	corn	C	d	2	N_{min}	-	0.52	-	-	-	-	-
	[16]	CAL.	CHN	Cfb	corn	C	d	2	N_{min}	-	0.56	-	-	-	-	-
	[16]	CAL.	CHN	Cfb	corn	C	c	2	N_{min}	-	0.3	-	-	-	-	-
	[16]	CAL.	CHN	Cfb	corn	C	c	2	N_{min}	-	0.67	-	-	-	-	-
	[16]	CAL.	CHN	Cfb	corn	C	c	2	N_{min}	-	0.5	-	-	-	-	-
	[16]	VAL.	CHN	Cfb	winter wheat–corn	C	c	-	Overall	-	0.74	0.71	-	-	-	-
	[16]	VAL.	CHN	Cfb	winter wheat–corn	C	c	-	Overall	-	0.76	0.63	-	-	-	-
	[16]	VAL.	CHN	Cfb	winter wheat–corn	C	d	1	N_0	-	0.05	0.01	-	-	-	-
	[16]	VAL.	CHN	Cfb	winter wheat–corn	C	d	2	N_{min}	-	-	-	-	-	-	-
	[16]	VAL.	CHN	Cfb	winter wheat–corn	C	d	3	N_{min}	-	0.38	0.03	-	-	-	-
	[16]	VAL.	CHN	Cfb	winter wheat–corn	C	d	4	N_{org} + N_{min}	-	0.4	0.03	-	-	-	-
	[16]	VAL.	CHN	Cfb	winter wheat–corn	C	d	1	N_0	-	0.08	0.01	-	-	-	-
	[16]	VAL.	CHN	Cfb	winter wheat–corn	C	d	2	N_{min}	-	-	-	-	-	-	-
	[16]	VAL.	CHN	Cfb	winter wheat–corn	C	d	3	N_{min}	-	0.45	0.03	-	-	-	-
	[16]	VAL.	CHN	Cfb	winter wheat–corn	C	d	4	N_{org} + N_{min}	-	0.47	0.02	-	-	-	-
CERES-EGC	[90]	VAL.	IT	Csa	faba beans	C	d	1	N_{org}		0.74	0.002	2.09×10^{-3}		-	
	[89]	VAL.	SW	Cfb	sugar beet–winter wheat	N	d	1	N_0		0.37	0.006	6.18×10^{-3}	-	-	-
CoupModel	[7]	CAL.	SE	Cfb	red clover–winter wheat	N	c	1–16	N_{min} + SWC	-	0.96	0.82	-	-	275	-
	[7]	CAL.	SE	Cfb	red clover–winter wheat	N	c	16	Overall	-	0.47	0.71	-	-	278	-
	[91]	VAL.	DE	Cfb	rapeseed	N	d	1	N_0	-	0.26	0.04	-	-	-	-
	[91]	VAL.	DE	Cfb	rapeseed	N	d	2	N_{min}	-	0.18	0.04	-	-	-	-
	[91]	VAL.	DE	Cfb	rapeseed	N	d	3	N_{min}	-	0.5	0.05	-	-	-	-
DAYCENT	[11]	VAL.	USA	Bsk	grassland	N	c	1	SL		0.35	-	-	-	-	0.045
	[11]	VAL.	USA	Bsk	grassland	N	c	3	SCL	-	0.18	-	-	-	-	0.19
	[11]	VAL.	USA	Bsk	grassland	N	c	2	N_{min} + SL	-	0.46	-	-	-	-	0.16
	[11]	VAL.	USA	Bsk	grassland	N	c	5	CL	-	0.64	-	-	-	-	0.01
	[11]	VAL.	USA	Bsk	grassland	N	c	-	Overall	-	0.26	-	-	-	-	0.0001
	[93]	VAL.	USA	Bsk	corn	N	c	1	Overall	-	0.29	-	-	-	-	-
	[92]	VAL.	CH	Cfb	rotation 1	N	c	1	Overall	-	0.89	1.04	-	-	25	-
	[11]	VAL.	USA	Bsk	grassland	N	c	4	N_{min} + SCL	-	0.02	-	-	-	-	0.69
	[11]	VAL.	USA	Bsk	grassland	N	d	1	SL		0.07	-	-	-	-	0.0001
	[11]	VAL.	USA	Bsk	grassland	N	d	3	SCL	-	0.08	-	-	-	-	0.0006
	[11]	VAL.	USA	Bsk	grassland	N	d	2	N_{min} + SL	-	0.19	-	-	-	-	0.0001
	[11]	VAL.	USA	Bsk	grassland	N	d	5	CL	-	0.02	-	-	-	-	0.1
	[11]	VAL.	USA	Bsk	grassland	N	d	-	Overall	-	0.09	-	-	-	-	0.0001
	[11]	VAL.	USA	Bsk	grassland	N	d	4	N_{min} + SCL	-	0.02	-	-	-	-	0.14
DNDC v.9.5	[95]	VAL.	CHN	Cfa	rotation 3	C	c	-	Overall	-	0.95	-	-	-	-	-
	[94]	CAL.	CHN	Cfa	rotation 2	N	c	4	Overall	-	0.75	0.51	-	-	-	-
	[95]	VAL.	CHN	Cfa	rotation 3	C	d	1	N_{org} + N_{min}	-	0.4	-	-	-	-	-
	[95]	VAL.	CHN	Cfa	rotation 3	C	d	2	N_{org} + N_{min}	-	0.28	-	-	-	-	-
	[94]	CAL.	CHN	Cfa	rotation 2	N	d	1 + 2	$Crop_{mng}$ (rice)	-	-	0.01–0.03	-	-	-	-
	[94]	CAL.	CHN	Cfa	rotation 2	N	d	3 + 4	$Crop_{mng}$ (vegetable)	-	-	0.11	-	-	-	-
	[95]	VAL.	CHN	Cfa	rotation 3	C	d	3	N_{org} + N_{min} + nitr. inhibitor	-	0.3	-	-	-	-	-

Table A9. *Cont.*

Model	Ref.	Ev.	Coun.	K. C.	Crop	Meas.	Fit.	n°	Tr.	*r*	R^2	*RMSE*	$RMSE_{95}$	*EF*	*RRMSE*	*p*-Value
EPIC	[96]	VAL.	USA	Dfa	rotation 5	N	c	1–7	(4) N_{min} + (3) $Crop_{mng}$	-	0.54	1.32	-	-	-	-
	[82]	CAL.	USA	Dfa	rotation 4	N	c	-	Overall (2007)	-	0.88	0.67	-	-	-	-
	[82]	CAL.	USA	Dfa	rotation 4	N	c	-	Overall (2008)	-	0.78	0.39	-	-	-	-
	[96]	CAL.	USA	Dfa	rotation 5	N	c	1–7	(4) N_{min} + (3) $Crop_{mng}$	-	0.41	1.25	-	-	-	-
	[82]	CAL.	USA	Dfa	rotation 4	N	d	1	N_0 (2007)	-	0.31	-	-	-	-	-
	[82]	CAL.	USA	Dfa	rotation 4	N	d	2	N_{min} (2007)	-	0.63	-	-	-	-	-
	[82]	CAL.	USA	Dfa	rotation 4	N	d	3	N_{min} (2007)	-	0.82	-	-	-	-	-
EPIC	[82]	CAL.	USA	Dfa	rotation 4	N	d	4	N_{min} (2007)	-	0.78	-	-	-	-	-
	[82]	CAL.	USA	Dfa	rotation 4	N	d	5	N_{min} (2007)	-	0.58	-	-	-	-	-
	[82]	CAL.	USA	Dfa	rotation 4	N	d	6	N_{min} (2007)	-	0.7	-	-	-	-	-
	[82]	CAL.	USA	Dfa	rotation 4	N	d	-	Overall (2007)	-	0.92	0	-	-	-	-
	[82]	CAL.	USA	Dfa	rotation 4	N	d	1	N_0 (2008)	-	0.1	-	-	-	-	-
	[82]	CAL.	USA	Dfa	rotation 4	N	d	2	N_{min} (2008)	-	0.32	-	-	-	-	-
	[82]	CAL.	USA	Dfa	rotation 4	N	d	3	N_{min} (2008)	-	0.55	-	-	-	-	-
	[82]	CAL.	USA	Dfa	rotation 4	N	d	4	N_{min} (2008)	-	0.77	-	-	-	-	-
	[82]	CAL.	USA	Dfa	rotation 4	N	d	5	N_{min} (2008)	-	0.64	-	-	-	-	-
	[82]	CAL.	USA	Dfa	rotation 4	N	d	6	N_{min} (2008)	-	0.75		-	-	-	-
	[82]	CAL.	USA	Dfa	rotation 4	N	d	-	Overall (2008)	-	0.78	0.04	-	-	-	-
	[96]	CAL.	USA	Dfa	rotation 5	N	d	1–7	(4) N_{min} + (3) $Crop_{mng}$	-	0.45	0.01	-	-	-	-
	[96]	VAL.	USA	Dfa	rotation 5	N	d	1–7	(4) N_{min} + (3) $Crop_{mng}$	-	0.14	0.02	-	-	-	-
SPACSYS	[98]	VAL.	U.K.	Cfb	permanent pasture	C	d	1	N_{min}	0.49	0.74	0.07	-	−0.2	-	-
	[71]	VAL.	GB–SCT	Cfb	grassland	N	c	1	N_0	0.06	-	0.494	0.87	−22.25	-	-
	[71]	VAL.	GB–SCT	Cfb	grassland	N	c	3	N_{org}	0.5	-	0.177	0.747	0.2	-	-
	[71]	VAL.	GB–SCT	Cfb	grassland	N	c	2	N_{min}	0.34	-	0.52	0.736	0.04	-	-
	[97]	VAL.	U.K.	Cfb	grassland	N	c	1	N_{min}	0.98	-	0.1305	0.17415	-	-	-
	[97]	CAL.	U.K.	Cfb	grassland	N	c	1	N_{min}	0.88	-	0.3841	0.24733	-	-	-
STICS	[99]	VAL.	SP, SP–C, FR	Cfa (SP), Csa (SP-C), Cfb (FR)	Durum wheat –faba bean	C	c	12	N_{min} + $Crop_{mng}$	-	0.4	-	-	0.24	45.6	

References

1. Mosier, A.; Kroeze, C. Potential impact on the global atmospheric N_2O budget of the increased nitrogen input required to meet future global food demands. *Chemosphere Glob. Chang. Sci.* **2000**, *2*, 465–473. [CrossRef]
2. Monson, R.K.; Holland, E.A. Biospheric Trace Gas Fluxes and Their Control Over Tropospheric Chemistry. *Annu. Rev. Ecol. Syst.* **2001**, *32*, 547–576. [CrossRef]
3. Myhre, G.; Shindell, D.; Bréon, F.-M.; Collins, W.; Fuglestvedt, J.; Huang, J.; Koch, D.; Lamarque, J.-F.; Lee, D.; Mendoza, B.; et al. Anthropogenic and Natural Radiative Forcing. In *Climate Change 2013: The Physical Science Basis. Contribution of Working Group I to the Fifth Assessment Report of the Intergovernmental Panel on Climate Change*; Stocker, T.F., Qin, D., Plattner, G.-K., Tignor, M., Allen, S.K., Boschung, J., Nauels, A., Xia, Y., Bex, V., Midgley, P.M., Eds.; Cambridge University Press: Cambridge, UK; New York, NY, USA, 2013.
4. Northrup, D.L.; Basso, B.; Wang, M.Q.; Morgan, C.L.S.; Benfey, P.N. Novel technologies for emission reduction complement conservation agriculture to achieve negative emissions from row-crop production. *Proc. Natl. Acad. Sci. USA* **2021**, *118*, e2022666118. [CrossRef] [PubMed]
5. Borken, W.; Matzner, E. Reappraisal of drying and wetting effects on C and N mineralization and fluxes in soils. *Glob. Chang. Biol.* **2009**, *15*, 808–824. [CrossRef]
6. Stein, L.Y.; Nicol, G.W. Nitrification. In *Encyclopedia of Life Sciences*; John Wiley & Sons, Ltd.: Hoboken, NJ, USA, 2018. [CrossRef]
7. Zhang, J.; Zhang, W.; Jansson, P.-E.; Petersen, S.O. Modeling nitrous oxide emissions from agricultural soil incubation experiments using CoupModel. *Biogeosciences* **2022**, *19*, 4811–4832. [CrossRef]
8. Pu, Y.; Zhu, B.; Dong, Z.; Liu, Y.; Wang, C.; Ye, C. Soil N_2O and NO_x emissions are directly linked with N-cycling enzymatic activities. *Appl. Soil Ecol.* **2019**, *139*, 15–24. [CrossRef]
9. Smith, K.A. Changing views of nitrous oxide emissions from agricultural soil: Key controlling processes and assessment at different spatial scales. *Eur. J. Soil Sci.* **2017**, *68*, 137–155. [CrossRef]
10. Ottaiano, L.; Di Mola, I.; Di Tommasi, P.; Mori, M.; Magliulo, V.; Vitale, L. Effects of irrigation on N_2O emissions in a maize crop grown on different soil types in two contrasting seasons. *Agriculture* **2020**, *10*, 623. [CrossRef]
11. Parton, W.J.; Holland, E.A.; Del Grosso, S.J.; Hartman, M.D.; Martin, R.E.; Mosier, A.R.; Ojima, D.S.; Schimel, D.S. Generalized model for NO_x and N_2O emissions from soils. *J. Geophys. Res.* **2001**, *106*, 17403–17419. [CrossRef]

12. Weier, K.L.; Doran, J.W.; Power, J.F.; Walters, D.T. Denitrification and the Dinitrogen/Nitrous Oxide Ratio as Affected by Soil Water, Available Carbon, and Nitrate. *Soil Sci. Soc. Am. J.* **1993**, *57*, 66–72. [CrossRef]
13. Butterbach-Bahl, K.; Baggs, E.M.; Dannenmann, M.; Kiese, R.; Zechmeister-Boltenstern, S. Nitrous oxide emissions from soils: How well do we understand the processes and their controls? *Philos. Trans. R. Soc. B Biol. Sci.* **2013**, *368*, 20130122. [CrossRef] [PubMed]
14. Hénault, C.H.; Grossel, A.; Mary, B.; Roussel, M.; Eonard, J.L. Nitrous Oxide Emission by Agricultural Soils: A Review of Spatial and Temporal Variability for Mitigation. *Pedosphere* **2012**, *22*, 426–433. [CrossRef]
15. Maag, M.; Vinther, F.P. Nitrous oxide emission by nitrification and denitrification in different soil types and at different soil. *Appl. Soil Ecol.* **1996**, *4*, 5–14. [CrossRef]
16. Li, J.; Wang, L.; Luo, Z.; Wang, E.; Wang, G.; Zhou, H.; Li, H.; Xu, S. Reducing N_2O emissions while maintaining yield in a wheat–maize rotation system modelled by APSIM. *Agric. Syst.* **2021**, *194*, 103277. [CrossRef]
17. Del Grosso, S.J.; Ojima, D.S.; Parton, W.J.; Stehfest, E.; Heistemann, M.; DeAngelo, B.; Rose, S. Global scale DAYCENT model analysis of greenhouse gas emissions and mitigation strategies for cropped soils. *Glob. Planet. Chang.* **2009**, *67*, 44–50. [CrossRef]
18. Schwenke, G.D.; Haigh, B.M. Can split or delayed application of N fertiliser to grain sorghum reduce soil N_2O emissions from sub-tropical Vertosols and maintain grain yields? *Soil Res.* **2019**, *57*, 859–874. [CrossRef]
19. Kravchenko, A.N.; Toosi, E.R.; Guber, A.K.; Ostrom, N.E.; Yu, J.; Azeem, K.; Rivers, M.L.; Robertson, G.P. Hotspots of soil N_2O emission enhanced through water absorption by plant residue. *Nat. Geosci.* **2017**, *10*, 496–500. [CrossRef]
20. Miller, L.T.; Griffis, T.J.; Erickson, M.D.; Turner, P.A.; Deventer, M.J.; Chen, Z.; Yu, Z.; Venterea, R.T.; Baker, J.M.; Frie, A.L. Response of nitrous oxide emissions to individual rain events and future changes in precipitation. *J. Environ. Qual.* **2022**, *51*, 312–324. [CrossRef]
21. Bouwman, A.F.; Boumans, L.J.; Batjes, N.H. Emissions of N_2O and NO from fertilized fields: Summary of available measurement data. *Glob. Biogeochem. Cycles* **2002**, *16*, 6-1–6-13. [CrossRef]
22. Aguilera, E.; Lassaletta, L.; Sanz-Cobeña, A.; Garnier, J.; Vallejo, A. The potential of organic fertilizers and water management to reduce N2O emissions in Mediterranean climate cropping systems. A review. *Agric. Ecosyst. Environ.* **2013**, *164*, 32–52. [CrossRef]
23. Li, R.; Cameira, M.R.; Fangueiro, D. *Modelling nitrous oxide emissions from an oats cover crop with the RZWQM2: In Advances in Agricultural Systems Modeling 8. Bridging Among Disciplines by Synthesizing Soil and Plant Processes*; Li, R., Cameira, M.R., Fangueiro, D., Eds.; American Society of Agronomy, Crop Science Society of America, and Soil Science Society of America, Inc.: Madison, WI, USA, 2019.
24. Pattey, E.; Edwards, G.C.; Desjardins, R.L.; Pennock, D.J.; Smith, W.; Grant, B.; MacPherson, J.I. Tools for quantifying N_2O emissions from agroecosystems. *Agric. For. Meteorol.* **2007**, *142*, 103–119. [CrossRef]
25. Beheydta, D.; Boeckxa, P.; Sleutelb, S.; Lic, C.; Van Cleemput, O. Validation of DNDC for 22 long-term N_2O field emission measurements. *Atmos. Environ.* **2007**, *41*, 6196–6211. [CrossRef]
26. Flessa, H.; Ruser, R.; Schilling, R.; Loftfield, N.; Munch, J.C.; Kaiser, E.A.; Beese, F. N_2O and CH_4 fluxes in potato fields: Automated 24 measurement, management effects and temporal variation. *Geoderma* **2002**, *105*, 307–325. [CrossRef]
27. Smith, K.A.; Dobbie, K.E. The impact of sampling frequency and sampling times on chamber-based measurements of N_2O emissions from fertilized soils. *Glob. Chang. Biol.* **2001**, *7*, 933–945. [CrossRef]
28. Rochette, P.; Desjardins, R.L.; Pattey, E.; Lessard, R. Instantaneous Measurement of Radiation and Water Use Efficiencies of a Maize Crop. *Agron. J.* **1996**, *88*, 627–635. [CrossRef]
29. Eugster, W.; Merbold, L. Eddy covariance for quantifying trace gas fluxes from soils. *Soil* **2015**, *1*, 187–205. [CrossRef]
30. Grant, R.F.; Pattey, E. Modelling variability in N_2O emissions from fertilized agricultural fields. *Soil Biol. Biochem.* **2003**, *35*, 225–243. [CrossRef]
31. Cowan, N.J.; Norman, P.; Famulari, D.; Levy, P.E.; Reay, D.S.; Skiba, U.M. Spatial variability and hotspots of soil N_2O fluxes from intensively grazed grassland. *Biogeosciences* **2015**, *12*, 1585–1596. [CrossRef]
32. Denmead, O.T. Micrometeorological methods for measuring gaseous losses of nitrogen in the field. In *Gaseous Loss of Nitrogen from Plant-Soil Systems. Developments in Plant and Soil Sciences*; Freney, J.R., Simpson, J.R., Eds.; Springer: Dordrecht, The Netherlands, 1983; Volume 9. [CrossRef]
33. Baldocchi, D.D.; Hincks, B.B.; Meyers, T.P. Measuring Biosphere-Atmosphere Exchanges of Biologically Related Gases with Micrometeorological Methods. *Ecology* **1988**, *69*, 1331–1340. [CrossRef]
34. Foken, T.; Aubinet, M.; Leuning, R. The Eddy Covariance Method. In *A Practical Guide to Measurement and Data Analysis*; Aubinet, M., Vesala, T., Papale, D., Eds.; Springer: Dordrecht, The Netherlands; Berlin/Heidelberg, Germany; London, UK; New York, NY, USA, 2012; ISBN 978-94-007-2350-4.
35. Shi, R.; Su, P.; Zhou, Z.; Yang, J.; Ding, X. Comparison of eddy covariance and automatic chamber-based methods for measuring carbon flux. *Agron. J.* **2022**, *114*, 2081–2094. [CrossRef]
36. Liang, L.L.; Campbell, D.I.; Wall, A.M.; Schipper, L.A. Nitrous oxide fluxes determined by continuous eddy covariance measurements from intensively grazed pastures: Temporal patterns and environmental controls. *Agric. Ecosyst. Environ.* **2018**, *268*, 171–180. [CrossRef]
37. Shurpali, N.J.; Rannik, Ü.; Jokinen, S.; Lind, S.; Biasi, C.; Mammarella, I.; Peltola, O.; Pihlatie, M.; Hyvönen, N.; Räty, M.; et al. Neglecting diurnal variations leads to uncertainties in terrestrial nitrous oxide emissions. *Sci. Rep.* **2016**, *6*, 25739. [CrossRef]

38. Giltrap, D.L.; Kirschbaum, M.U.; Liáng, L.L. The potential effectiveness of four different options to reduce environmental impacts of grazed pastures. A model-based assessment. *Agric. Syst.* **2021**, *186*, 102960. [CrossRef]
39. Uddin, S.; Islam, M.R.; Jahangir, M.M.R.; Rahman, M.M.; Hassan, S.; Hassan, M.M.; Abo-Shosha, A.A.; Ahmed, A.F.; Rahman, M.M. Nitrogen release in soils amended with different organic and inorganic fertilizers under contrasting moisture regimes: A laboratory incubation study. *Agronomy* **2021**, *11*, 2163. [CrossRef]
40. Schädel, C.; Beem-Miller, J.; Aziz Rad, M.; Crow, S.E.; Hicks Pries, C.E.; Ernakovich, J.; Hoyt, A.M.; Plante, A.; Stoner, S.; Treat, C.C.; et al. Decomposability of soil organic matter over time: The Soil Incubation Database (SIDb, version 1.0) and guidance for incubation procedures. *Earth Syst. Sci. Data* **2020**, *12*, 1511–1524. [CrossRef]
41. Lapitan, R.; Wanninkhof, R.; Mosier, A. Methods for stable gas flux determination in aquatic and terrestrial systems. *Dev. Atmos. Sci.* **1999**, *24*, 29–66. [CrossRef]
42. Avadí, A.; Galland, V.; Versini, A.; Bockstaller, C. Suitability of operational N direct field emissions models to represent contrasting agricultural situations in agricultural LCA: Review and prospectus. *Sci. Total Environ.* **2022**, *802*, 149960. [CrossRef]
43. Dorich, C.D.; Conant, R.T.; Albanito, F.; Butterbach-Bahl, K.; Grace, P.; Scheer, C.; Snow, V.O.; Vogeler, I.; van der Weerden, T.J. Improving N_2O emission estimates with the global N_2O database. *Curr. Opin. Environ. Sustain.* **2020**, *47*, 13–20. [CrossRef]
44. Nemecek, T.; Gaillard, G. Challenges in assessing the environmental impacts of crop production and horticulture. In *Environmental Assessment and Management in the Food Industry—Life Cycle Assessment and Related Approaches*; Sonesson, U., Berlin, J., Ziegler, F., Eds.; Woodhead Publishing Limited: Oxford, UK, 2010; Chapter 6; pp. 98–116.
45. Nevison, C. Review of the IPCC methodology for estimating nitrous oxide emissions associated with agricultural leaching and runoff. *Chemosphere Glob. Chang. Sci.* **2000**, *2*, 493–500. [CrossRef]
46. Shang, Z.; Abdalla, M.; Kuhnert, M.; Albanito, F.; Zhou, F.; Xia, L.; Smith, P. Measurement of N_2O emissions over the whole year is necessary for estimating reliable emission factors. *Environ. Pollut.* **2020**, *259*, 113864. [CrossRef]
47. Yan, H.P. A Dynamic, Architectural Plant Model Simulating Resource-dependent Growth. *Ann. Bot.* **2004**, *93*, 591–602. [CrossRef] [PubMed]
48. Bouwman, A.F. Direct emission of nitrous oxide from agricultural soils. *Nutr. Cycl. Agroecosystems* **1996**, *46*, 53–70. [CrossRef]
49. Freibauer, A.; Kaltschmitt, M. Controls and models for estimating direct nitrous oxide emissions from temperate and sub-boreal agricultural mineral soils in Europe. *Biogeochemistry* **2003**, *63*, 93–115. [CrossRef]
50. Tonitto, C.; Woodbury, P.B.; McLellan, E.L. Defining a best practice methodology for modeling the environmental performance of agriculture. *Environ. Sci. Policy* **2018**, *87*, 64–73. [CrossRef]
51. Mummey, D.L.; Smith, J.L.; Bluhm, G. Assessment of alternative soil management practices on N_2O emissions from US agriculture. *Agric. Ecosyst. Environ.* **1998**, *70*, 79–87. [CrossRef]
52. Li, C.S. Modeling Trace Gas Emissions from Agricultural Ecosystems. *Nutr. Cycl. Agroecosystems* **2000**, *58*, 259–276. [CrossRef]
53. Chen, D.; Li, Y.; Grace, P.; Mosier, A.R. N_2O emissions from agricultural lands: A synthesis of simulation approaches. *Plant Soil* **2008**, *309*, 169–189. [CrossRef]
54. Brilli, L.; Bechini, L.; Bindi, M.; Carozzi, M.; Cavalli, D.; Conant, R.; Dorich, C.D.; Doro, L.; Ehrhardt, F.; Farina, R.; et al. Review and analysis of strengths and weaknesses of agro-ecosystem models for simulating C and N fluxes. *Sci. Total Environ.* **2017**, *598*, 445–470. [CrossRef]
55. Wang, C.; Amon, B.; Schulz, K.; Mehdi, B. Factors That Influence Nitrous Oxide Emissions from Agricultural Soils as Well as Their Representation in Simulation Models: A Review. *Agronomy* **2021**, *11*, 770. [CrossRef]
56. Perego, A.; Giussani, A.; Sanna, M.; Fumagalli, M.; Carozzi, M.; Alfieri, L.; Brenna, S.; Acutis, M. The ARMOSA simulation crop model: Overall features, calibration and validation results. *Ital. J. Agrometeorol.* **2013**, *3*, 23–38.
57. Holzworth, D.P.; Huth, N.I.; deVoil, P.G.; Zurcher, E.J.; Herrmann, N.I.; McLean, G.; Chenu, K.; van Oosterom, E.J.; Snow, V.; Murphy, C.; et al. APSIM—Evolution towards a new generation of agricultural systems simulation. *Environ. Model. Softw.* **2014**, *62*, 327–350. [CrossRef]
58. Gabrielle, B.; Da-Silveira, J.; Houot, S.; Michelin, J. Field-scale modelling of carbon and nitrogen dynamics in soils amended with urban waste composts. *Agric. Ecosyst. Environ.* **2005**, *110*, 289–299. [CrossRef]
59. Stöckle, C.O.; Donatelli, M.; Nelson, R. CropSyst, a cropping systems simulation model. *Eur. J. Agron.* **2003**, *18*, 289–307. [CrossRef]
60. Brisson, N.; Launay, M.; Mary, B.; Beaudoin, N. *Conceptual Basis, Formalisations and Parameterization of the STICS Crop Model*; Edition Quae: Versailles, France, 2008.
61. Jones, J.W.; Hoogenboom, G.; Porter, C.H.; Boote, K.J.; Batchelor, W.D.; Hunt, L.A.; Wilkens, P.W.; Singh, U.; Gijsman, A.J.; Ritchie, J.T. The DSSAT cropping system model. *Eur. J. Agron.* **2003**, *18*, 235–265. [CrossRef]
62. Sharpley, A.N.; Williams, J.R. *EPIC—Erosion/Productivity Impact Calculator Model Documentation*; U.S. Department of Agriculture Technical Bulletin No. 1768; USA Government Printing Office: Washington, DC, USA, 1990.
63. Li, C.; Frolking, S.; Frolking, T.A. A model of nitrous oxide evolution from soil driven by rainfall events: 1. Model structure and sensitivity. *J. Geophys. Res.* **1992**, *97*, 9759–9776. [CrossRef]
64. Parton, W.J.; Ojima, D.S.; Cole, C.V.; Schimel, D.S. A General Model for Soil Organic Matter Dynamics: Sensitivity to Litter Chemistry, Texture and Management. In *Quantitative Modeling of Soil Forming Processes*; Bryant, R.B., Arnold, R.W., Eds.; John Wiley & Sons, Inc.: Hoboken, NJ, USA, 1994. [CrossRef]
65. Jansson, P.-E. CoupModel: Model use, calibration and validation. *Trans. ASABE* **2012**, *55*, 1335–1344.

66. Wu, L.; McGechan, M.B.; McRoberts, N.; Baddeley, J.A.; Watson, C.A. SPACSYS: Integration of a 3D root architecture component to carbon, nitrogen and water cycling—Model description. *Ecol. Model.* **2007**, *200*, 343–359. [CrossRef]
67. Thorburn, P.J.; Biggs, J.S.; Collins, K.; Probert, M.E. Using the APSIM model to estimate nitrous oxide emissions from diverse Australian sugarcane production systems. *Agric. Ecosyst. Environ.* **2010**, *136*, 343–350. [CrossRef]
68. Jansson, P.-E.; Karlberg, L. *Coupled Heat and Mass Transfer Model for Soilplant-Atmosphere Systems*; Royal Institute of Technology: Stockholm, Sweden, 2010; Available online: www2.lwr.kth.se/CoupModel/coupmanual.pdf (accessed on 16 January 2024).
69. Stöckle, C.; Higgins, S.; Kemanian, A.; Nelson, R.; Huggins, D.; Marcos, J.; Collins, H. Carbon storage and nitrous oxide emissions of cropping systems in eastern Washington: A simulation study. *J. Soil Water Conserv.* **2012**, *67*, 365–377. [CrossRef]
70. Hoogenboom, G.; Porter, C.H.; Boote, K.J.; Shelia, V.; Wilkens, P.W.; Singh, U.; White, J.W.; Asseng, S.; Lizaso, J.I.; Moreno, L.P.; et al. The DSSAT crop modeling ecosystem. In *Advances in Crop Modelling for a Sustainable Agriculture*; Boote, K., Ed.; Burleigh Dodds Science Publishing: Cambridge, UK, 2019; pp. 173–216. ISBN 9781786762405.
71. Wu, L.; Rees, R.M.; Tarsitano, D.; Zhang, X.; Jones, S.K.; Whitmore, A.P. Simulation of nitrous oxide emissions at field scale using the SPACSYS model. *Sci. Total Environ.* **2015**, *530–531*, 76–86. [CrossRef]
72. Meier, E.A.; Thorburn, P.J.; Probert, M.E. Occurrence and simulation of nitrification in two contrasting sugarcane soils from the Australian wet tropics. *Aust. J. Soil Res.* **2006**, *44*, 1–9. [CrossRef]
73. Stöckle, C.O.; Martin, S.A.; Campbell, G.S. CropSyst, a cropping systems simulation model: Water/nitrogen budgets and crop yield. *Agric. Syst.* **1994**, *46*, 335–359. [CrossRef]
74. Wu, L.; McGechan, M.B. A Review of Carbon and Nitrogen Processes in Four Soil Nitrogen Dynamics Models. *J. Agric. Eng. Res.* **1998**, *69*, 279–305. [CrossRef]
75. Eckersten, H.; Jansson, P.-E.; Johnsson, H. *SOILN Model User's Manual: Version 9.2*; Avdelningsmeddelande 98:6 Communications: Uppsala, Sweden, 1998; ISRN SLU-HY-AVDM--98/6--SE 0282-6569.
76. Lehuger, S. Modélisation des Bilans de Gaz à Effet de Serre des Agro-Écosystèmes en Europe. Ph.D. Thesis, AgroParisTech, Paris, France, 2009.
77. Available online: https://github.com/DSSAT/dssat-csm-os (accessed on 16 November 2023).
78. EPIC v.1102. Software Executable. Available online: https://epicapex.tamu.edu/software/ (accessed on 16 November 2023).
79. Institute for the Study of Earth, Oceans, and Space. *DNDC Scientific Basis and Processes: Version 9.5*; Institute for the Study of Earth, Oceans, and Space: Durham, NH, USA, 2017.
80. Parton, W.J.; Mosier, A.R.; Ojima, D.S.; Valentine, D.W.; Schimel, D.S.; Weier, K.; Kulmala, A.E. Generalized model for N_2 and N_2O production from nitrification and denitrification. *Glob. Biogeochem. Cycles* **1996**, *10*, 401–412. [CrossRef]
81. Del Grosso, S.J.; Parton, W.J.; Mosier, A.R.; Ojima, D.S.; Kulmala, A.E.; Phongpan, S. General model for N_2O and N_2 gas emissions from soils due to dentrification. *Glob. Biogeochem. Cycles* **2000**, *14*, 1045–1060. [CrossRef]
82. Izaurralde, R.C.; McGill, W.B.; Williams, J.R.; Jones, C.D.; Link, R.P.; Manowitz, D.H.; Schwab, D.E.; Zhang, X.; Robertson, G.P.; Millar, N. Simulating microbial denitrification with EPIC: Model description and evaluation. *Ecol. Model.* **2017**, *359*, 349–362. [CrossRef]
83. Hénault, C.; Bizouard, F.; Laville, P.; Gabrielle, B.; Nicoullaud, B.; Germon, J.C.; Cellier, P. Predicting in situ soil N_2O emission using NOE algorithm and soil database. *Glob. Chang. Biol.* **2005**, *11*, 115–127. [CrossRef]
84. APSIM 7.10. Soil Modules Documentation: SoilN. Available online: https://www.apsim.info/documentation/model-documentation/soil-modules-documentation/soiln/ (accessed on 16 November 2023).
85. Available online: https://www.nrel.colostate.edu/projects/daycent-executables/ (accessed on 16 November 2023).
86. Franzluebbers, A.J. Microbial activity in response to water-filled pore space of variably eroded southern Piedmont soils. *Appl. Soil Ecol.* **1999**, *11*, 91–101. [CrossRef]
87. Linn, D.M.; Doran, J.W. Effect of water-filled pore space on carbon dioxide and nitrous oxide production in tilled and nontilled soils. *Soil Sci. Soc. Am. J.* **1984**, *48*, 1267–1272. [CrossRef]
88. Arnfield, A.J. Köppen Climate Classification. Available online: https://www.britannica.com/science/Koppen-climate-classification (accessed on 16 November 2023).
89. Haas, E.; Carozzi, M.; Massad, R.S.; Scheer, C.; Butterbach-Bahl, K. Testing the Performance of CERES-EGC and LandscapeDNDC to Simulate Effects of Residue Management on Soil N_2O Emissions. ResidueGas Deliverable Report 4.1. 2021. Available online: https://projects.au.dk/fileadmin/projects/residuegas/D_reports/ResidueGas_D4.1.pdf (accessed on 16 November 2023).
90. Ferrara, R.M.; Carozzi, M.; Decuq, C.; Loubet, B.; Finco, A.; Marzuoli, R.; Gerosa, G.; Di Tommasi, P.; Magliulo, V.; Rana, G. Ammonia, nitrous oxide, carbon dioxide, and water vapor fluxes after green manuring of faba bean under Mediterranean climate. *Agric. Ecosyst. Environ.* **2021**, *315*, 107439. [CrossRef]
91. Köbke, S.; He, H.; Böldt, M.; Wang, H.; Senbayram, M.; Dittert, K. Climate Overrides Effects of Fertilizer and Straw Management as Controls of Nitrous Oxide Emissions After Oilseed Rape Harvest. *Front. Environ. Sci.* **2022**, *9*, 773901. [CrossRef]
92. Necpalova, M.; Lee, J.; Skinner, C.; Büchi, L.; Wittwer, R.; Gattinger, A.; van der Heijden, M.; Mäder, P.; Charles, R.; Berner, A.; et al. Potentials to mitigate greenhouse gas emissions from Swiss agriculture. *Agric. Ecosyst. Environ.* **2018**, *265*, 84–102. [CrossRef]
93. Del Grosso, S.; Parton, W.; Mosier, A.; Hartman, M.; Brenner, J.; Ojima, D.; Schimel, D. Simulated Interaction of Carbon Dynamics and Nitrogen Trace Gas Fluxes Using the DAYCENT Model. In *Modeling Carbon and Nitrogen Dynamics for Soil Management*; Hansen, S., Shaffer, M., Ma, L., Eds.; CRC Press: Boca Raton, FL, USA, 2001; ISBN 978-1-56670-529-5.

94. Sun, X.; Yang, X.; Hou, J.; Wang, B.; Fang, Q. Modeling the Effects of Rice-Vegetable Cropping System Conversion and Fertilization on GHG Emissions Using the DNDC Model. *Agronomy* **2023**, *13*, 379. [CrossRef]
95. Zhang, H.; Deng, Q.; Schadt, C.W.; Mayes, M.A.; Zhang, D.; Hui, D. Precipitation and nitrogen application stimulate soil nitrous oxide emission. *Nutr. Cycl. Agroecosystems* **2021**, *120*, 363–378. [CrossRef]
96. Gaillard, R.K.; Jones, C.D.; Ingraham, P.; Collier, S.; Izaurralde, R.C.; Jokela, W.; Osterholz, W.; Salas, W.; Vadas, P.; Ruark, M.D. Underestimation of N_2O emissions in a comparison of the DayCent, DNDC, and EPIC models. *Ecol. Appl.* **2018**, *28*, 694–708. [CrossRef] [PubMed]
97. Abalos, D.; Cardenas, L.M.; Wu, L. Climate change and N_2O emissions from South West England grasslands: A modelling approach. *Atmos. Environ.* **2016**, *132*, 249–257. [CrossRef]
98. Liu, Y.; Li, Y.; Harris, P.; Cardenas, L.M.; Dunn, R.M.; Sint, H.; Murray, P.J.; Lee, M.R.; Wu, L. Modelling field scale spatial variation in water run-off, soil moisture, N_2O emissions and herbage biomass of a grazed pasture using the SPACSYS model. *Geoderma* **2018**, *315*, 49–58. [CrossRef]
99. Plaza-Bonilla, D.; Léonard, J.; Peyrard, C.; Mary, B.; Justes, É. Precipitation gradient and crop management affect N_2O emissions: Simulation of mitigation strategies in rainfed Mediterranean conditions. *Agric. Ecosyst. Environ.* **2017**, *238*, 89–103. [CrossRef]
100. Ehrhardt, F.; Soussana, J.-F.; Bellocchi, G.; Grace, P.; McAuliffe, R.; Recous, S.; Sándor, R.; Smith, P.; Snow, V.; de Antoni Migliorati, M.; et al. Assessing uncertainties in crop and pasture ensemble model simulations of productivity and N_2O emissions. *Glob. Chang. Biol.* **2018**, *24*, e603–e616. [CrossRef]
101. Donatelli, M.; Acutis, M.; Bellocchi, G.; Fila, G. New Indices to Quantify Patterns of Residuals Produced by Model Estimates. *Agron. J.* **2004**, *96*, 631–645. [CrossRef]
102. Brown, L.; Brown, S.A.; Jarvis, S.C.; Syed, B.; Goulding, K.W.T.; Phillips, V.R.; Sneath, R.W.; Pain, B.F. An inventory of nitrous oxide emissions from agriculture in the UK using the IPCC methodology: Emission estimate, uncertainty and sensitivity analysis. *Atmos. Environ.* **2001**, *35*, 1439–1449. [CrossRef]
103. Mosier, A.; Kroeze, C.; Nevison, C.; Oenema, O.; Seitzinger, S.; Van Cleemput, O. An overview of the revised 1996 IPCC guidelines for national greenhouse gas inventory methodology for nitrous oxide from agriculture. *Environ. Sci. Policy* **1999**, *2*, 325–333. [CrossRef]
104. Lokupitiya, E.; Paustian, K. Agricultural Soil Greenhouse Gas Emissions. *J. Environ. Qual.* **2006**, *35*, 1413–1427. [CrossRef] [PubMed]
105. Amon, B.; Çinar, G.; Anderl, M.; Dragoni, F.; Kleinberger-Pierer, M.; Hörtenhuber, S. Inventory reporting of livestock emissions: The impact of the IPCC 1996 and 2006 Guidelines. *Environ. Res. Lett.* **2021**, *16*, 075001. [CrossRef]
106. Leip, A.; Busto, M.; Winiwarter, W. Developing spatially stratified N_2O emission factors for Europe. *Environ. Pollut.* **2011**, *159*, 3223–3232. [CrossRef]
107. Millar, N.; Robertson, G.P.; Grace, P.R.; Gehl, R.J.; Hoben, J.P. Nitrogen fertilizer management for nitrous oxide (N_2O) mitigation in intensive corn (Maize) production: An emissions reduction protocol for US Midwest agriculture. *Mitig. Adapt. Strateg. Glob. Chang.* **2010**, *15*, 185–204. [CrossRef]
108. Tonitto, C.; David, M.B.; Drinkwater, L.E. Modeling N_2O flux from an Illinois agroecosystem using Monte Carlo sampling of field observations. *Biogeochemistry* **2009**, *93*, 31–48. [CrossRef]
109. Smith, P.; Davies, C.A.; Ogle, S.; Zanchi, G.; Bellarby, J.; Bird, N.; Boddey, R.M.; McNamara, N.P.; Powlson, D.; Cowie, A.; et al. Towards an integrated global framework to assess the impacts of land use and management change on soil carbon: Current capability and future vision. *Glob. Chang. Biol.* **2012**, *18*, 2089–2101. [CrossRef]
110. Basche, A.D.; Miguez, F.E.; Kaspar, T.C.; Castellano, M.J. Do cover crops increase or decrease nitrous oxide emissions? a meta-analysis. *J. Soil Water Conserv.* **2014**, *69*, 471–482. [CrossRef]
111. Van Kessel, C.; Venterea, R.; Six, J.; Adviento-Borbe, M.A.; Linquist, B.; Jan van Groenigen, K. Climate, duration, and N placement determine N_2O emissions in reduced tillage systems: A meta-analysis. *Glob. Chang. Biol.* **2013**, *19*, 33–44. [CrossRef]
112. Villa-Vialaneix, N.; Follador, M.; Ratto, M.; Leip, A. A comparison of eight metamodeling techniques for the simulation of N_2O fluxes and N leaching from corn crops. *Environ. Model. Softw.* **2012**, *34*, 51–66. [CrossRef]
113. Robertson, G.P.; Paul, E.A.; Harwood, R.R. Greenhouse Gases in Intensive Agriculture: Contributions of Individual Gases to the Radiative Forcing of the Atmosphere. *Science* **2000**, *289*, 1922–1925. [CrossRef] [PubMed]
114. Del Prado, A.; Crosson, P.; Olesen, J.E.; Rotz, C.A. Whole-farm models to quantify greenhouse gas emissions and their potential use for linking climate change mitigation and adaptation in temperate grassland ruminant-based farming system. *Animal* **2013**, *7* (Suppl. 2), 373–385. [CrossRef] [PubMed]
115. Louhichi, K.; Kanellopoulos, A.; Janssen, S.; Flichman, G.; Blanco, M.; Hengsdijk, H.; Heckelei, T.; Berentsen, P.; Lansink, A.O.; Van Ittersum, M. FSSIM, a bio-economic farm model for simulating the response of EU farming systems to agricultural and environmental policies. *Agric. Syst.* **2010**, *103*, 585–597. [CrossRef]
116. Shang, L.; Wang, J.; Schäfer, D.; Heckelei, T.; Gall, J.; Appel, F.; Storm, H. Surrogate modelling of a detailed farm-level model using deep learning. *J. Agric. Econ.* **2023**, 1–26. [CrossRef]
117. Cann, D.J.; Hunt, J.R.; Malcolm, B. Long fallows can maintain whole-farm profit and reduce risk in semi-arid south-eastern Australia. *Agric. Syst.* **2020**, *178*, 102721. [CrossRef]
118. Loague, K.; Green, R.E. Statistical and graphical methods for evaluating solute transport models: Overview and application. *J. Contam. Hydrol.* **1991**, *7*, 51–73. [CrossRef]

119. Nash, J.E.; Sutcliffe, J.V. River flow forecasting through conceptual models part I—A discussion of principles. *J. Hydrol.* **1970**, *10*, 282–290. [CrossRef]
120. Addiscott, T.M.; Whitmore, A.P. Computer simulation of changes in soil mineral nitrogen and crop nitrogen during autumn, winter and spring. *J. Agric. Sci.* **1987**, *109*, 141–157. [CrossRef]
121. Probert, M.E.; Dimes, J.P.; Keating, B.A.; Dalal, R.C.; Strong, W.M. APSIM's Water and Nitrogen Modules and Simulation of the Dynamics of Water and Nitrogen in Fallow Systems. *Agric. Syst.* **1998**, *56*, 1–28. [CrossRef]
122. Blagodatsky, S.A.; Richter, O. Microbial growth in soil and nitrogen turnover: A theoretical model considering the activity state of microorganisms. *Soil Biol. Biochem.* **1998**, *30*, 1743–1755. [CrossRef]